THERMAL HAZARD ASSESSMENT OF THE STYRENE POLYMERIZATION SYSTEM

A Dissertation

by

LIN ZHAO

Submitted to the Office of Graduate and Professional Studies of
Texas A&M University
in partial fulfillment of the requirements for the degree of

DOCTOR OF PHILOSOPHY

Chair of Committee,	Mustafa Akbulut
Committee Members,	Jodie Lutkenhaus
	Joseph Kwon
	Jerald Caton
Head of Department,	Arul Jayaraman

August 2020

Major Subject: Chemical Engineering

ABSTRACT

Polymerization reactions are prone to runaway risks due to the unstable nature of monomers and the complex interactions between reactants. The major direct cause of polymerization runaway incidents is the deviation from the standard recipe or designed operation conditions. These unintended reactions may lead to auto-accelerated temperature and pressure rise, followed by rupture of reaction vessels, fire, and explosion.

To minimalize the risk, the polymerization reaction runaway behavior under various hazardous scenarios should be fully identified and carefully quantified. The understanding of the thermal/pressure behaviors and mechanisms during thermal runaway is essential to facilitate safer handling and storage of the reactive styrene system.

In this work, three most credible hazardous scenarios have been identified regarding the styrene system during polymerization and storage, including the deviation in monomer mass fraction, the deviation in initiator type and concentration, and the contact between monomer and a variety of impurities. Runaway hazards of these scenarios were calorimetrically investigated. Lumped kinetic models have been developed to predict reaction hazards.

Calorimetric results showed that the onset of the runaway reaction was strongly affected by the co-existing chemicals in the polymerization recipe. Polymerization inhibitor retarded the initial stage of the runaway reaction. The mischarging of the solvent had a complex effect on the runaway hazards of the polymerization reaction, as the addition of solvent monotonically reduced temperature-related thermal hazards and

increased the pressure hazards. Experiment and thermodynamic calculations indicated that volatile diluent increased system vapor pressure even at a lower adiabatic temperature rise. The mischarging effect of two different radical initiators, including benzoyl peroxide (BPO) and azobisisobutyronitrile (AIBN), was investigated at a series of elevated concentrations in both screening and adiabatic calorimeters. The onset temperature shifted to lower values with higher initiator dosage in the system. The overall heat generation, pressure building-up rate monotonically increased with initiator concentration. Finally, screening calorimeters were employed to quantify the contamination effects of styrene in contact with impurities, including water, alkaline, and acid. The exothermic characteristics of styrene mixed with contaminating substances were significantly related to the impurity concentrations and mixing conditions, especially for strong acids.

DEDICATION

To my husband Liangfeng, my mother, my father for all their love and support.

To my professors, Dr. Mustafa Akbulut and Dr. M. Sam Mannan for all their guidance and support.

ACKNOWLEDGEMENTS

I would like to express my sincere gratitude to my advisor Dr. Mustafa Akbulut. I would like to thank Dr. Akbulut for his support, guidance, and encouragement throughout my research at Texas A&M University, especially during difficult times. He has been most kind and supportive to take me into his group and guide me through my research. Without his guidance and constant support, this Ph.D. would not have been achievable.

I want to give my special appreciation to my deceased advisor, Dr. M. Sam Mannan. He has been a role model in the process safety research. His dedication to "make safety second nature" has inspired me along with my study, and this legacy will continue to be remembered.

I also want to thank all my committee members, Dr. Jodie Lutkenhaus, Dr. Joseph Kwon, and Dr. Jerald Caton, for their guidance and support throughout my graduate study. Their insights and suggestions have enabled me to go for a bigger picture and think deeper.

I would like to give special thanks to Dr. James Holste, Dr. Maria Papadaki, and Dr. Eric Petersen. They have been friends of the safety center for years and showed tremendous support to the group and the students. Dr. Papadaki's insights and expertise in chemical reactivity has inspired me to generate research ideas.

Finally, I would like to express my deepest gratitude to all my family members and friends at Texas A&M University, Mary Kay O'Connor Safety Center, and back in China. This dissertation would not have been possible without their support and help.

CONTRIBUTORS AND FUNDING SOURCES

Contributors

This work was supervised by a dissertation committee consisting of Dr. Mustafa Akbulut (advisor and committee chair) of Artie McFerrin Department of Chemical Engineering at Texas A&M University, Dr. M. Sam Mannan (deceased) (advisor) of Artie McFerrin Department of Chemical Engineering at Texas A&M University, Dr. Jodie Lutkenhaus (committee member) of Artie McFerrin Department of Chemical Engineering at Texas A&M University, Dr. Joseph Kwon (committee member) of Artie McFerrin Department of Chemical Engineering at Texas A&M University, and Dr. Jerald Caton (committee member) of Department of Mechanical Engineering at Texas A&M University.

Funding Sources

Graduate study was supported by Mary Kay O'Connor Process Safety Center and the Artie McFerrin Department of Chemical Engineering at Texas A&M University.

NOMENCLATURE

ΔH	Heat of reaction, J/g or kJ/mol
ΔH_d	Specific heat of decomposition, J/g
ΔT_{ad}	Adiabatic temperature rise, K or °C
C_p	Heat capacity, J/ (g·°C) or J/ (K·g)
$C_{p,c}$	Heat capacity of the test cell, J/ (g·°C) or J/ (K·g)
$C_{p,s}$	Heat capacity of the sample, J/ (g·°C) or J/ (K·g)
dT/dt	Self-heating rate, K/min or °C/min
$(dT/dt)_{max}$	Maximum self-heating rate, °C/min
dP/dt	Pressure-rising rate, (kPa/min) or (psi/min)
$(dP/dt)_{max}$	Maximum self-pressurization rate, (kPa/min) or (psi/min)
E_a	Overall activation energy, kJ/mol
E_d	Activation energy for the decomposition step, kJ/mol
E_p	Activation energy for the propagation step, kJ/mol
E_t	Activation energy for the termination step, kJ/mol
f	Radical efficiency factor, unitless
k_d	Decomposition rate coefficient of the initiator
k_p	Propagation rate coefficient of the free-radical polymerization
k_t	Termination rate coefficient of the free-radical polymerization
k_{tr}	Transfering rate coefficient of the free-radical polymerization

k_H	Huggins coefficient
m_c	Mass of the test cell, g
m_s	Mass of the sample, g
M_w	Molar weight of the chemical, g/mol
P_0	Initial pad pressure of the test, kPa or psig
P_{max}	Maximum pressure, kPa or psig
R	Universal gas constant, 8.3145 J/(mol·K)
R_d	Decomposition rate of the initiator
R_p	Propagation rate of the free-radical polymerization
R_t	Termination rate of the free-radical polymerization
T_0	Onset temperature, °C
T_p	Peak temperature, °C
T_f	Final temperature under adiabatic condition, °C
T_{max}	Maximum temperature under adiabatic condition, °C
TMR	Time to maximum rate, s or min
x	Reactant conversion
Greek symbol	
α	Conversion of the reaction, unitless
β	Heating rate, °C/min or K/min
φ	Thermal inertia factor, unitless
ϕ	Volume fraction of components in a polymer solution system
ρ	Density, kg/m^3

η	Apparent viscosity of the system, cp
$[\eta]$	Intrinsic viscosity of polymer chain in the solvent, cp
η_{sp}	Specific viscosity of polymer solution, cp
η_0	Viscosity of the solvent, cp

TABLE OF CONTENTS

Page

Page

Page

LIST OF FIGURES

Page

Page

Page

LIST OF TABLES

Page

1. INTRODUCTION [1]

1.1. Chemical Reactivity Hazards

Reactive chemical runaway is defined as a situation that the potential for an uncontrolled chemical reaction results directly or indirectly in serious harm to people, property, or the environment.[1] Such catastrophic reactive chemical runaway incidents keep reoccurring all over the world, leading to server consequences such as fire, explosion, toxic gas/liquid release, injuries, and fatalities.

According to the Guidelines for Safe Storage and Handling of Reactive Materials published by the Center for Chemical Process Safety (CCPS),[2] understanding chemical reactivity hazard is crucial to control runaway hazards and reduce the risk of the potential loss event. In general, the reactivity hazards are grouped into two major types: Self-reactive and reactive with other materials. Major hazardous reaction types include thermal decomposition, polymerization, exothermic rearrangement, reaction with oxygen, reaction with water. The hazards of these reactions are tightly linked to the process chemistry, kinetic parameters, operation conditions, and the scale of the process [3]. If the heat, energy, or gaseous products are not properly contained or accommodated, the uncontrolled reaction will lead to catastrophic consequences.[4]

Among all the runaway incidents happened all over the world, one particular type of reaction has caused significant numbers of incidents. Barton and Nolan[5] reported that

[1] Part of this section is reprinted with permission from "Probing into Styrene Polymerization Runaway Hazards: Effects of the Monomer Mass Fraction" by Lin Zhao, Wen Zhu, Maria I. Papadaki, M. Sam Mannan, and Mustafa Akbulut. *ACS Omega*, 4(5), 8136-8145. Copyright 2019 by ACS Publications.

48% of total runaway incidents that occurred over the period from 1962 to 1987 in the UK were polymerization reactions. A reactive chemical incidents report published by the Chemical Safety Board (CSB)[6] also denoted that almost 15% of incidents involving uncontrolled chemical reactions in 1980-2001 in the US are polymerization thermal runaways. An incident statistical study by Sales[7] in 2006 showed that 17 out of 132 (13%) reactive chemical incidents recorded by the Major Accident Reporting System (MARS) in the European Commission were caused by the polymerization runaway reactions. More recently, Mihailidou[8] analyzed 319 major industrial incidents with significant consequences based on the United Nations Environment Program (UNEP) criterion and found 34 out of 319 (11%) the major incidents worldwide during the years 1917 to 2011 were related to the reactive monomer/polymer process. Saada[9] analyzed 30 runaway incidents in a specific unit process during 1988-2013 and showed that over 33% of those were polymerization incidents.

Polystyrene is the fourth most consumed commodity general-purpose thermoplastics in the world,[10] following polyethylene, polypropylene, and polyvinyl chloride. Styrene monomer, the building block of the polystyrene, has also found use in the manufacturing of expandable polystyrene (EPS), acrylonitrile-butadiene-styrene (ABS) plastic, and high impact polystyrene plastics (HIP). However, process safety concerns have been raised during the handling and processing of the styrene monomer, as it has led to reoccurring runaway incidents all over the world in recent years.

Table 1.1 summarizes some of the major runaway incidents caused by styrene monomer that led to either injuries or fatalities. These runaway incidents happened in

various types of processing vessels such as storage tanks and reactors. The incidents investigation showed that the direct causes of the incidents included mischarging of reaction recipe, overheating of the reactants, and insufficient cooling due to the improper scaling-up of the polymerization reaction.

Table 1.1 Selected thermal runaway incidents related to styrene process

Date	**Location**	**Consequences**	
		Injury	Fatality
07/05/1994	Kaohsiung, Taiwan	0	1
01/26/1996	Chiayi, Taiwan	1	0
01/21/1998	Kaohsiung, Taiwan	4	0
12/24/1998	Kanagawa, Japan	0	0
06/27/1998	Channahon, IL, US	1	0
06/23/1999	Pasadena, TX, US	21	2
10/06/1999	Chiayi, Taiwan	1	0
03/27/2000	Pasadena, TX, US	71	1
04/02/2003	Addyston, OH, US	0	1
04/08/2004	Jiangsu, China	8	6
06/30/2005	Mesa, AZ, US	0	1

1.2. Chemical Reactivity Hazards Identification and Evaluation

1.2.1. Regulations and Guidelines

In order to prevent the runaway incidents from happening and minimize the risk associated with handling reactive chemicals, a variety of regulations and standards have been developed for hazardous chemical manufacturers to follow.

The primary regulations and standards have been summarized and compared by Besserman[11] across the United States, European Union, United Kingdom, China, and India. Most of these regulations were established after major reactive chemical loss events and aimed to provide a systematic tool focused on preventing the release of highly hazardous chemicals from both engineering and management perspectives. In the United States, the manufacturing and handling of the hazardous chemicals are covered by CFR 1910.119-Process Safety Management of Highly Hazardous Chemicals (PSM). This program contains fourteen elements to effectively identify hazards and control the potential risk caused by processes and procedures. Leggett[12] summarized the five most critical elements in the PSM program, which help enhance the management of reactive chemical hazards, including process safety information, process hazards analysis, operating procedures, pre-startup safety review, and incident investigation.

The Center for Chemical Process Safety (CCPS) provides a series of detailed guidelines regarding hazardous chemical reactivity evaluation and risk control. The guidelines for engineering design for process safety[13] summarized a life-cycle approach for inherently safer chemical process design, including identification and analysis of hazards, assessment of the risk, design of protection layers, and proper documentation

systems. The guideline for safe storage and handling of reactive materials[2] listed different chemical reactivity hazard types and classifications, material assessment tools, consequence analysis approaches, and industry best practice surveys. The guidelines for chemical reactivity evaluation and application to process design[14] provided a comprehensive illustration of the chemical thermal stability test methods and the corresponding application in process design, scaling-up, storage, and handling.

Regulations, guidelines, and industry best practices all denoted that the proper hazard identification and evaluation is the key and foundation of hazard elimination and risk control of the reactive chemical processes, and the overall implementation strategy consists of two major steps: the desk screening and the calorimetry tests.

1.2.2. Desktop Screening

Desk screening of reactive chemical runaway hazards usually involves the following steps:

- Safety data sheets (SDS)
- Handbooks and databases
- Theoretical thermal hazard calculation

The safety data sheet (SDS) is a 16-section, mandatory document regulated by Hazard Communication Standard (HCS) (29 CFR 1910.1200 (g)) to provide safety-related information of hazardous chemicals. Section 1 and section 2 contain general information on chemical identification, hazard classification, signal word, and hazard statements. Important flammability and firefighting information such as flash point, autoignition point, and explosion limits (lower and upper) are documented in section 5 and section 9.

In addition to the flammability hazards, chemical thermal instability rating evaluated per the National Fire Protection Association (NFPA) 704 standards is usually available in section 15, showing in an NFPA diamond label. The thermal instability is evaluated by calculating the Instantaneous Power Density (IPD) of the chemical under 250 °C during the exothermic reaction. IPD is defined as the product of exothermic energy release and the initial rate of the reaction[15] and is categorized into five levels to denote the energy release potential of a chemical upon heating. The above information in SDS provides a convenient way to screen potential reactivity/thermal hazards associated with a chemical.

A variety of chemical hazard handbooks are available as sources for detailed chemical hazard information. Sax's Dangerous Properties of Industrial Materials[16] summarizes general physical properties, reactivity, flammability, toxicology, and regularity information of over 28000 hazardous chemicals. The Hazardous Chemicals Handbook[17] also provides similar information on chemicals related to safe practice. Bretherick's Handbook of Reactive Chemical Hazards[18] contains more detailed and comprehensive reactivity related hazards of over 5000 chemicals, as well as the reactive interactions between incompatible species. A list of major reactive functional groups is also provided in this handbook for quick screening of potential reactive structures. Wiley Guide to Chemical Incompatibilities[19] also serves as an easy-to-use, portable guide regarding identifying incompatible chemical pairs. Other useful data sources for chemical thermal instability and flammability hazard include the National Institute for Occupational Safety and Health (NIOSH) Data and Statistics Gateway, the TOXNET (Toxicology Data

Network) database by the National Library of Medicine, and the CAMEO Chemicals Database by National Oceanic and Atmospheric Administration (NOAA).

Theoretical calculation tools and criteria have also been developed for qualitative or semi-quantitative screening of chemical reactivity hazards. The most straightforward and commonly used criterion is the oxygen balance (OB) value of a chemical, which represents the extent to which the chemical can be oxidized to convert carbon atoms to CO_2 and hydrogen atoms to H_2O.[20, 21] Generally, an oxygen balance close to zero (+80 to −120) denotes a highly chemical instability hazard. However, Shanley and Melhem[22] compared the hazardous rating obtained from the oxygen balance criterion and calorimeter test of over 20 chemicals. They argued that the OB criterion did not apply to oxygen-free but hazardous species such as polymerizable components, nitrides, diazo compounds, and others.

The calculated adiabatic reaction temperature (CART) is another useful criterion on the estimation of chemical reactivity hazard. It was first developed by the National Aeronautics and Space Administration (NASA) as part of the Lewis computer program CET89 in 1989 and later modified by Murphy[23] in 2003 to predict the energy release potential of a chemical reaction under adiabatic conditions. The method calculates the energy release of the decomposition of a chemical based on the most stable equilibrium products. The adiabatic reaction temperature is obtained by adopting the energy balance of the reactant/products system, assuming no heat loss to the environment. Experiment test results confirmed that chemicals with a CART higher than 1200 K had higher

explosive potential upon heating; however, the observation did not apply to organic peroxides.[20]

The Chemical Thermodynamics and Energy Release (CHETAH) program is a thermodynamic and energy release evaluation program developed by the American Society for Testing and Materials (ASTM) to calculate the chemical reactivity hazards of chemicals, mixtures, and chemical reactions theoretically. CHETAH programs adopted Benson group contribution methods to predict the heat of formation, heat capacity, Gibbs free energy, and other thermodynamic properties of a chemical in different phases. These values are further used to calculate a variety of the chemical thermal hazard indicators, including the maximum heat of decomposition, overall energy release potential, and net plosive density, as summarized by Shanley and Melhem.[24] Grewera[25] collected the experimental decomposition reaction enthalpy of nine highly hazardous functional groups and compared with the calculated value obtained by CHETAH and concluded that the agreement was satisfactory. It was also addressed that some important functional groups were not available as Benson groups, and the estimation using substitution groups were adopted. Another comparison of experimental and CHETAH simulated energy release value was carried out by Pasturenzi[26] for over 300 chemicals covering a variety of chemical types. CHETAH program successfully predicted the energy release potential of around 90% of chemicals except for nitriles and heterocyclic compounds.

1.2.3. Calorimetric Tests

Desktop screening methods provide an efficient and easy way to scan possible thermal instability information of chemicals or chemical reactions. Thermal stability tests

using calorimeters, on the other hand, enable a more accurate and reliable evaluation of thermal hazards at various scales, under both intended and unintended conditions.

A comprehensive review of conventional calorimetric techniques used for thermal hazard screening has been provided by CCPS.[27] Three major types of calorimeters are prevalent in thermal hazard screening applications: thermal screening calorimeters, adiabatic calorimeters, and isothermal calorimeters.

Thermal screening calorimeters such as Differential Scanning Calorimeter (DSC), Advanced Reactive System Screening Tool (ARSST), and Thermal Screening Unit (TSU) generally require small sample size. They are used for screening the heat release of samples under isothermal conditions or fixed heating ramp. These techniques are extremely critical in the early stage of process development.

After possible thermal reactivity hazards are discovered by the screening methods, adiabatic calorimeters including Accelerating Rate Calorimeter (ARC), Phi-TEC, Vent Sizing Package (VSP), and Automatic Pressure Tracking Adiabatic Calorimeter (APTAC) are adopted to obtain heat release information and pressure profile of chemical reactions under near-adiabatic conditions.

While the screening and adiabatic calorimeters provide comprehensive information regarding the thermal behavior of chemicals and chemical reactions under unintended/abnormal operation conditions, the isothermal calorimeters are used to understand the thermodynamics of a reaction under intended/desired reaction conditions. The dominant workhorse of the isothermal calorimeter is the Reaction Calorimeter (RC1e)

developed by Mettler Toledo, which measures the heat flow of the reaction under isothermal conditions by adopting a precise temperature control of the jacket fluid.

A summary and comparison of major hazard evaluation calorimeters is listed in Table 1.2. These techniques differ in sensitivity, test size, and also data acquisition. In general, a combination of these experimental tools is utilized following a specific test strategy to provide both temperature and pressure hazards of chemicals or chemical reactions under various conditions. A simplified procedure for prioritizing tests and proper interpretation of the data has been summarized by Rowe,[28] Donoghue,[29] and Gustin.[30]

Table 1.2 A summary of calorimetric techniques for chemical reactivity hazard evaluation

Type	Method	Sample gram	Operation mode	Data output
Screening	DSC	0.001–0.01	Isothermal Heat ramp	T_o, ΔH_r, kinetics
	ARSST	1–10		T_o, ΔH_r, $(dT/dt)_{max}$, $P_{max,}$ $(dP/dt)_{max,}$ kinetics
	TSU	1–7	Isothermal Dual-Scan Soak & Scan	T_o, ΔH_r, $(dT/dt)_{max}$, $P_{max,}$ $(dP/dt)_{max,}$ Time from exotherm to explosion, kinetics
Adiabatic	ARC	2–10	Heat-wait-search Isothermal Heat ramp	T_o, ΔH_r, ΔT_{ad}, $(dT/dt)_{max}$, $P_{max,}$ $(dP/dt)_{max,}$ Time to maximum rate, kinetics
	APTAC	2–10		
	VSP	10–100		
	Phi-Tec	1–100		

Table 1.2 Continued

Type	Method	Sample gram	Operation mode	Data output
Isothermal	RC1e	500–2000	Isothermal Isoperibolic Heat ramp	Jacket temperature, heat flux, ΔH_r

1.3. Literature Review

1.3.1. Reactivity Hazards in Polymerization Systems

Over time, an extensive literature has been developed on understanding the thermal hazard associated with the polymerization system by adopting the simulation and experiment techniques summarized in the previous section. Polymerization systems have attracted research attention due to the frequency of the runaway incidents, inherent self-reacting nature of the monomer, and also the self-accelerating characteristic of the polymerization system.

Vinyl-type monomers such as styrene, acrylonitrile, and vinyl acetate, carry unsaturated double bonds and have the potential to self-react to initiate unwanted polymerization reactions upon heating. The typical value of exothermic heat of polymerization is around −20 kcal/mol (−83.6 kJ/mol),[31] which corresponds to an adiabatic temperature rise of over 300 ºC assuming no heat loss to the environment. To prevent the self-reaction and extend the shelf life of monomers, inhibitors are usually added to the system to scavenge free radicals and stop polymerization reactions. Several chemicals have been experimentally studied and proven to effectively retard the free-radical polymerization of styrene including benzoquinone,[32, 33] tetraphenyl hydrazine,[32]

hydroquinones,[32, 34, 35] 4-tert-butylcatechol (TBC),[33, 35-38] and oxygen.[39, 40] A detailed inhibition mechanism has been proposed by Caldwell and Ihrig,[41] suggesting that in the presence of both oxygen and antioxidant type inhibitors, the peroxyl radicals primarily react with the inhibitor to form retarder radical instead of the usual chain propagation reaction to stop the polymerization reaction. When no inhibitors are present, the monomers are prone to initiate the self-polymerization or in the presence of initiators.

The polymerization reaction of the monomers to produce polymers is a complex process involving multiple reaction steps, including the initiation, propagation, termination, and chain transfer. Typically, free-radicals are produced upon initiator decomposition or the self-reaction of the monomer, followed by the growth of the long polymer chain. Finally, the free-radicals combine to cease the reaction. A well-recognized kinetic of free-radical polymerization reaction has been documented by Flory[42] and shown in Figure 1.1.

Initiation	$I \xrightarrow{k_d} 2R^{\bullet}$
Propagation	$R^{\bullet} + M \xrightarrow{k_i} M^{\bullet}$ $M^{\bullet} + nM \xrightarrow{k_p} P^{\bullet}_{n+1}$
Termination	$P^{\bullet}_{n+1} + P^{\bullet}_{m+1} \xrightarrow{k_t} polymer$
Chain transfer	$P^{\bullet}_{n} + S \xrightarrow{k_{tr}} P_n + S^{\bullet}$ $S^{\bullet} + nM \longrightarrow P_n + SM^{\bullet}_{n}$

Figure 1.1 The reaction steps in a polymerization reaction

The corresponding rate expressions for each step are listed in Equation (1) to Equation (5).

Initiation:

$$R_d = 2fk_d[I] \tag{1}$$

Propagation:

$$\frac{d[\mathrm{R}^\bullet]}{dt} = k_i[\mathrm{R}^\bullet][\mathrm{M}] \tag{2}$$

$$R_p = k_p[\mathrm{M}^\bullet][\mathrm{M}] \tag{3}$$

Termination:

$$R_t = 2k_t[\mathrm{M}^\bullet][\mathrm{M}^\bullet] \tag{4}$$

Overall:

$$R_p = k_p[\mathrm{M}]\sqrt{\frac{fk_d[\mathrm{I}]}{k_t}} \tag{5}$$

In the above expressions, I is the initiator molecule which generates free radicals upon heating, $\mathrm{R}^\bullet$ is the primary radical from the initiator decomposition, M is the monomer molecule, $\mathrm{M}^\bullet$ is the monomer radical, $\mathrm{P}^\bullet$ is the polymer radical, and S is the chain transfer agent, which could be solvent, monomer, or other chemical compounds. The rate coefficient and the reaction rate are also derived from the kinetic as denoted in the above equations. R_d represents the initiator decomposition rate with k_d as the corresponding rate coefficient. f is the correction factor for initiator efficiency. The propagation rate and rate coefficient are represented by R_p and k_p, respectively. The termination rate R_t is the overall effect of two different termination mechanisms, the recombination and disproportionation. k_t is the sum of these two rate rate coefficients.

k_{tr} is the chain transfer rate coefficient. If the pseudo-steady-state assumption is adopted to assume the concentration of radical components keeps constant during the reaction, an overall rate expression can be derived, as shown in Equation (5). The rate equation denotes that the overall polymerization rate is proportional to the molar concentration of the monomer, the square root of the molar concentration of the initiator.

However, the above kinetic equation gives good agreement with experimental data only within a limited monomer conversion range. For most of the free-radical polymerization processes, an auto-acceleration of the reaction is observed that the rate of polymerization significantly increases as the reaction progresses. This phenomenon is usually unknown as the Trommsdorff–Norrish effect, or the gel effect.

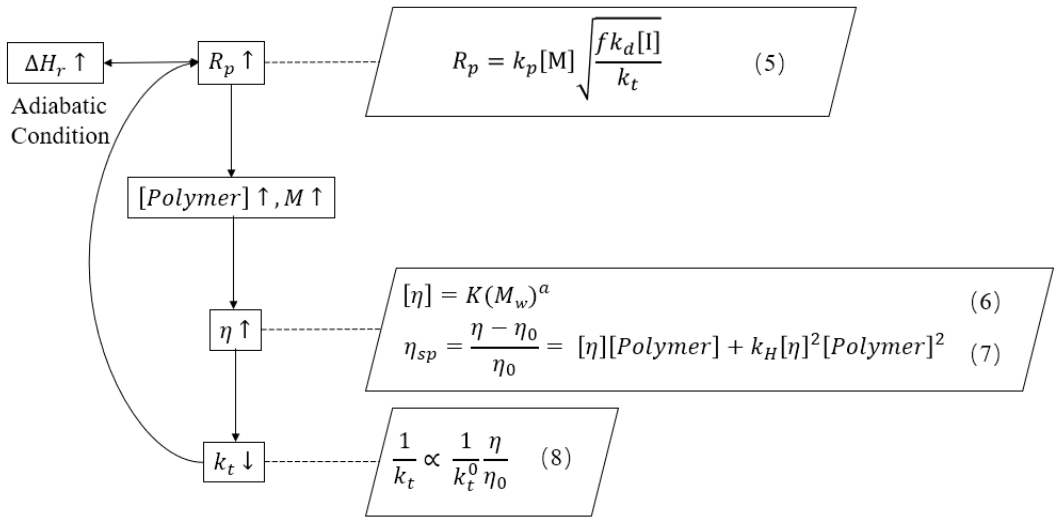

Figure 1.2 An illustration of the gel effect in the polymerization system

Figure 1.2 gives a brief illustration of the origin and mechanism of the gel effect during the free-radical polymerization reaction. As the monomers are consumed, the polymer concentration [polymer], as well as polymer molecular weight M_w increases, and the latter can increase by orders of magnitudes compared to monomer molar weight. These long-chain polymers significantly elevate system viscosity η via two different mechanisms. The intrinsic viscosity of polymer chains [η] increases exponentially with molecular weight M_w due to the increase of the length of polymer chains, which can be described by the Mark-Houwink as Equation (6). Parameters a and K depend on the specific polymer-solvent system pairs. At the same time, the apparent viscosity of the system increases with polymer concentration, as formulated by Huggins in Equation (7), where η_{sp} is the specific viscosity, η_0 is the solvent viscosity, k_H is the Huggins coefficient. Thus, the mobility of polymer chains and diffusion is strongly hindered such that the termination rate dramatically drops compared to the initial termination rate k_t^0 according to Equation (8), resulting in a fastened overall polymerization reaction rate. This synergetic process can further develop under adiabatic conditions, as reaction heat generated during exotherm elevated the system temperature and the reaction rate. If the reaction heat and rate are not controlled correctly, the auto-accelerated rate will result in explosive polymerization, leading to catastrophic runaway incidents, loss of containments, fire, and explosion.

In the modern chemical industry, the free-radical polymerization of styrene is usually carried out in a continuous process in the presence of a solvent to reduce system viscosity and avoid thermal runaway. This process is called solution polymerization, while

the polymerization of styrene without the addition of solvent is known as bulk polymerization. A simplified process flowsheet diagram of the solution polymerization process of styrene is shown in Figure 1.3.

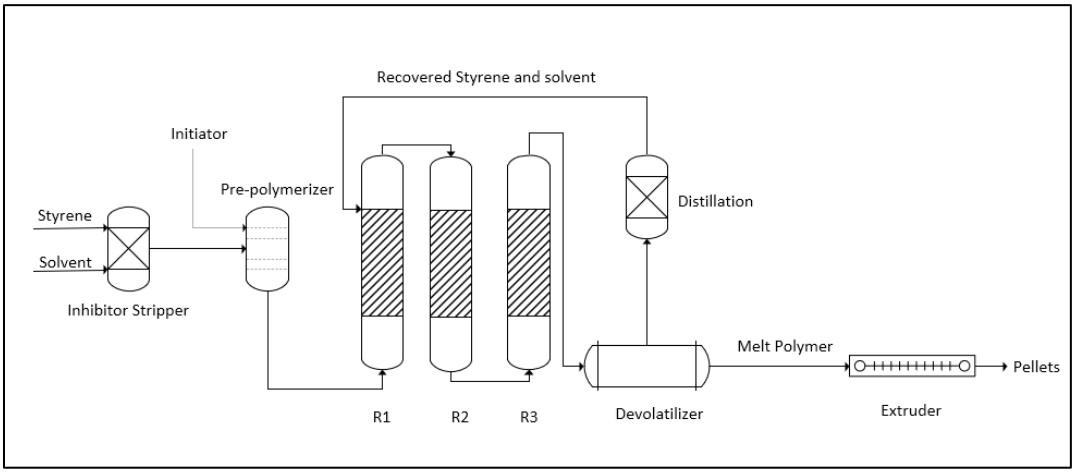

Figure 1.3 Simplified flow sheet diagram of the industrial styrene polymerization process

Ethylbenzene and toluene are two typical solvents (diluents) used in this process[43] and are mixed with the styrene monomer with a weight percentage between 5−25% before the reaction. TBC was removed from the feed stream by passing the inhibited monomer through a stripping column, as the residue of inhibitors usually results in unwanted color in the final product.[44] Oil-soluble initiators such as organic peroxides and azo compounds are commonly added to lower the polymerization temperature and alter the polymer structure. The reaction mixture is heated to the desired temperature according to the thermal decomposition behavior of the initiator and passes through multiple reactors (usually 3 or 4) to gradually polymerize into long-chain molecules. The continuous

polymerization reactor comes in different shapes, including stirred tank reactors (CSTR), plug flow reactors (PFR), agitated tower reactors, and static mixing reactors (SMR).[45, 46] The reactor operation temperature increases with monomer conversion as well as the system viscosity, and finally reaches a temperature range between 200−220 ºC. The polymer-monomer-solvent mixture finally passes through a vacuum devolatilizer to recover the light components for reuse, and the polymer slurry is sent to extruders to produce plastic pellets.[47]

It is obvious that multiple hazardous chemicals are present in a commercial polystyrene production process, including initiators, organic solvents, styrene monomer. The complex interaction between these components would strongly affect the thermal runaway hazard of the system and needs to be analyzed and quantified systematically. A thorough understanding of the thermal hazard of the polymerization system using different calorimeters is critical to inherent safer process design, protection layer and control measure installation, and prevention of the unwanted runaway incidents from happening. The following sections will give a comprehensive literature review on the research progresses regarding the thermal hazard assessment of the styrene polymerization system.

1.3.2. Styrene Thermal Polymerization System

The self-initiation of the free-radical polymerization of styrene in the absence of initiators is known as thermal initiation. The initiation mechanism involves the formation of styrene dimers and trimers following the Diels–Alder type reaction, as proposed by Mayo[48] and Flory.[49] Hui and Hamielec further developed an empirical model to relate the conversion of the monomer during the thermal polymerization with the polymer mass

fraction and temperature using polynomial correlations.[50, 51] This model found good agreement with the mg-scale isothermal experimental data during the temperature range of 100–220 ℃.

Whiting and Tou[52] evaluated the thermal behavior of styrene in an Accelerating Rate Calorimeter (ARC) under a heat-wait-search mode to address the effects of the system thermal inertia on the temperature profile during thermal runaway. After a correction on adiabaticity, the measured overall heat of polymerization ΔH was around −65 kJ/mol, which was slightly lower than the value obtained in DSC. In their study, the styrene sample contained 15 ppm of TBC as an inhibitor, which could significantly retard the thermal polymerization of styrene.

Gibson[53] tested the runaway reaction of inhibited styrene (12−15 ppm TBC) starting from 150 °C in an adiabatic Dewar bottle and calculated the relief valve size. The heat of reaction obtained in this study was around −17.7 kcal/mol (−73.9 kJ/mol), and the corrected maximum adiabatic temperature was between 375–379 ℃. A simplified kinetic correlation assuming a pseudo-first-order reaction resulted in overall activation energy of around 79.4 kJ/mol.

Frurip[31] discussed some general practices regarding hazard evaluation of polymerizable compounds and performed ARC tests on uninhibited styrene with oxygen-induced peroxide at various concentrations. The results denoted that with the presence of styrene (po1y) peroxide, the major exothermic peak shifted to a lower temperature. A DSC test was also conducted to compare the thermal behavior of inhibited and distillated

styrene up to 300 ℃. It was noticed that the presence of inhibitor delayed the onset of exothermic reaction by over 20 ℃.

Chen performed isothermal studies on inhibited[54] and uninhibited[55] styrene to investigate the runaway behavior and kinetic parameters of styrene at low temperatures using microcalorimeters. Isothermal test of uninhibited styrene was conducted in Thermal Activity Monitor (TAM) between 50–80 ℃ with 0.2 g of sample. The overall heat of polymerization linearly increased with storage temperature and had an average of around −70 kJ/mol. The activation energy was calculated to be −63 kJ/mol. A more detailed estimation of kinetic parameters was performed using isothermal data obtained from both DSC and TAM. The overall activation energy was verified to be 84 kJ/mol, while the thermal initiation step and chain transfer step had activation of 125 kJ/mol and 60 kJ/mol, respectively.

Liao[36] compared the thermal behavior of purified styrene and inhibited styrene with 10 ppm of TBC in DSC and TAM. It was noticed that TBC significantly retarded the thermal polymerization of styrene and postponed the exothermic reaction by 20 ℃. The DSC results of TBC inhibited styrene showed two consecutive exothermic peaks, which were identified to follow autocatalytic reaction kinetics and n^{th} order kinetics, respectively. The activation energy of these two peaks fell into a similar range of around 160 kJ/mol.

Leung[56] utilized the ARC to investigate the thermally initiated polymerization of inhibited styrene with 20% ethylbenzene added to the system under an air pad. The adiabatic exothermic onset temperature for the solvent-containing system was around 110 ℃, and the maximum temperature was observed to be around 343 ℃. The activation

energy obtained in this study was 80 kJ/mol using a lumped pseudo-first-order reaction model.

Many efforts have also been made to develop detailed models to match the experimental data of the polymerization system, as summarized by Achilias.[57] One of the most challenging parts of this field is the proper description of the gel effect. At the same time, many of these researches have been limited to simulate the polymerization reaction at the desired reaction condition, giving no information on the thermal behavior of the system during a thermal runaway incident. Noronha[58] proposed a second-order kinetic model and related the termination rate with system viscosity to mimic the auto-acceleration behavior of styrene thermal polymerization. The calculated thermal behavior data were compared with the experimental data acquired from a self-made Dewar reactor, and the results agreed with the measured data within orders of magnitudes below 200 ℃. Hungenberg[59] further compared three more advanced kinetic models developed by Hui and Hamielec, Weickert, and Marten and Hamielec, respectively. All three models considered the gel effect and matched well with the isothermal experimental data below 140 ℃. Thermal runaway simulation was also carried out by Hungenberg for the thermal polymerization of styrene started from 80 ℃ and 150 ℃, and all three models predicted similar temperature profiles for a runaway reaction, with temperature difference within 15 ℃. However, no comparison between simulated and experimental data was performed for the runaway study, primarily due to the lack of data in the open literature.

One of the drawbacks in the hazard analysis of the thermally initiated styrene runaway polymerization is that the evaluations were usually conducted at the microscale

or massive scale but under poor adiabaticity. Most of the literature failed to rule out the effect of inhibitors before testing, which might result in underestimation of the real hazard and provide misleading guidelines regarding the installation of safe control measures. Moreover, atmospheric control was not adopted to avoid the inhibition effect of oxygen on the thermal polymerization in adiabatic calorimeters. The kinetic modeling and comparison between simulation results and experimental data were very limited to isothermal conditions at low-temperature ranges (< 200 °C). In addition to that, there is no open literature available that discusses the effect of solvent on the runaway behavior of the thermal polymerization of styrene.

1.3.3. Styrene-Initiator Polymerization System

In most of the production process of polystyrene, the system is not thermally initiated. Instead, initiators that generate free radicals are added to lower the activation energy (energy barrier) and fasten the polymerization reaction. As illustrated in Equation (1) and (2), primary radicals are first produced and attack the carbon-carbon double bond of the monomer to further produce initiating radicals. As the initiation is the first step in free-radical polymerization, understanding the initiator decomposition behavior and its interaction with the monomer is essential in determining the thermal runaway hazards of the polymerization system.

Different types of initiators can be adopted to trigger the polymerization reaction via a variety of mechanisms. Typical reactions lead to the formation of free-radicals include the thermal decomposition of initiators, the redox reaction of initiator pairs, and the photo-induced decomposition of initiators.[60] In the production of polystyrene, the

thermal initiators, typically azo compounds and peroxides, are most prevalent. The decomposition mechanism of thermal initiators involves the cleavage of weak valency bonds and subsequent dissociation of the molecule to produce single or multiple radicals. The decomposition rate of the initiators strongly depends on the structure of the molecule, the temperature, and also the surrounding solvent. Most of the open literature assumes the overall decomposition rate follows first-order reaction rate law, and the concentration change of the initiator upon heating can be expressed in Equation (9).

$$[I] = [I]_0 e^{-k_d t} \tag{9}$$

In Equation (9), $[I]_0$ denotes the initial concentration of the initiator before thermal decomposition. If Equation (9) is integrated with respect to time, the time required for 50% of the initiator to decompose can be calculated as Equation (10).

$$t_{1/2} = 0.693/k_d \tag{10}$$

$t_{1/2}$ is named as the half-life of the initiator. Shorter half-life is usually associated with a higher decomposition rate of the initiator. It was noticed that in Equation (1), factor *f* is used as the correction for radical generation efficiency, which is less than unity. This correction is added to describe the cage effect that hinders the complete decomposition of initiators in a specific monomer/solvent system. A detailed description of the theory and mechanism of the cage effect is summarized by Denisov.[61] In general, the cage effect, as well as the induced decomposition of certain types of initiators, deplete the initiator and reduced initiation capability.

Many research efforts have been made to assess the thermal hazards during the thermal decomposition of the initiators, especially for peroxides. The uncontrolled

decomposition of pure initiators is usually explosive and has caused numerous major incidents, as summarized by Graham[62] and Ho.[63] Duh[64] compared the thermal decomposition behavior of eight organic peroxides in DSC, microcalorimeter, and VSP. The test results denoted that these compounds had the potential to thermally decompose, starting from as low as 70 °C, releasing a significant amount of heat and non-condensable gas.

Two of the most commonly used initiators in the production of styrene are azobisisobutyronitrile (AIBN) and benzoyl peroxide (BPO), and many researchers have theoretically and experimentally studied the thermal hazards of these two compounds. Liu[65] investigated the thermal decomposition of pure AIBN and AIBN mixed with diluted acid and hydroxide in DSC. The onset temperature of AIBN identified in this research was around 105 °C, and the addition of acid slightly promoted the initial stage of the decomposition. The measured heat of decomposition for AIBN was around −1065 J/g. Further study by the same research group[66] using kinetic modeling showed that the decomposition reaction had an activation energy of around 142 kJ/mol. Guo[67] performed DSC tests and kinetic modeling on the thermal decomposition of AIBN, and the fitting results showed a decomposition heat of −1124 J/g and activation energy of 124 kJ/mol according to Ozawa method. Bessiere's work on AIBN decomposition measurement in DSC adopted both isothermal and heat ramping test,[68] and the heat of reaction obtained was −230 kJ/mol (−1402 J/g), with an activation energy of 127 kJ/mol. One of the difficulties in obtaining accurate thermal hazard data of AIBN is that the major exothermic peak overlaps with the endothermic melting peak, and the coupling of these two heat

effects generates a complex heat release curve during a DSC test. Zhang[69] performed two decoupling methods to isolate the exothermic effect from the integrated thermal curve by dissolving AIBN into an organic solvent before the test or by extrapolating the two peaks. The solvent method showed an onset temperature of 86.2 °C and an exothermic heat of −1119 J/g, while the mathematical extrapolating yielded a slightly higher onset temperature of 93.5 °C and a heat release of −1169 J/g.

The heat release of 75% BPO in water has been investigated by Tsai in both DSC and VSP2.[70] The DSC curve denoted a heat release of around −1045 J/g, and sulfuric acid was identified to be a promotor of the thermal decomposition. Huang[71] analyzed the thermal behavior of pure BPO in microcalorimeters, including DSC and TAM, and obtained the low-temperature heat of decomposition of BPO was around −1010 J/g. This research also calculated the self-accelerating decomposition temperature (SADT) of BPO and suggested that the material required a storage temperature below 90 °C to ensure safety. Lv[72] performed thermal hazard analysis of BPO in both DSC, TSU, and ARC and obtained the onset temperature and heat release under various conditions. After proper correction regarding the adiabatic thermal inertia factor, the measured heat release during the decomposition was around −1120 J/g, and the exothermic was first observed at 94.3 °C. The decomposition activation energy obtained in this research was 191 kJ/mol, denoting the auto acceleration characteristic associated with BPO decomposition due to the induced decomposition mechanism.

In industrial practice, initiators are usually added into the system to facilitate styrene polymerization at hundreds of ppm-level. Even at such low concentrations, the

addition of initiators brings substantial change to the thermal behavior of the polymerization system as the initiation reaction pathway is altered. Several studies have been carried out to investigate the interaction between initiator decomposition and monomer polymerization in different calorimeters.

Maschio[73] investigated the free-radical polymerization of purified methyl methacrylate (MMA) using Phi-tec at initiator concentrations up to 0.075 M. The test results showed that the celling temperature and initial polymerization rate varied with initiator types. Both BPO and AIBN resulted in similar overall activation energy of around 87 kJ/mol using a pseudo-first-order model. The study of Theis[74] on the copolymerization of MMA and styrene with a pseudo-adiabatic calorimeter ARSST showed an increase of over 100 °C/min on self-heating rate when the diazo type initiator concentration was doubled from 5000 ppm to 10000 ppm. Lee[75] performed an isothermal test of the initiator-MMA polymerization system using four different types of initiators under low temperatures (60−90 °C). The isothermal curves obtained revealed the auto-acceleration characteristic of the free-radical polymerization system and were split into three consecutive stages to perform kinetic modeling. The rate coefficients and activation energies at different stages were calculated and compared with an initiator dosage of 5000 ppm.

For the pure styrene polymerization system (bulk/solution), Rowe[76] tested the thermal runaway behavior of styrene with 5000 ppm BPO in an adiabatic Dewar bottle and noticed that three exothermic peaks were present on the self-heating rate curve. It was speculated that the first two peaks were related to the primary and secondary radical

generation, and the last peak (main exotherm) was the thermally initiated polymerization peak. Uchida[77] carried out a thermal hazard analysis of the initiator-styrene system with 7000−70000 ppm BPO added to bulk styrene. Calorimeters, including DSC, RSST, and ARC, were utilized to obtain the thermal behavior of the system under different BPO concentrations, and the test results confirmed that higher initiator dosage led to lower onset temperature of exothermic activity and also higher maximum self-heating rate under pseudo-adiabatic conditions. Two more recent studies have been carried out by researchers at Nanjing Tech University, covering the BPO-styrene system thermal runaway behavior. Wang[78] performed a calorimeter study of the above system by changing the BPO concentration between 0−44000 ppm in both DSC and Phi-tec. The DSC results showed that the onset temperature of styrene polymerization shifted from 127 °C for thermal polymerization to 70 °C for 40000 ppm BPO initiated polymerization. The adiabatic tests also identified a decreasing trend in activation energy and overall heat release when BPO dosage was elevated. The lowest activation energy obtained in this study was 62 kJ/mol. Liang[79] observed similar runaway behavior patterns by comparing the thermally-initiated polymerization with BPO-induced styrene polymerization in DSC and Phi-tec. Gel permeation chromatography (GPC) tests on the polymer products revealed that BPO-initiated polymerization generated polymers with lower molecular weight and viscosity.

Research has tended to understand the difference in thermal hazards between thermal polymerization and initiator-induced polymerization, primarily for the bulk styrene system (no solvent). These results provide a fundamental understanding of the thermal behavior of different polymerization routines; however, more research effort is

needed to guide realistic styrene production by investigating the styrene solution polymerization system. General industrial practice avoids polymerizing pure styrene; instead, a solvent is usually added to reduce system viscosity, enhance heat/mass transfer, and thus mitigate production difficulty. It is crucial to perform the thermal hazard study of the initiator-styrene with the presence of a solvent. In addition to that, the comparison between different types of initiators on the runaway behavior of styrene is not well documented. Experimental work needs to be carried out to provide data and guide the selection of an inherently safer initiator.

1.3.4. Styrene-Contaminant Incompatible System

The previous sections summarize research work on thermal hazard analysis of the styrene polymerization system with desired chemical compounds in the normal recipe (styrene, inhibitor, solvent, and initiators). Another critical piece towards a comprehensive hazard analysis of the system covers the assessment of the interaction between styrene and other unwanted components; in other words, the contaminants. Contamination of the reactant is a common and credible scenario during the production and processing of styrene and polystyrene and has been the direct cause of many past major chemical runaway incidents, according to the statistics summarized by Sales.[7]

A growing body of research has been carried out to investigate the effect of contaminants/impurities on runaway reactions, specifically on the polymerization systems. According to Gustin,[80] contaminant species at a small amount could pose significant threats to monomer storage due to the fastened inhibitor consumption rate, especially for ethylene oxide (EO) and vinyl acetate (VAM). Liu[81] performed a comprehensive literature

review on the current research progress regarding contamination effects on EO polymerization, including water, iron oxide (rust), and alkaline. Casson[82] confirmed that alkyl anilines accelerated the thermal polymerization of methyl methacrylate (MMA) in ARC by elevating the maximum self-heating temperature rate and reducing the time to the maximum rate. A more detailed kinetic simulation was carried out by the same research group adopting isothermal hazard analysis in DSC.[83] The kinetic fitting results suggested that the possible interaction between alkyl anilines and monomer-peroxide was the culprit of the unwanted exothermic reaction. Liu[84] recently investigated the contamination effect of three inorganic acids on the thermal polymerization of isoprene in DSC. It was confirmed that sulfuric acid, hydrochloric acid, and nitric acid promoted the highly exothermic thermal polymerization reaction by lowering the onset temperature from over 200 °C to room temperature.

However, very limited research effort has been made to address the incompatibility between styrene and possible contaminants. Hankin[85] studied the thermal polymerization of various vinyl type monomers in contact with silica absorbents in ARC and confirmed that silica-based absorbent lowered styrene thermal polymerization onset temperature by around 20 °C and accelerated the runaway reaction. Frurip[31] also observed a lowered onset temperature as well as the maximum self-heating rate of styrene polymerization in ARC when styrene was mixed with clay absorbent.

Other chemical components that have the incompatibility issues with styrene were documented by chemical hazard handbooks introduced in section 1.2.2. Unwanted thermal runaway reaction is possible if styrene gets in contact with strong acids, strong oxidizers,

peroxides, and other initiators, aluminum chloride, butyllithium, and also air under elevated temperatures.[16, 18, 19] However, no detailed thermal hazard analysis data are currently available in open literature documenting the temperature profile, pressure profile, and kinetic parameters for styrene/contaminative components mentioned above. Experimental investigation using calorimeters needs to be carried out to provide quantitative data regarding the incompatibility hazards of the styrene polymerization system.

2. PROBLEM STATEMENT AND OBJECTIVES

As discussed in the previous section, the processing and storage of styrene to produce polystyrene is an inherently hazardous process that has caused numerous major incidents, resulting in injuries, fatalities, asset loss, and environmental damage. The underlying root cause of these incidents is the inadequate understanding of the thermal hazards of the system under unintended reaction conditions. A comprehensive, in-depth study on the quantification and prediction of the reactivity hazards serves as the very first step to proper control and elimination of the risk during operation.

The literature review revealed the complexity and inadequacy regarding the thermal hazard analysis of the styrene reaction system as multiple hazardous chemical compounds could be present, including reactive monomer, flammable solvent, initiators, inhibitors, and possible contaminants. The research gaps identified in the first chapter are summarized as follows:

- For most of the calorimetric analysis, especially under adiabatic conditions, the retardation effect of the inhibitor was not properly ruled out.
- For the hazard analysis of thermally-initiated polymerization of styrene, the kinetic model validation was conducted at low-temperature ranges. Thus, the results cannot represent the runaway hazard under worst-case scenarios.
- Few researchers addressed the solvent effect on the thermal and pressure hazard of styrene polymerization. Bulk polymerization without solvent is not

favored in the commercial polystyrene production, and the hazard analysis for this solution polymerization system is missing.

- For the ternary polymerization system containing initiator, monomer, and solvent, no hazard elevation was performed to compare the difference between the effect of different types of initiators. Most of the open literature fails to address the thermal behavior of the system when the dosage of the initiator was in the normal operation range (hundreds of ppm level).
- The quantification of the incompatibility hazards of styrene with possible contaminants was not available.

To fill these gaps, this work will first carry out a systematic analysis of the multi-component styrene polymerization reaction system to develop credible hazardous scenarios. For each of these scenarios, experimental measures will be conducted using different calorimetric techniques to accurately assess the thermal/pressure hazard during the course of thermal runaway. These data will be further fitted into kinetic models to generate kinetic parameters and guide the prediction of thermal runaway hazard. The various sub-objectives of this work are listed as follows:

- To perform systematic root cause analysis of the multi-component styrene reaction system and identify the most credible unintended incident scenarios.
- To perform different inhibitor removal techniques and calorimetrically evaluate the effect of the inhibitor on the thermal runaway polymerization hazard.

- To assess the thermal hazard of the styrene-solvent polymerization system and identify the contribution of solvent on the runaway behavior. Further, this work targets the kinetic model validation of the runaway reaction at high temperatures and conversions.
- To study the initiator-solvent-monomer interaction during the runaway reaction in various calorimeters. The concentration of the components will reflect both normal operation conditions and abnormal situations.
- To obtain quantitative thermal hazard data of the styrene-contaminants system and discuss the incompatibility hazards under different concentrations and mixing conditions.

3. METHODOLOGY

As addressed earlier in the previous chapter, for the hazard evaluation of a complex styrene polymerization system, the very first step is to obtain credible scenarios. Following that, calorimetric analysis and kinetic fitting methods will be adopted to quantify and further predict the hazards. This section covers detailed methodologies used in this work to fulfill the proposed research objectives. Root cause analysis tool, various calorimetric techniques and corresponding data processing procedures, and kinetic models will be elaborated.

3.1. Fault Tree Analysis

Fault tree analysis (FTA) technology, also known as the negative analysis tree, is a kind of logical cause and effect diagram. It correlates the outcome or state of the system (top event) according to the causes or the state of the element (base event). Similar to reliability block diagrams, fault tree analysis diagrams are also a graphical design method. The technique was first developed by Bell Telegraph's Telephone Laboratory in 1962 and has been widely adopted by the National Aeronautics and Space Administration (NASA) and the chemical industry to facilitate hazard identification and subsequent risk analysis.

Fault tree analysis utilizes Boolean type logic components to analyze hazards visually. It is intuitive, clear, and logical. It fits into both qualitative analysis and quantitative analysis. It embodies the systematisms, accuracy, and predictability when studying safety issues with a system. Some of the important features of FTA include the capability to handle complex systems, visually display the interaction between complex

cause-consequence combinations, the simplicity regarding the interpretation, and the possibility to combine with risk analysis to provide quantitative data.[86, 87]

FTA is commonly used to perform root cause analysis by identifying all relevant events and contributing factors that could lead to an unwanted situation (the outcome of the top event). Then these contributing factors are connected by Boolean logical operators to identify the sequence of the events and their interaction patterns. This process will be repeated on each event until the most common and fundamental event (root) is identified.

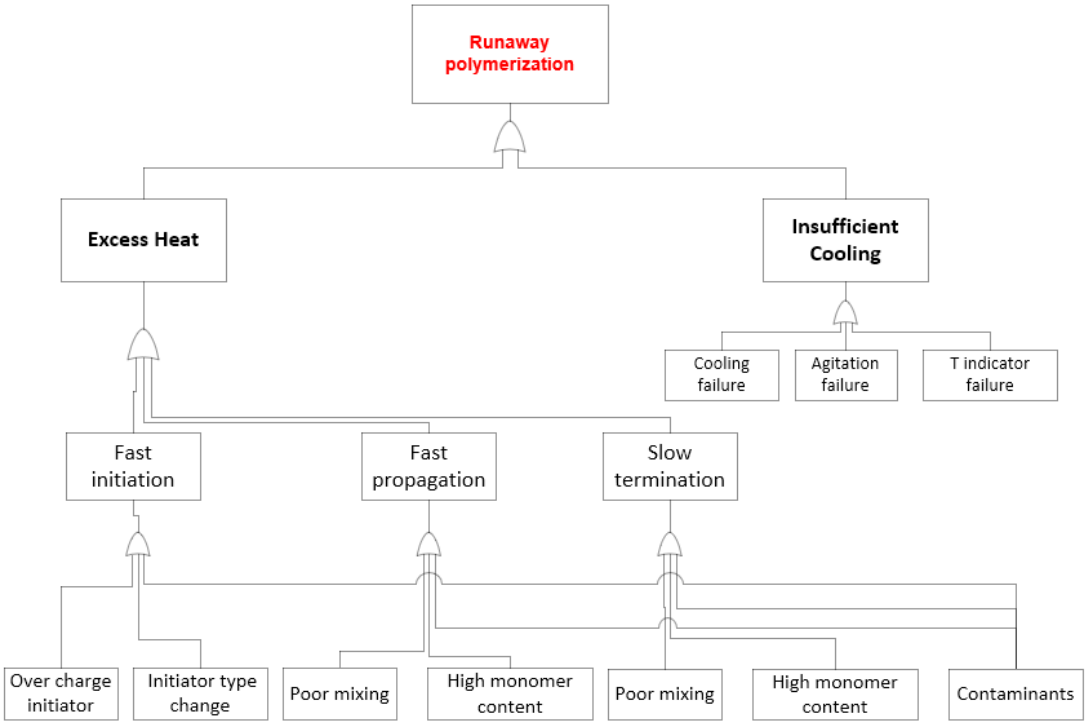

Figure 3.1 Fault tree analysis of the styrene polymerization system

A detailed FTA used in this research is shown in Figure 3.1. Fault tree analysis starts with the proper definition of the system of interest. In this research, the system was defined as the styrene free-radical polymerization process, which involves multiple hazardous chemical compounds, as listed in the previous sections. Next, the top event was identified as the uncontrolled thermal runaway reaction of the styrene system. This event could be possibly initiated by two deviations from the normal operation condition: the insufficient cooling or excessive heat generation. In this layer, these two events were independent of each other, and if at least one event is true, the output (top event) is true. Thus, the second layer components were connected with the top event with the OR gate.

Next, for the "insufficient cooling" event, three possible root events were identified, including the failure of cooling, the failure of agitation, and also the failure of the temperature indicator. These components were connected to the upper event with the OR gate.

The contributing factors for the "excessive heat generation" event were identified according to the overall polymerization rate expression shown in Equation (5). Since the polymerization reaction is a highly exothermic process, the heat released during the reaction is proportional to the rate that the monomers are consumed. Any deviation caused the increase of reaction rate would result in excessive and unwanted heat generation.

From the previous analysis on reaction mechanism and rate equation, it was noticed that the fastened polymerization rate could be contributed to three events: fast initiation step, fast propagation step, and the slow termination step. The three events

served as the third layer of the FTA and were connected to the second layer event by the OR gate.

Moving forward to lower layers, the fast initiation was supposed to be the results of initiator concentration change or initiator type change. Mischarging of initiator concentration beyond normal recipe led to an increase of [I], and the change in initiator type would strongly affect the decomposition rate k_d and initiator efficiency *f*. Similarly, fast propagation was most possibly related to the elevation of monomer concentration [M], and the boost of the propagation rate coefficient k_p when the gel effect was significant. Finally, the slow termination was the direct consequence of lowered termination rate k_t due to the gel effect, which appeared as a denominator term in Equation (5). At the same time, the origin of the gel effect was the reduced mobility of polymer chains in the system, which could be caused by a higher [M] or poor mixing. Last but not least, all these three contributing factors in the third layer were supposed to be affected by the contaminant components.

The fault tree analysis provided a convenient way to identify the underlying contributing factors regarding the runaway polymerization of the styrene system. The root causes obtained from this fault tree include the overcharging of initiator concentration, the change in initiator type, the change in monomer concentration, the inadequate mixing, and possible contamination. These deviations would strongly affect the system reaction rate coefficients, system viscosity, and the subsequent gel effect, thus alternating the overall reaction rate and stimulating excessive heat generation. If these heats were not properly controlled, runaway polymerization was expected to occur.

3.2. Experimental Design

In section 3.1, the fault tree analysis was adopted to obtain a series of root causes that would contribute to the thermal runaway polymerization of styrene. For each of these causes, detailed calorimeter tests and kinetic modeling (if applicable) will be carried out to provide a quantitative assessment of the thermal hazards during thermal runaway.

Table 3.1 The experiment plan for the thermal hazard assessment

Scenario	Reaction recipe	Experimental setup
1. Lack of inhibitor	Styrene ± Inhibitor	• As-is styrene • Caustic wash of inhibitor • Adsorption of inhibitor
2. High monomer content	Styrene + Diluent	• 0%, 15%, 30%, 45% wt EB
3. Initiator type change 4. Overcharge of initiator	Styrene + 15% Diluent + Two Initiators	• Solid BPO/AIBN • BPO/AIBN 5% in EB • 0, 500, 1000, 2500, 5000, 10000 ppm
5. Contamination	Styrene + Contaminants	• 5%, 20% wt H_2O • 5N H_2SO_4/ 5N NaOH • 5% wt concentrated H_2SO_4

A detailed experimental plan is summarized in Table 3.1 to showcase the hazardous scenarios investigated in this research. The first scenario was the testing of the inhibitor retardation effect on the thermal runaway behavior of styrene thermal polymerization. Two inhibitor removal methods were compared. In all the following investigations, the inhibitor was properly removed to rule out the retardation effect. Scenario 2 studied the consequence of monomer concentration change by altering the diluent concentration from 0% up to 45% in the system (wt.). Ethylbenzene (EB) was used as the diluent as it is most prevalent in the commercial production of polystyrene. The term diluent and solvent were used interchangeably in this research. In scenario 3, the initiator concentration, as well as the initiator type, were altered in the styrene-diluent-initiator system to investigate the thermal behavior change. The thermal decomposition of BPO and AIBN was first studied in the solid form and when dissolved in the diluent. Then the initiators were added varying from 0 ppm to 10000 ppm to mimic the overcharging of the initiator. Finally, the incompatibility study of styrene with possible contaminants was studied in scenario 4, covering water, acid solution, caustic solution, and concentrated acid. Different types of calorimeters were adopted to obtain the thermal runaway data of interest, which will be discussed in detail in the following section.

3.3. Calorimetric Techniques

As discussed in section 1.2.3, calorimeters in different types are the workhorse of the quantitative assessment of thermal runaway hazards. The calorimeters used in this work include the screening tool DSC, the adiabatic tool APTAC, and the pseudo-adiabatic tool ARSST.

3.3.1. Differential Scanning Calorimeter (DSC)

Differential scanning calorimetry (DSC) is a powerful tool for thermal analysis of chemicals or chemical reactions under isothermal and ramped heating conditions. DSC records the heat flow during the reaction as a function of temperature or time. There are two major types of DSC: The heat flux type and the power compensation type[88]. In this research, a Q20 DSC from TA Instruments was used, which functions in the heat flux mode. A simplified schematic of the DSC is shown in Figure 3.2.

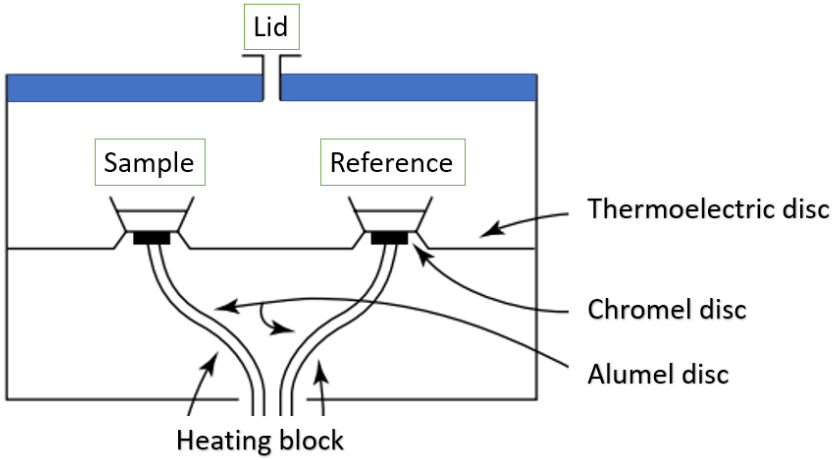

Figure 3.2 Schematic diagram of the heat flux DSC

1−10 mg of the sample was contained in the sample holder and heated up by the furnace according to the pre-programmed heating mode to increase the temperature linearly or keep the temperature at the desired isothermal condition. The heat flux difference needed to heat the two samples to the same temperature was recorded. In this research, an empty pan was used as a reference for all tests.

When utilizing DSC as a thermal hazard analysis tool, it is critical to choose the proper sample holder to ensure the containment of all reactive components (reactants and products) during the reaction. Table 3.2 summarizes the comparison between the conventional sample pan and the high-pressure sample pan used particularly in the thermal hazard evaluation application.

Table 3.2 A comparison between different sample pans in the DSC test

Type	Material	T range (°C)	Max P (MPa)	Notes
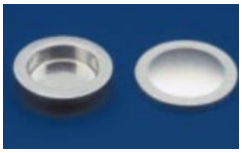 **Tzero Hermetic**	Aluminum	25–600	0.2	Heat conduction Sensitivity Loss of reactant
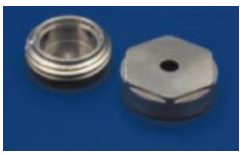 **High-pressure**	Stainless-steel	25–300	10	Poor heat conduction T gradient

The standard Tzero hermetic aluminum pan is light-weighted and provides excellent sensitivity regarding small heat flow. However, when samples with the huge exothermic effect are tested, an expansion of headspace gas will be observed as well as the vapor or non-condensable gas generation. The pressure change in these processes can

reach 100 bar and cannot be appropriately contained in the aluminum pan. Thus, the stainless-steel pan, which can withstand high pressure needs to be used.

The DSC test on the melting process of metal Indium was carried out to testify if the heat flow data obtained in both types of sample pans were in agreement. The DSC was first calibrated by a blank sample, then 5 mg of indium was sealed in both pans and heated up to 300 °C at a constant heating ramp of 4 °C/min. The heat flow curves and calculated heat of melting are summarized in Figure 3.3. Several important thermal hazard indicators were obtained from the DSC heat flow curve, as listed below:

1) the onset temperature T_0, shown as the intercept of the extrapolated slope of the heat flow curve and the continuation of the baseline.

2) The peak temperature T_p, at which temperature the heat flow reaches maximum.

3) The heat of reaction ΔH_r, calculated by integrating the specific heat flow signal (W/g) with respect to time (s).

The comparison denoted that both pans gave almost identical T_p on the heat flow curve, which is known as the melting point of indium. The melting heat of indium integrated was near 28 kJ/mol, which was in good agreement with the literature value.[89] The difference was noticed in the shape of the baseline and the peak in two pans. The aluminum pan provided a flat baseline and symmetric Gaussian peak, while the stainless-steel pan introduced a tilted baseline and a tailing peak. These non-idea features might be introduced by the relatively poor heat conduction of the stainless-steel material and the thermal-sink effect caused by the high-weight sample pan.

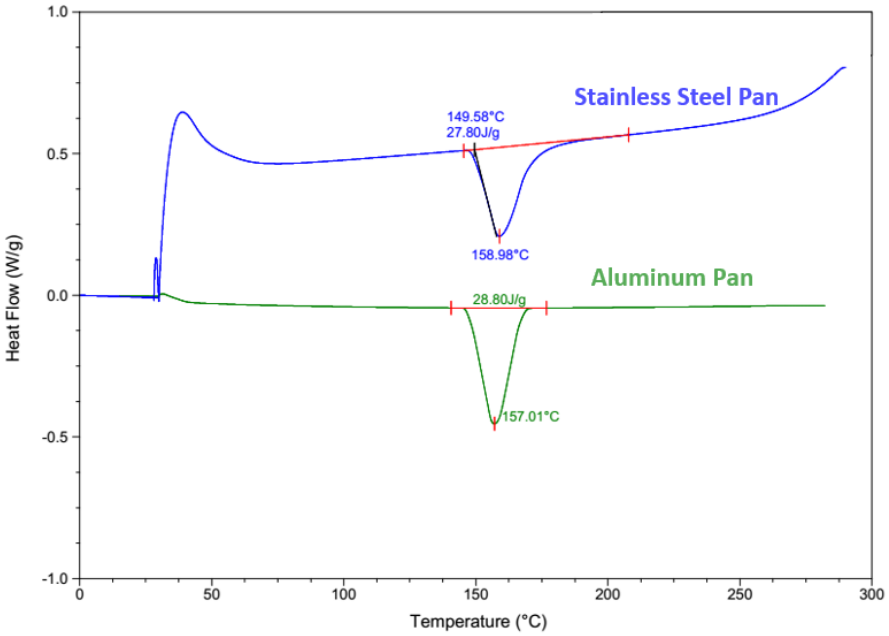

Figure 3.3 The heat flow of Indium melting in DSC using two different pans

Besides the thermodynamic information mentioned above, DSC is also capable of providing kinetic information about the reaction. A comprehensive review of these kinetic methods was documented by TA Instruments[90] using the curing of epoxy resin as the model system. The kinetic evaluation can be conducted under both isothermal[91] and heat-ramping mode following different kinetic models, namely Borchardt and Daniels method,[92] Kissinger method,[93] and the Flynn/Wall/Ozawa Method.[94] The detailed elaboration and application of the Flynn/Wall/Ozawa Method will be covered in section five.

3.3.2. Adiabatic Calorimeter (APTAC)

The Automatic Pressure Tracking Adiabatic Calorimeter (APTAC) developed by Netzsch is a powerful adiabatic calorimeter for the worst-case scenario assessment of the

thermal runaway reaction. The device has the capability to track the sudden elevated temperature and pressure in the test cell by keeping the temperature and pressure identical in and outside of the cell. The maximum operating temperatures of the APTAC is up to 500 °C and pressures up to 2000 psi (13000 kPa). A simplified diagram of the reaction vessel part of APTAC is shown in Figure 3.4.

The test samples, usually liquid of solid of highly reactive chemicals, are contained in the test cell, and the temperature is recorded by the thermal couple (TC) inserted into the sample. The test cell comes in different materials (glass, titanium, and stainless steel) and sizes (10 ml, 25 ml, 50 ml to 100 ml) depending on the research interest and the hazardous nature of the chemical been tested. In this research, a 25 mL glass cell was adopted for all the test runs, and the liquid chemical or chemical mixtures were loaded up to 9 g.

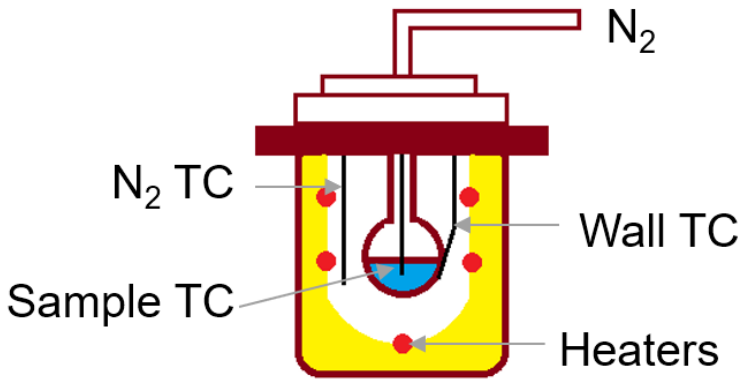

Figure 3.4 A simplified diagram of the APTAC reaction vessel

The sample test cell is connected to the pressure transmitter to record the pressure building up information. It is noticed in the above figure that the sample and the headspace gas coexist during the runaway reaction test. In order to avoid the unwanted side reaction introduced by oxygen and other reactive gases, the sample was purged with nitrogen under the protection of an ice bath for 30 min before the test. When the test sample cell was loaded and connected to the gas stream, three pressurizing-depressurizing cycles using nitrogen were performed to further eliminate the trace oxygen left in the pipelines.

During the thermal runaway test, the samples and the surrounding nitrogen filled in the outside chamber were heated up by the heaters located on the bottom, top, side of the chamber, and also the tube heater connected directly to the test cell. A sophisticated control program monitored the temperature difference between the sample TC, wall TC, and nitrogen TC and kept the temperature difference as small as possible to obtain a near-adiabatic system. The pressure was also balanced in and out of the test cell to prevent cell rupture.

APTAC can be operated under various heating modes, including the heat-wait-search (HWS) mode, the constant temperature ramping mode, and the isothermal mode. In this research, the HWS mode was applied to all the samples tested in APTAC.

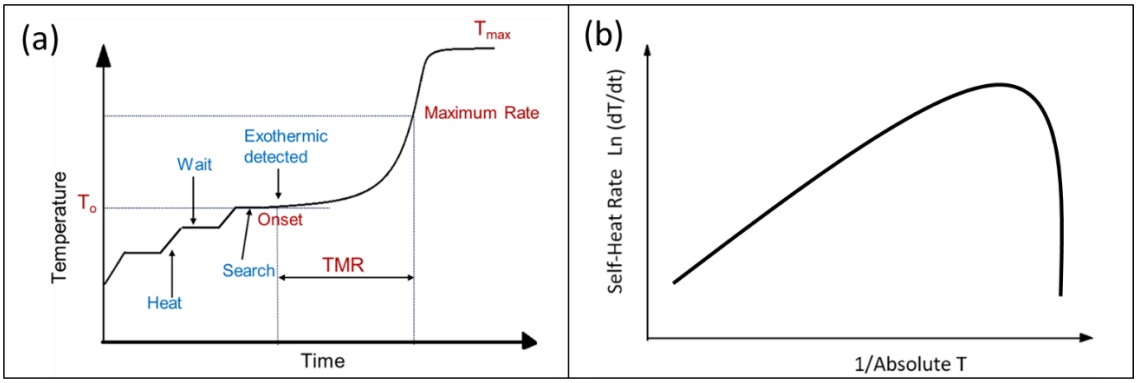

Figure 3.5 Thermal hazard curve during a heat-wait-search test in APTAC: (a) temperature vs. time trajectory, (b) self-heating curve vs. reciprocal of absolute temperature

Figure 3.5 illustrates the temperature trajectory (a) and the self-heating rate curve (b) of the sample during an HWS test in APTAC. After the sample was purified, purged, and sealed in the test cell, the sample was heated up by a small temperature increment of around 5 °C at a slow speed of 1 °C/min. Then the temperature was kept constant for 30 min (wait) to search for exothermic activities. The criterion for the self-sustaining exothermic activity used in this research was 0.1 °C/min. If no exothermic signal was detected that exceeded the criteria, the next round of heat-wait-search cycle would be performed. When an exotherm was identified to release heat greater than 0.1 °C/min, the APTAC entered adiabatic operation mode that the heaters were controlled to only compensate the heat loss and maintain adiabaticity without adding any extra heat. The temperature and pressure of the test sample were recorded until the end of the exotherm. Several critical thermal hazard indicators obtained in the APTAC test were listed below:

1) T_0, the onset temperature of the exothermic reaction when the heat release rate exceeds the 0.1 °C/min criterion. In Figure 3.5(a), it was identified as the intercept between

the baseline during the waiting period and the extrapolated exothermic peak. This temperature was identical to the onset temperature obtained from the self-heating rate curve.

2) $T_{\max}$, the maximum temperature obtained at the end of the adiabatic reaction, also known as the final temperature of the reaction T_f.

3) *dT/dt*, the self-heating rate of the reaction, which is calculated by taking the derivative of sample temperature with respect to time. The self-heating rate denotes how fast the heat is released during the self-sustaining exothermic reaction. It is usually plotted in a semi-log scale figure regarding the reciprocal of the absolute temperature (1/T), as shown in Figure 3.5(b). The peak value of the self-heating rate is known as the maximum self-heating rate $(dT/dt)_{\max}$.

4) Pressure, maximum pressure, pressure-rising rate *dP/dt*, and the maximum pressure rising rate $(dP/dt)_{\max}$. These values represent the pressure building up inside the test cell as well as the pressure building-up rate.

5) TMR, the time to the maximum rate. It is defined as the time needed to reach the maximum reaction rate and is commonly used to assess the severity of the runaway reaction, as proposed by Stoessel.[95] A reaction with shorter TMR has a higher potential to result in an uncontrolled runaway incident as less time is left for responding and containing the initiating events.

The experiment data obtained from the APTAC test need to be further processed to calculate other crucial thermal hazard indicators and kinetic parameters. As can be noticed in Figure 3.4 that during the adiabatic runaway reaction test in APTAC, the

surrounding heaters minimize the temperature difference between the sample TC and the wall TC. In other words, the adiabatic system includes both the sample and the sample cell. As a result, during the adiabatic reaction regime, part of the heat generated by the reactants are used to elevate the temperature of the test cell. Thus, the measured heat underestimates the real thermal hazard and is usually corrected by the thermal inertia factor φ, as shown in Equation (11). In this expression, m_{c} stands for the mass of the test cell; m_{s} is the mass of the sample contained in the cell; $C_{\mathrm{p,c}}$ is the heat capacity of the cell, and $C_{\mathrm{p,s}}$ is the heat capacity of the sample.

$$\varphi = 1 + \frac{m_{\mathrm{c}} \times C_{\mathrm{p,c}}}{m_{\mathrm{s}} \times C_{\mathrm{p,s}}} \tag{11}$$

The heat capacity of the cell and test sample changes with temperature and is usually empirically related to the absolute temperature using a polynomial type expression as shown in Equation (12), where $C_0 - C_3$, and the power m and n are coefficients documented by other researchers by fitting the experimental data to the equation. The coefficients used in this research were taken from Leung[56] for styrene and ethylbenzene. For the glass test cell, the data of fused silica from Schick[96] were used. For polystyrene produced during the reaction, the heat capacity data from Aras[97] were adopted, assuming the molecular weight is around 11000 g/mol.

$$C_{\mathrm{p}} = C_0 + C_1 T + C_2 T^m + C_3 T^n \tag{12}$$

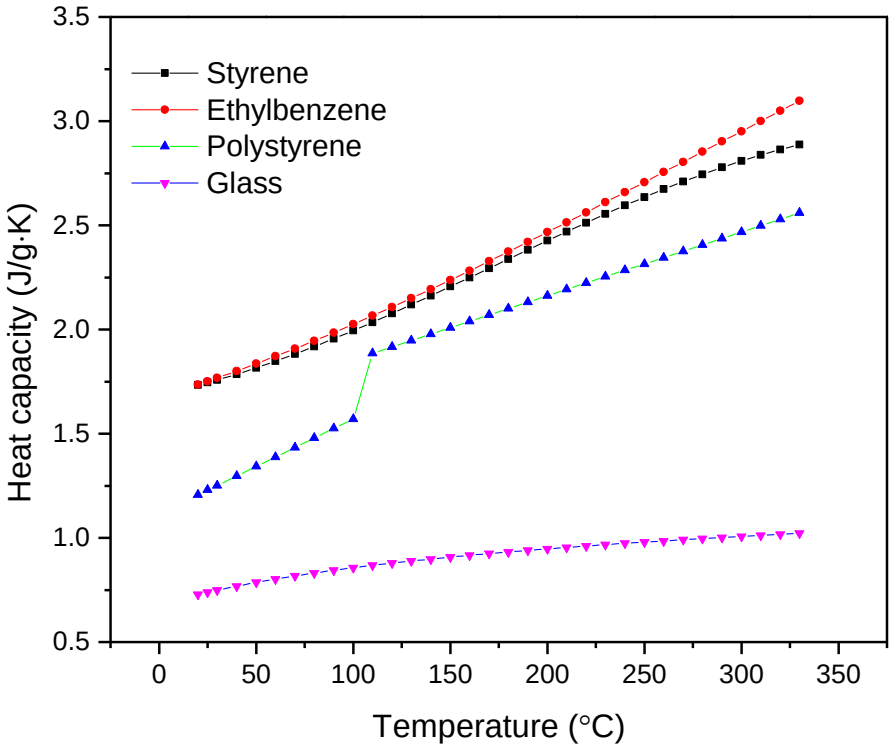

Figure 3.6 Heat capacity of the test cell and reactants

The heat capacity of all components in the system are plotted in Figure 3.6 regarding the temperature. It is noticed that for the cell and various species present in the sample, heat capacity monotonically increased with temperature. Styrene and ethylbenzene had very similar heat capacity, especially below 250 °C. The polystyrene had a glass transition at around 100 °C, resulting in a step-change in heat capacity. During our calculation, an approximation was made to average the heat capacity during the temperature range between the onset temperature T_0 and the final temperature T_f. The thermal inertia factor was calculated according to Equation (11) using the averaged heat capacity of the test cell and samples.

The ΔT_{ad}, the adiabatic temperature rise of the reaction was calculated following Equation (13) as the difference between the final temperature T_f (or $T_{\max}$) and T_0 corrected by the thermal inertia factor φ. This value is a reasonable estimate on the temperature increase during the thermal runaway reaction for a real reaction vessel. The large-scale processing vessels usually have a high volume-surface area ratio that the phi factor approaches one[98]. In an adiabatic calorimetric experiment, it is essential to use a larger sample size to minimize the thermal inertia factor.

$$\Delta T_{\mathrm{ad}} = \varphi \times (T_f - T_0) \tag{13}$$

The heat of polymerization ΔH was calculated by multiplying the averaged heat capacity by the adiabatic temperature rise ΔT_{ad}, as shown in Equation (14), to indicate how much heat was released from the exothermic reaction if no heat loss to the environment.

$$\Delta H = \Delta T_{\mathrm{ad}} \times C_{\mathrm{p,s}} \tag{14}$$

The data acquired in the APTAC test can be further processed to obtain critical kinetic parameters. A well-known kinetic model was developed by Townsend and Tou[99, 100] to determine the activation energy and the overall reaction rate based on the self-heating rate. The method assumes the reaction follows *n*th-order reaction rate law, and the overall rate constant is expressed in Equation (15) and Equation (16), where C is the concentration of the reactant, k is the rate constant, and E_a is the activation energy of the reaction.

$$\frac{dC}{dt} = -kC^n \tag{15}$$

$$k = A \cdot \exp(-\frac{E_a}{RT}) \tag{16}$$

Assuming the heat capacity is constant during the reaction, then the conversion α of the reactant is proportional to the heat released, as shown in Equation (17). C_0 is the initial concentration of the reactant.

$$\alpha = \frac{T - T_0}{\Delta T_{\mathrm{ad}}} = 1 - \frac{C}{C_0} \tag{17}$$

Differentiate the temperature with respect to time would result in the self-heating rate, as expressed in Equation (18):

$$\frac{dT}{dt} = kC_0^{n-1}\left[\frac{T_f - T}{\Delta T_{\mathrm{ad}}}\right]^n \Delta T_{\mathrm{ad}} \tag{18}$$

For a pseudo-first-order reaction, rearranging Equation (18) yields to Equation (19). By further substituting the rate constant *k* with the Arrhenius expression shown in Equation (16), the initial self-heat rate can be related to the kinetic parameters, as shown in Equation (20). Plotting the self-heating rate regarding the reciprocal of the absolute temperature would result in a linear line, and the activation energy of the reaction can be obtained from the slope of this curve.

$$k = \frac{dT}{dt} \cdot \left(\frac{1}{T_f - T}\right) \tag{19}$$

$$\ln\left(\frac{dT}{dt}\right)_0 = \ln(A \cdot \Delta T_{\mathrm{ad}}) - \frac{E_a}{R}\left(\frac{1}{T}\right) \tag{20}$$

3.3.3. Advanced Reactive System Screening Tool (ARSST)

The Advanced reactive system screening tool (ARSST) developed by Fauske & Associates is another powerful tool to evaluate the near-adiabatic thermal runaway behavior of the reaction system in a fast and cost-effective way.

The runaway reaction can be tested in ARSST up to 700 °C and 500 psig. Similar to APTAC, ARSST utilizes a larger sample size and is capable of tracking both temperature and pressure change during the runaway reaction. The pressure data obtained from ARSST tests were usually used to guide the relief valve sizing to ensure the safe containment of a reaction system.[101] It is a pseudo-adiabatic tool that the heat lost to the environment is compensated by the heat generated by the heating tape. Figure 3.7 gives a simplified schematic diagram of the test chamber of ARSST. A more detailed illustration of the containment vessel and internal settings was well documented by Burelbach.[102]

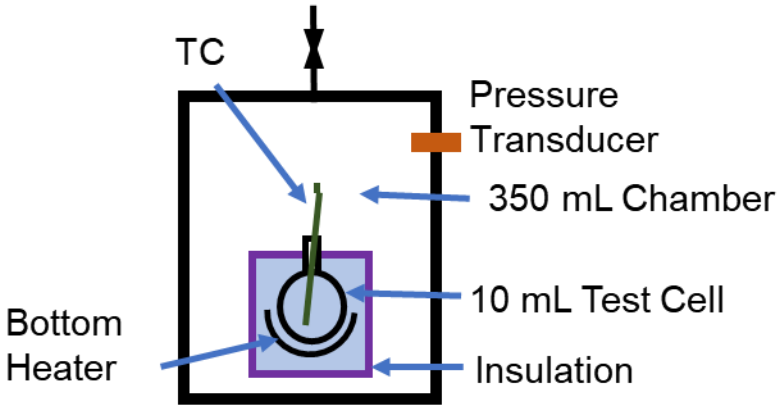

Figure 3.7 The simplified schematic diagram of the ARSST main chamber

In an ARSST experiment, up to 10 g of reactive sample (usually liquid) was loaded into the 10 mL glass test cell, and a thermal couple (TC) was inserted to detect the sample temperature. An electric heating tape was wrapped and firmly attached to the bottom of the test cell as the heating source. The test cell was insulated and placed in a 350 mL test chamber, and the pressure in the larger chamber was recorded by the pressure transducer.

The 10 mL test cell was open to the 350 mL chamber that the pressure building up inside the test cell was "diluted" by the larger space outside of it. If the test sample contains volatile species, the evaporization of the chemical upon heating will result in a loss of active component in the test cell. To prevent the sample loss and contain the reactant in the test cell, a nitrogen pressure pad at around 300 psig was applied to increase the initial system pressure before heating. Similar to the APTAC test, several pressurize-depressurize cycles were conducted to eliminate the oxygen in the test chamber. The sample was also purged with nitrogen for 30 min under the protection of an ice bath to rule out the retardation effect of dissolved oxygen.

Both isothermal heating and constant ramp heating are available in the ARSST test to heat the sample. In this research, the constant heating ramp was used to increase sample temperature at a constant speed of around 0.25 °C/min to 3 °C/min. A polynomial control program was calibrated using an inert organic solvent (pentadecane) to obtain the desire heating power curve. Details of heating power calibration can be found in Wen's work.[103] The shutdown criteria of temperature and pressure were 420 °C and 400 psig, respectively.

Similar to the APTAC test, the adiabaticity correction (phi factor) was made to the data obtained to compensate for the heat loss to the test cell. Safety indicators obtained in an ARSST test include T_0, $T_{\max}$, *dT/dt,* $(dT/dt)_{\max}$, *dP/dt,* $(dP/dt)_{\max}$, TMR, and kinetic parameter E_a. It is important to address that there are different ways regarding defining the onset of exothermic temperature T_0 for an ARSST test. Figure 3.8 shows the typical temperature rising and the self-heating curve obtained form an ARSST test. From the temperature-time curve, the intercept of the constant temperature ramping period and the

first exothermic peak is defined as the onset point A, as shown in Figure 3.8(a). The onset point B obtained from the self-heating curve shown in Figure 3.8(b) is a more direct indicator of when the exothermic reaction starts. In this work, the onset point of all ARSST tests was defined by the latter method.

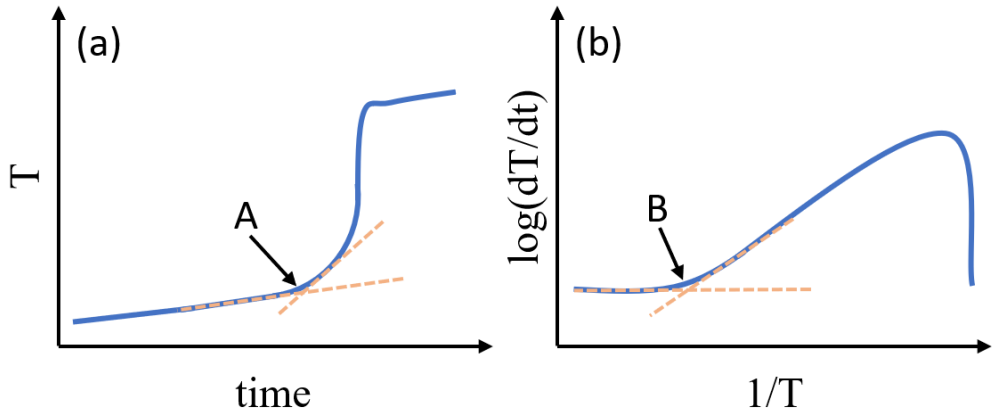

Figure 3.8 Onset temperature determination in ARSST test: (a) based on temperature rise, (b) based on self-heating rat**e**

3.4. Materials and Procedures

3.4.1. Chemicals

The chemical species used in this research and corresponding specifications are listed in Table 3.3. The styrene contained 15 ppm of 4-tert-butylcatechol (TBC) as an inhibitor and was purified before the runaway reaction test. Deionized water (DI) was used in the preparation of purified styrene. The purified sample was used immediately after the purification and nitrogen purging. All the other reagents were used without further

purification. An explosion-proof refrigerator operated at 4 ºC was used to store the monomers and initiators to avoid the slow self-reaction of these chemicals.

Table 3.3 List of chemicals used in the experiment

Chemical	CAS NO.	Formulation	Grade	Supplier
Ethylbenzene	100-41-4	C_8H_{10}	ReagentPlus, 99%	Sigma-Aldrich
Styrene, stabilized	100-42-5	C_8H_8	ReagentPlus, 99%	Sigma-Aldrich
Sodium sulfate, anhydrous	7757-82-6	Na_2SO_4	ACS reagent, ≥99.0%	Sigma-Aldrich
Inhibitor remover	1344-28-1	Al_2O_3	N/A	Sigma-Aldrich
Sodium hydroxide	1310-73-2	NaOH	Reagent, >98%	Sigma-Aldrich
Benzoyl peroxide	94-36-0	$C_{14}H_{10}O_4$	ReagentPlus, 99%	Sigma-Aldrich
2,2'-Azobis (2-methylpropionitrile	78-67-1	$C_8H_{12}N_4$	ReagentPlus, 99%	Sigma-Aldrich
Sulfuric acid	7664-93-9	H_2SO_4	ACS reagent, 95.0-98.0%	Sigma-Aldrich

Table 3.3 Continued

Chemical	CAS NO.	Formulation	Grade	Supplier
Methanol	67-56-1	CH_4O	ReagentPlus, 99%	Sigma-Aldrich
Sulfuric acid, 5N Solution	7664-93-9 7732-18-5	H_2O H_2SO_4	Reagent	Fisher Chemical
Sodium hydroxide, 5N Solution	1310-73-2 7732-18-5	H_2O NaOH	Reagent	Fisher Chemical

3.4.2. Calorimetric Test Procedures

Before each calorimetric test, the monomer styrene was purified to remove the inhibitor and rule out the retardation effect. Details of these purification methods and their effects on the thermal runaway behavior will be discussed in the next chapter.

After purification, styrene was mixed with other species and transfer into a 25 mL round flask. The flask was merged in an ice bath to maintain the sample temperature below 4 ºC. A needle head was then inserted below the surface of the sample, and nitrogen was bubbled into the sample for 30 min to eliminate the dissolved oxygen. All weight measurements and calorimeter tests were repeated three times to ensure the reproducibility of the data.

In a DSC test, around 5 mg of the reactive sample containing styrene and other species (solvent, initiator, contaminant) was loaded into the high-pressure sample pan. The pan was covered by a gold-plated seal and screwed tightly with the stainless-steel cap. An

empty stainless-steel capsule with a golden seal containing air was used as the reference for all tests. The two capsules were heated up at the desired rate (between 1−8 °C/min) from room temperature to the end of the exothermic reaction (~300 °C). The heat flow change regarding heating time, and the temperature was recorded in watt. This signal was then normalized by the mass of the sample to obtain the specific heat flow of the sample in mW/g. Integrating the specific heat flow regarding time resulted in the overall heat release during the reaction. For the polymerization system, the sample was rescanned after the cooling, and the signal from the second heating cycle was used as the baseline of integration.

For an APTAC test, the test sample was purified using the same procedure as the DSC test. After that, around 10 g of the sample was loaded into the 25 mL glass test-cell. In order to eliminate the dissolved oxygen, the sample was purged with nitrogen for 30 min in an ice bath before being tested. Styrene polymerization generates only condensable gases and has been identified as the *Vapor System* by the Center for Chemical Process Safety (CCPS) regarding relief valve design[104]. To suppress the boiling of the sample and minimalize the tempering effects brought by the reflux of the volatile components, the APTAC cell, together with the contained reactant, was pressurized with nitrogen to around 1000 kPa (147 psig) before heating. A heat-wait-search operating mode was applied with temperature steps of 5 °C, with a heating rate of 5 °C/min, and a 30 min waiting period followed between temperature steps. APTAC entered adiabatic mode once the self-heating rate exceeded the exothermic threshold of 0.1 °C/min. A polytetrafluoroethylene (PTFE) coated magnetic stir bar was used to mix the sample at 300 RPM throughout the

experiment. Temperature and pressure, as well as the rate of self-heating and pressure-rise, was measured and recorded throughout the experiment. The data were corrected by the thermal inertial factor, and the kinetic parameters were calculated.

The ARSST test followed the same procedure as the APTAC test to purify and purge the sample before testing. The reaction mixture containing styrene and contaminants (around 5 g) was then loaded into a 10 ml glass test cell where the open-cup cell was contained in the 350 mL containment vessel. The containment vessel was purged with nitrogen for several times and pressurized to around 300 psig before conducting heating. The mixture was heated up using a single ramp-polynomial control program from room temperature to the end of the exothermic reaction. The heating rate of pure styrene samples kept constant between 3−4 °C/min. For the styrene/contaminant system, the mixture samples experienced slightly different heating rates due to the variation in mixture heat capacity. The magnetic stirring was performed for all tests at a fixed speed of 300 RPM to enhance the mass transfer between styrene and the immiscible contaminants. The temperature of the mixture was recorded and used to calculate the thermal characteristics and kinetic parameters.

The ARSST was also used to perform injection experiments to understand the instantaneous contamination effect between styrene and the concentrated sulfuric acid. Styrene was first loaded into the test cell and heated up to 30 °C under ambient pressure. A small amount of concentrated sulfuric acid was then injected into the cell under the protection of nitrogen at different mixing conditions. The temperature rise during the reaction was recorded by the thermal couple.

4. THERMAL HAZARD ANALYSIS OF THE PURE STYRENE SYSTEM

The very first step of this research was to obtain the thermal runaway hazard data of the styrene monomer as the basis for the hazard evaluation of the polymerization system. There were two critical steps to obtain accurate data and maintain data repeatability. First of all, as mentioned in the previous sections, the styrene monomer purchased usually contains a ppm level inhibitor to increase the shelf-life and stop self-reaction. Removing the inhibitor and ruling out the retardation effect was the pre-requisite of the accurate and conservative thermal hazard data. Next, for the adiabatic calorimeter tests, proper phi factor correction must be made to maintain a good adiabaticity of the test system to mimic the reaction that happened in real vessels.

In this section, two different inhibitor removal methods were applied to remove the inhibitor. Their effect on the thermal hazard of styrene thermal polymerization was compared in both screening calorimeter DSC and adiabatic calorimeter APTAC. Experiments were also carried out to locate the optimum test sample mass in APTAC to minimize the thermal inertia factor.

4.1. Comparison of Two Inhibitor Removal Methods

4.1.1. Inhibitor Removal Mechanism

The inhibitor presents in the styrene monomer is 4-tert-butylcatechol (TBC), which is an antioxidant and usually added at up to 15 ppm. There many different ways to remove the TBC from styrene as summarized by Matsas:[105]

(1) Distillation;

(2) Liquid-liquid extraction (caustic wash);

(3) Adsorption.

Distillation under vacuum usually consumes a large quantity of energy as the absolute concentration of the inhibitor is at ppm level and is not favored in the industrial production process. Many researchers have used caustic chemicals; usually, sodium hydroxide solution, to wash the styrene and eliminate the inhibitor.[106-108] However, Matsas argued that the liquid-liquid extraction was not effective enough when inhibitor concentration was low. The working mechanism of the caustic wash was explained by Loss,[109] and an illustration of the reaction is given in Figure 4.1(a).

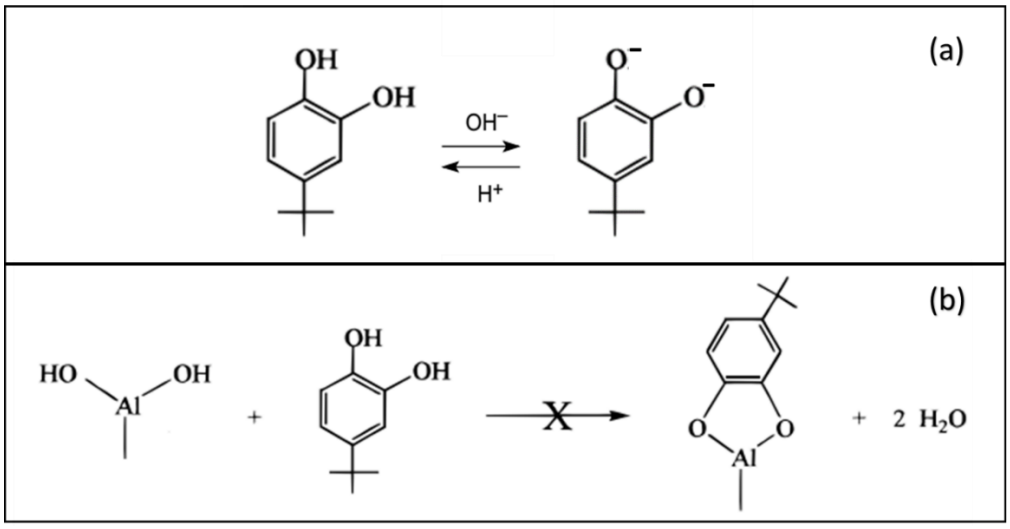

Figure 4.1 The mechanism of two inhibitor removal methods: (a) caustic wash, (b) adsorption

As a weak acid, TBC reversibly dissociates in caustic medium and can associate when the pH value is low. The water-solubility of the dissociated TBC is significantly higher than the associated form that the compound can be extracted to the water phase when a caustic solution is used, and the concentration of the associated TBC is reduced in the oil-phase styrene.The most important inhibitor removal method is the adsorption process of styrene on the surface of inorganic oxides. The working mechanism is the reaction between the hydroxyl group in TBC and the weak acid sites carried by the aluminum oxide. One possible reaction scheme is illustrated in Figure 4.1(b), according to Nedez.[110] More discussion on the adsorption mechanism was documented by Diaz[111] and Rivero.[112] This adsorption process is usually realized by passing the styrene through a packed column at a temperature below 10 °C, during which process the water is adsorbed and removed simultaneously as a by-product. It is critical to maintain a low-temperature operation of the adsorption, as the process is spontaneous and exothermic.

4.1.2. Inhibitor Removal Experiment

In this research, the caustic wash and aluminum oxide adsorption were carried out to remove TBC from styrene.

For the caustic wash, 10 g of 10% (wt) sodium hydroxide solution was mixed with 20 g inhibited styrene and mixed vigorously in a separation funnel. A color change was noticed immediately after the extraction reaction, as shown in Figure 4.2(a). The participation of the dissociated TBC resulted in a different color in the two-phase system. The upper oil phase had a yellowish color, while the water phase on the bottom showed a pink color. The water phase was separated, and the caustic solution was added again until

the water phase became colorless. DI wash was then carried out for several times to remove the sodium hydroxide until the pH of the water phase reached 7. After the water phase was drained from the system, anhydrous sodium sulfate powder was added to the purified styrene to further remove the trace moisture in the organic phase under the protection of an ice bath. Finally, the purified monomer was filtered using a 0.45 μm syringe filter to remove the sodium sulfate particles. The purified product from the caustic wash still showed a light yellow color.

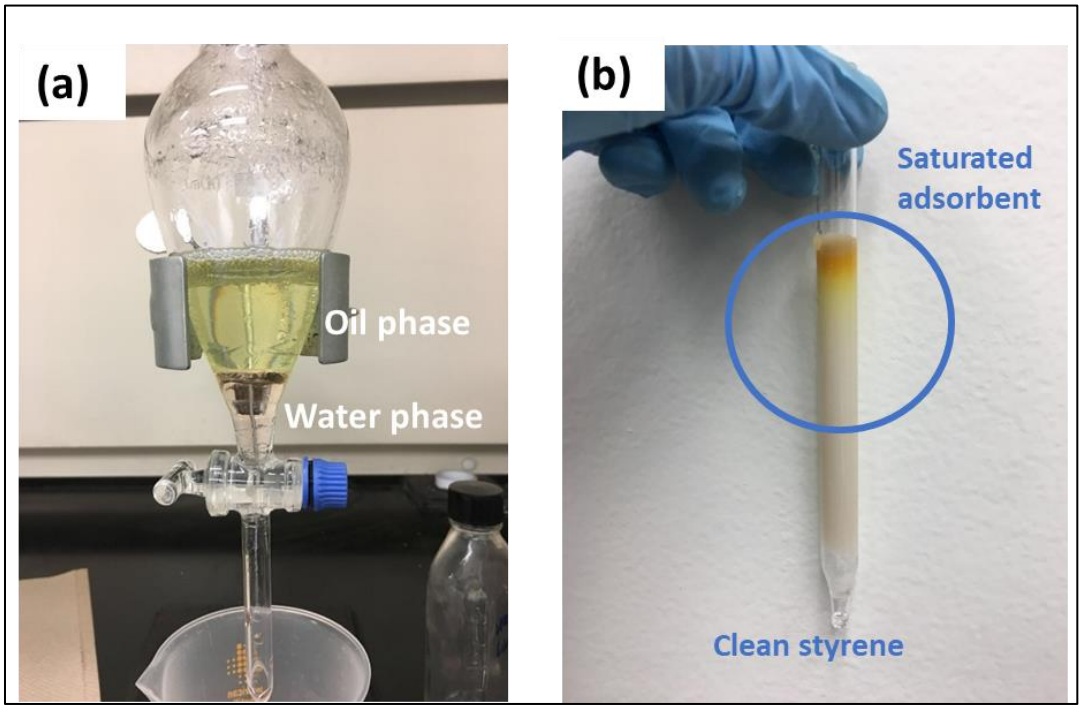

Figure 4.2 The digital photographs of the two inhibitor removal methods: (a) caustic wash and the phase separation, (b) adsorption over aluminum oxide

The adsorption process to remove the TBC in styrene is illustrated in Figure 4.2(b). Activated aluminum oxide particles are commercially available from Sigma-Aldrich, and the particles were densely packed into a glass column (10 mm O.D.). The inhibited styrene was drop-wisely added into the column. The purified product was collected at the bottom under the protection of an ice bath. As denoted in the previous section that aluminum oxide was capable of removing the inhibitor and the by-product water at the same time; thus, no further drying process was carried out for styrene obtained in this method. The aluminum oxide purified styrene was colorless.

4.1.3. Comparison of Inhibitor Removal Results in Calorimeter

DSC test was carried out on the inhibited styrene (as-is sample from Sigma-Aldrich) and styrene samples purified with both caustic wash and adsorption methods. The specific heat flow curve during the thermal polymerization is shown in Figure 4.3, and the safety indicators are summarised in Table 4.1. As can be seen in Figure 4.3, three exothermic peaks were displayed for all three cases. However, the time of their appearance and the heat flow generated is significantly different. For TBC inhibited styrene, the first exothermic peak was detected to be around 150 °C, followed by a higher peak (the maximum heat release peak) at 205 °C and an almost invisible one at around 250 °C. This multi-peak exothermic curve denoted a complex reaction pathway of thermal polymerization of styrene and had been observed in many other studies.[55, 99] Liao[36] reported similar peak behavior for TBC inhibited styrene and performed kinetic modeling on each peak. It was identified that the first peak was typical of an autocatalytic behavior while the second peak was an n^{th} order regarding styrene with reaction order around 1.8−2.

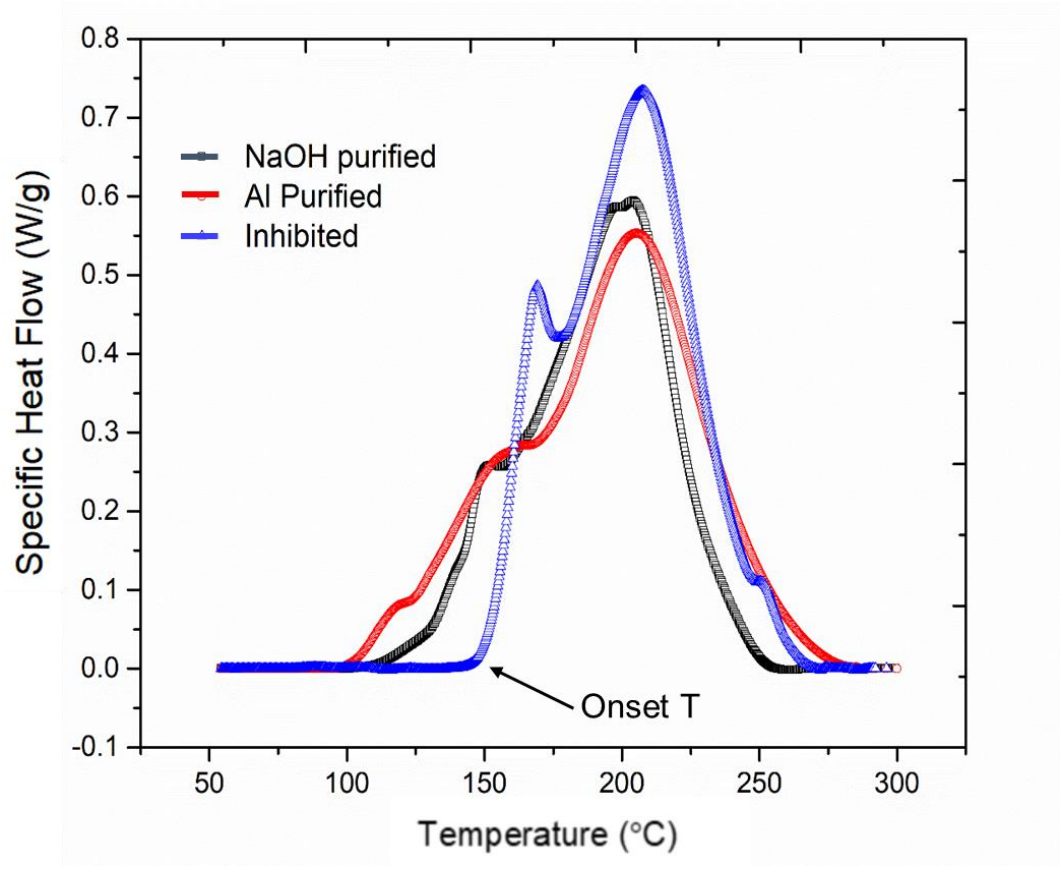

Figure 4.3 The comparison of inhibited and inhibitor-free styrene in DSC

Table 4.1 DSC comparison between different purification methods

Styrene sample	T_0 **(°C)**	ΔH **(J/g)**	T_p **(°C)**
TBC inhibited	149 (±4)	646 (±9)	205 (±3)
NaOH Purified	116 (±2)	601 (±17)	204 (±0.5)
Alumina Purified	101 (±1)	629 (±21)	205 (±0.1)

The purification of TBC using caustic wash showed a significant change in the thermal behavior in DSC, as shown in the same figure denoted in black color. First of all,

the onset of exothermic thermal polymerization was observed at around 116 °C (listed in Table 4.1), which was around 35 °C lower than the inhibited styrene. The inhibitor retarded the reaction by reacting with the primary free radicals thermally produced in the styrene, and thus the reaction was not able to proceed until all the inhibitors in the system were consumed. The DSC test showed a clear promotion effect when TBC was partially removed from the system. The most intensive heat release took place at around 205 °C, and this temperature kept constant regardless of whether TBC was present.

For aluminum oxide purified samples, the DSC curve showed a different thermal profile as three major exothermic peaks appeared at 120 °C, 150 °C, and 205 °C, respectively. As can be seen, the overall heat generation was approximately the same as the inhibited styrene. However, in the case of the aluminum oxide purified monomer, the reaction became notable at a much lower temperature (101 °C) while its rate of heat generation was much slower than that of the inhibited monomer. Also, the temperature range of the exothermic reaction was expanded. It is argued that thermally initiated radicals trigger the polymerization at a much lower temperature, which can be considered as a guiding value for deciding on styrene storage conditions in view of inhibitor depletion. When the TBC or other inhibitors are exhausted over time in a styrene tank, self-reaction may significantly accelerate at around 101 °C.

On the other hand, if unwanted polymerization occurs in an inhibited quantity of styrene, containment of the unwanted reaction may not be possible as the generation of heat will be more intense after 150 °C compared to uninhibited styrene. The maximum heat flow for either sample was detected at 205 °C, and this unaltered characteristic

temperature indicated that 15 ppm of TBC effectively inhibited self-polymerization but only at the early stage. It is plausible that the first peak denotes the primary radical production, where the TBC acts as a radical scavenger and thus delays the polymerization until it is depleted at a higher temperature. The main peak is likely to represent the main polymerization process in the course of which the monomers add up to build the extended polymer chain. The heat of polymerization of styrene obtained from this study was between 629−646 J/g. This number was in good agreement with the previous research for uninhibited styrene summarized in the literature review section.

By comparing the DSC curve and data, it was also noticed that the two removal methods showed different efficiency and had a substantial difference regarding the impact on the runaway behavior of styrene. The experiment observation denoted that after the caustic wash, TBC was not completely removed from styrene and resulted in a light-yellow color. The DSC test further confirmed that not all TBC was properly removed from styrene by caustic wash, as the onset temperature in DSC was around 20 °C higher than the uninhibited sample. The retardation effect remained, but at a lower level. Thus, the traditional caustic wash method could result in misleading information regarding the thermal runaway hazard analysis to styrene and other reactive monomer systems. In the following sections of this research, the adsorption method was used to eliminate TBC from styrene before all experiments.

A comparison of the adiabatic thermal runaway behavior of inhibited and inhibitor-free styrene processed by adsorption was also carried out using APTAC. Around 9 g of samples were used for both sample types, and the same heat-wait-search program

was adopted based on the procedure described in the experimental section. For the inhibitor-free styrene, the sample was purged with nitrogen to remove the dissolved oxygen. For the inhibited styrene, however, the oxygen was not removed before the test. The rationale for this difference in atmospheric control was that TBC is an oxygen-sensitive inhibitor[35, 38, 113]. Removing the dissolved oxygen would result in the deactivation of TBC. Thus, in order to tell the difference between effectively-inhibited styrene and inhibitor-free styrene, the oxygen was not removed from the system to maintain the reactivity of the inhibitor. The calorimeter results are listed in Table 4.2.

Table 4.2 APTAC comparison between inhibited and inhibitor-free styrene

Styrene sample	T_0 **(°C)**	ΔT_{ad} **(°C)**	**TMR (min)**	ΔP **(kPa)**	$(dP/dt)_{max}$ **(kPa/min)**	$(dT/dt)_{max}$ **(°C/min)**
Alumina Purified	106 (±2)	290 (±8)	121 (±6)	1299 (±16)	241 (±25)	58 (±6)
TBC inhibited	121 (±4)	128 (±3)	72 (±9)	993 (±31)	14 (±5)	4 (±2)

The runaway temperature trajectories are summarized in Figure 4.4. In the adiabatic thermal runaway test, an active inhibitor showed a significant effect on the thermally initiated polymerization of styrene. Under the same heat-wait-search ramp, inhibitor-free styrene showed an onset temperature as low as 106 °C, which was 15 °C lower than the inhibited styrene. It is a clear indicator that the thermal polymerization was strongly delayed when the inhibitor was present. At the same time, the corrected adiabatic

temperature-rise ΔT_{ad} was reduced by 260 °C if the inhibitor was not removed. In an adiabatic test, the difference regarding total heat release was more significant when compared to the data acquired from the DSC test. This observation could be explained that different monomer conversion was achieved in these two devices.

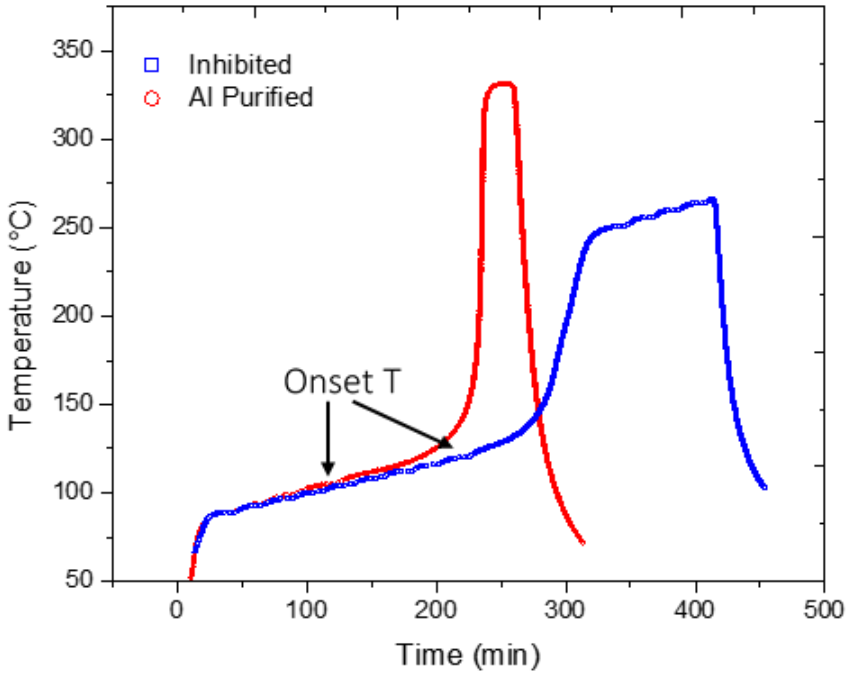

Figure 4.4 The comparison of inhibited and inhibitor-free styrene in APTA**C**

In an adiabatic test, the reaction was self-sustained until the self-heating rate dropped below the criteria (0.1 °C/min) for this case. Thus, when heat dissipation to the cell exceeds the exothermic heat produced by the retarded reaction, the reaction was not able to further develop to higher conversions. A significant reduction in the pressure rate and temperature rate was also observed.

4.2. Phi-Factor Correction of the Adiabatic Data

In the previous chapter, the effect of the inhibitor was ruled out to ensure the runaway polymerization reaction was not retarded in a calorimetric test. Another critical parameter in an APTAC test that would strongly affect the thermal runaway indicators was the thermal inertia factor (φ-factor). As discussed previously, φ-factor is the measure of how much heat is lost to the sample holder, and a value closer to unity would result in a more accurate and conservative value regarding the thermal hazard assessment.

There are different ways to reduce the phi-factor for an APTAC test. For example, using light-weight, thin-wall test cells effectively reduce the overall heat capacity of the sample holder. However, the mechanical strength of the cell would also be compromised and bring difficulties to test the high-pressure system. Increasing the sample mass also results in a decrease in the phi-factor.

Figure 4.5 shows the phi-factor change of a styrene-glass cell system when the styrene sample mass was elevated. The 25 mL glass test cell utilized in this research was not able to contain more than 23 g of styrene, considering the boiling and expansion of the organic compound. The reduction of the phi-factor was a monotonical line that when styrene sample mass was increased from 1 g to around 9 g, the thermal inertia factor quickly dropped. Further addition of styrene resulted in a lowered reduction speed of the phi-factor. The “elbow” of this curve was denoted as the intercept of two tangential dash lines, which was used to indicate the inflection point where the sample mass had a lowered effect on reducing the phi-factor.

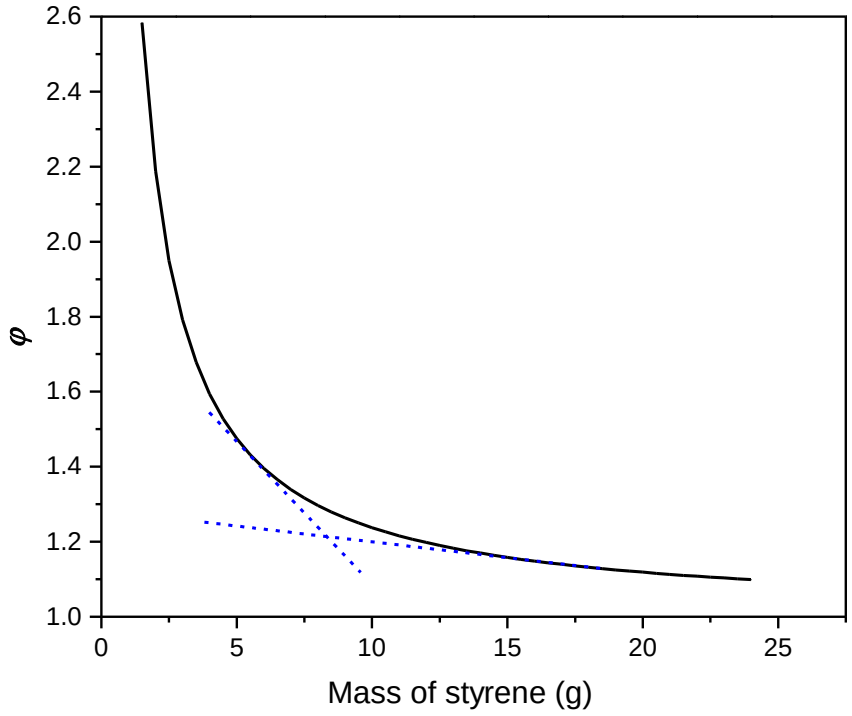

Figure 4.5 The relationship between styrene sample mass and APTAC thermal inertia factor

Another concern that stopped the researcher from using an extremely large sample size was the deterioration of mixing when more reactants were loaded. As mentioned in the experiment section, a magnetic stir bar was used in the APTAC test to ensure good heat and mass transfer in the test cell. Increasing the sample size would result in a less-effective mixing in the test cell and should be avoided. Other concerns regarding using a larger sample were the difficulty in maintaining the maximum pressure of the runaway reaction within the mechanical limit of the test cell.

Table 4.3 The APTAC runaway data of different styrene sample masses

Styrene mass (g)	φ	T_0 (°C)	$T_f - T_0$ (°C)	ΔH (J/g)	$(dT/dt)_{max}$ (°C/min)
2	2.19	108 (±4)	121 (±12)	643 (±36)	4 (±2)
3	1.79	115 (±2)	163 (±7)	715 (±7)	16 (±6)
4	1.59	112 (±2)	191 (±2)	742 (±28)	22 (±1)
5	1.48	108 (±4)	215 (±7)	772 (±9)	36 (±5)
7	1.34	106 (±1)	220 (±13)	718 (±10)	52 (±7)
9	1.26	106 (±2)	228 (±8)	708 (±20)	58 (±6)

Table 4.3 summarizes how the thermal runaway indicators changed when the sample mass of styrene was altered in the APTAC test. The first column was the calculated thermal inertia factor φ. When the sample mass increased from 2 g to 9 g, the ratio of sample heat capacity over system heat capacity also elevated, resulting in less heat loss to the cell and a decrease in the thermal inertia factor. In this research, a minimum φ of around 1.26 was achieved by using 9 g of styrene in the 25 mL glass test cell. The onset of the exothermic reactor was slightly delayed by using less sample size, as more heat dissipated to the test cell, and the higher temperature was required to generate enough heat that exceeded the test threshold of 0.1 °C/min. The second column denoted the difference between the maximum temperature of the runaway reaction and the onset temperature; in other words, the apparent adiabatic temperature-rise if the adiabaticity was not corrected. This value monotonically increased with the styrene sample size. The overall heat release was obtained after the φ-factor correction and listed in the fourth column. As the sample

mass changed from 2 g to 9 g, the heat release measured fell into the same range between 643−772 J/g, which was in good agreement of DSC and other calorimeter test results. It was obvious that the phi-factor correction was essential regarding obtaining uncompromised thermal runaway data. The self-heating rate of the runaway reaction at different sample mass is shown in Figure 4.6.

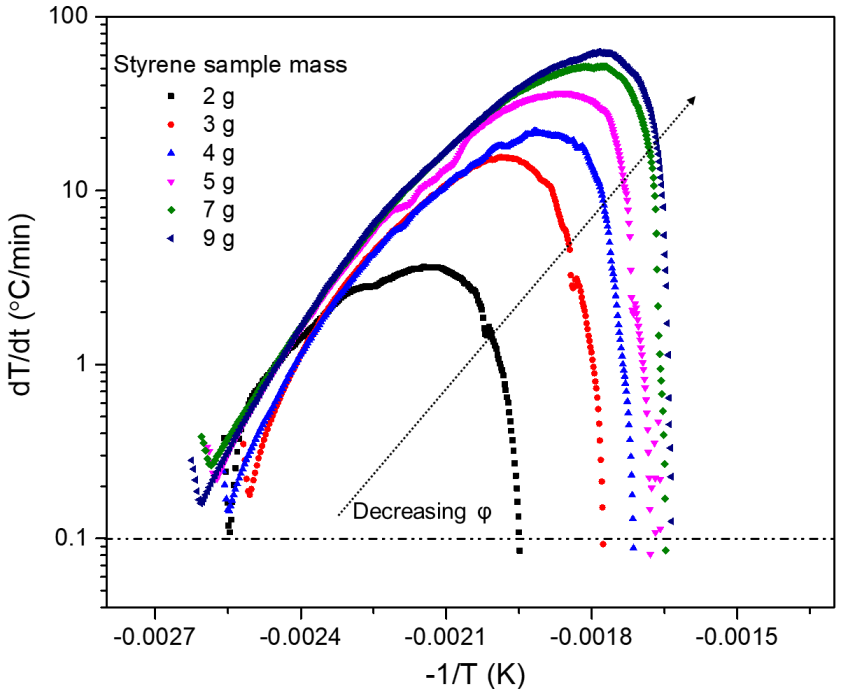

Figure 4.6 The self-heating rate from APTAC test with different styrene sample mass

It was noted in Figure 4.6 that the initial reaction rates obtained from different sample mass kept constant, as the curves almost overlapped below 150 °C. Referring to Equation (20), the logarithm of the initial self-heating can be linearly correlated to the reciprocal of the absolute temperature, and the slope of this curve is determined by the

activation energy of the reaction, which is an intrinsic characteristic value of the chemical. Thus, our observation confirmed that changing the sample size and adiabaticity of the reaction did not affect the initial reaction rate and the kinetic parameters. However, Figure 4.6 also denoted the phi-factor sharply lowered the maximum self-heating rate of the reaction. This observation was rarely discussed in previous literature, and it was speculated to relate to the different vaporization rates in the test cell when the headspace changes under different sample loadings. When the sample mass exceeded 7 g, the maximum self-heating rate showed a minor change. In the following research on all APTAC tests, the sample size of the reactant was kept constant at 9 g.

4.3. Conclusions

In this section, two critical experimental conditions that had a substantial effect on the thermal runaway behavior of styrene polymerization were investigated.

First of all, inhibitor in the commercial styrene was removed by both caustic wash and aluminum oxide adsorption methods, and the impact on the thermal runaway polymerization was compared in DSC and APTAC. The removal of inhibitor with caustic solution involved reversible hydrolysis reaction and significant liquid processing. During this process, the inhibitor TBC was not completely removed, and the trace amount of left inhibitor was still able to retard the reaction by delaying the exothermic onset and lowering the maximum heat release in a DSC ramped heating test. On the contrary, passing the styrene through an aluminum oxide packed column was approved to be an effective inhibitor elimination method if proper temperature control was adopted. Colorless, water-free styrene was obtained cost-effectively and conveniently.

The DSC test results confirmed that uninhibited styrene showed an exothermic reaction started at around 101 °C, and the heat of polymerization was measured to be around 629 J/g. There were multiple exothermic peaks during the heating process of the styrene thermal polymerization, denoting a complex reaction regime with multiple steps. The peak heat rerelease during the runway of thermal polymerization was around 205 °C and was altered by the presence or concentration of the inhibitor. The APTAC test results were carried out to compare the adiabatic runaway behavior of styrene under different inhibition status. With the presence of effective inhibitor (TBC + oxygen), the onset of thermal polymerization was delayed by 15 °C, and all the other thermal runaway indicators including the adiabatic temperature rise, the maximum pressure, the maximum self-heating rate, and the maximum pressure rising rate were significantly lowered. These test results reinforced the importance of proper removal of the inhibitor before any thermal runaway tests.

The effect of thermal inertia factor (φ-factor) on the adiabatic thermal runaway behavior of styrene thermal polymerization was analyzed in APTAC by using different styrene sample mass. The φ-factor monotonically decreased when a larger sample size was utilized. For the styrene-glass cell system used in this research, the φ-factor declined rapidly at a smaller sample size and approached around 1.3 when sample mass was higher than 7 g. The APTAC test results showed a trivial change on the onset threshold of the exothermic reaction when the sample mass was changed. At the same time, by applying the φ-factor correction, the heat release calculated was in good agreement with the value

obtained from the DSC tests. The self-heating rate plot derived from the APTAC test also denoted that the kinetic parameters were not altered by the adiabaticity of the tests.

5. EFFECT OF DILUENT ON THE THERMAL HAZARD OF STYRENE[2]

In the previous chapter, two important test parameters were investigated to lay a solid foundation regarding the accurate assessment of the thermal runaway hazard of a styrene system. The thermally initiated polymerization of styrene was investigated in both screening and adiabatic calorimeters. In this section, the thermal runaway behavior of the styrene-diluent binary system is analyzed using a combination of calorimetric tests and kinetic modeling.

The solution polymerization of styrene using ethylbenzene of the diluent is one of the most important commercial styrene polymerization processes. The diluent or solvent is added into the monomer to control the gel-effect and minimalize heat/mass transfer difficulties. However, the effect of diluent concentration on the thermal runaway polymerization has not been quantified and theoretically investigated from the safety perspective. In this chapter, the thermal runaway hazards of the ethylbenzene-styrene system with different monomer mass fractions were calorimetrically investigated up to temperatures where decomposition products are unlikely to be produced. DSC and APTAC were used to investigate how important safety indicators, including the onset temperature, heat release, pressure building-up change with diluent concentration under constant heating rate or adiabatic conditions. Thermodynamic calculations were carried out to fit the experimental data to different kinetic models. The Townsend model and a

[2] Part of this section is reprinted with permission from "Probing into Styrene Polymerization Runaway Hazards: Effects of the Monomer Mass Fraction" by Lin Zhao, Wen Zhu, Maria I. Papadaki, M. Sam Mannan, and Mustafa Akbulut. *ACS omega*, 4(5), 8136-8145. Copyright 2019 by ACS Publications.

lumped kinetic model developed by Hui & Hamielec were compared using the adiabatic thermal runaway data.

5.1. Thermal Hazard Analysis of the Styrene-Ethylbenzene System in DSC

Ramped-heating DSC scanning tests were conducted for thermal analysis of the styrene-ethylbenzene system with different ethylbenzene mass concentrations. 5 mg of reactant mixture was prepared by mixing the ethylbenzene with purified (inhibitor-free) styrene. The mass ratio of ethylbenzene in samples changed from 0% for pure styrene, to 15% (weight of ethylbenzene to the weight of mixture), 30%, and 45%. Samples were purged by nitrogen to remove dissolved oxygen before heating.

A stainless-steel high-pressure sample capsule was used to contain the reactant mixture. The heating ramp was kept constant at 4 °C/min for all tests during the temperature range from room temperature to 300 °C. The heat flow curved was normalized by both the total weight of the sample and the net weight of the reactive monomer.

The thermal runaway indicators from the DSC tests of the styrene-ethylbenzene system are summarized in Table 5.1. As can be seen from the table, the onset temperature (T_0) obtained from the DSC test was observed at around 100 °C and did not shift upon ethylbenzene addition. Similarly, the maximum exothermic peak temperature (T_p) appeared at approximately 205- 210 °C, and it was marginally, if not at all, affected by the mass of styrene. The normalized heat, however, was substantially affected by the mass fraction of styrene in the solution (the total mixture).

Table 5.1 Dynamic DSC results of styrene-ethylbenzene systems

Styrene mass fraction	T_0 (°C)	ΔH of mixture (J/g)	ΔH of styrene (J/g)	T_p (°C)
100%	101 (±1)	629 (±22)	629 (±22)	205 (±0.06)
85%	100 (±1)	468 (±9)	551 (±9)	209 (±3)
70%	100 (±0.1)	327 (±17)	468 (±17)	212 (±3)
55%	103 (±2)	231 (±24)	434 (±24)	211 (±0.7)

The specific heat flow profiles of the samples are shown in Figure 5.1(a). The total heat of reaction was calculated as described in the experimental section and summarized in Table 5.1 as ΔH of the solution.

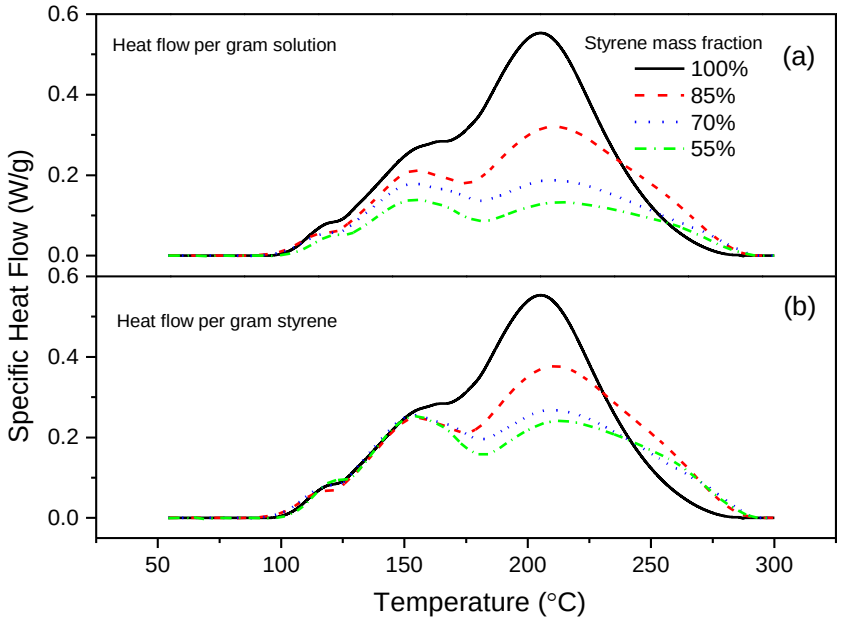

Figure 5.1 DSC results of thermal polymerization of styrene in ethylbenzene with various mass fractions: (a) specific heat flow per gram of solution (b) specific heat flow per gram of styrene

The heat of reaction of the samples was the total heat released by the samples. This value is useful for the calculation of the cooling system for the polymerization. The monotonically decreasing heat release indicated that the addition of solvent significantly reduced the overall thermal hazards. The heat flow was then divided by the styrene mass fraction to produce Figure 5.1(b), and the overall reaction heat of styrene is reported as ΔH of styrene in Table 5.1. Three major exothermic peaks for all polymerization reactions irrespectively of styrene concentrations were obtained. As can be seen in Figure 5.1(b), in all cases, the first two peaks had approximate the same position and area. In other words, the same amount of heat was produced by styrene regardless of ethylbenzene addition up to around 150 °C. This observation led to the hypothesis that the thermally initiated polymerization process of styrene was not affected by the addition of solvent at the initial stage (before around 150 °C). The last exothermic peak shifted from 205 °C to 210 °C as styrene mass fraction in the solution was reduced from 100% to 55%. In addition to that, the respective peak became wider as the solvent increased; the severity of the reaction step was decreased as the specific heat released in each case was declining (smaller peak area) with a lower monomer mass fraction. This is a clear indication that the final peak corresponds to the chain-addition/termination course, a process that has been known to be strongly affected by the gel effect.

The DSC results denoted the decline of the overall reaction heat resulted from the reduced severity of the main exothermic step, as shown in Figure 5.1(b). When the mass fraction of styrene in the test sample was lowered, the collisions between active reactant species were significantly reduced, resulting in a slower chain addition process. At the

same time, in the more diluted solution, the mobility of the polymer chains was increased, which facilitated the termination process, thus resulting in reduced chain length and therefore reduced reaction severity. Therefore, the DSC results confirmed that when the reaction takes place in a dilute solution, it becomes significantly less thermally hazardous due to the reduced heat generated. However, as this is partially owed to the shorter polymer chains production, product quality standards also need to be considered so that the objective of performing the polymerization is not compromised.

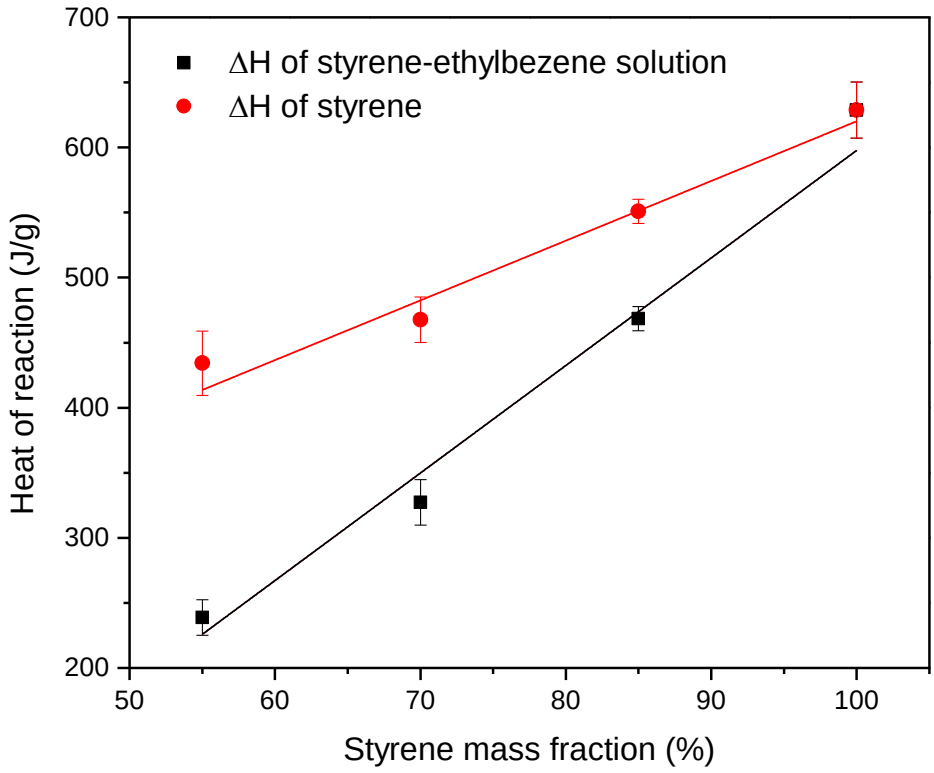

Figure 5.2 The heat of reaction of the styrene-ethylbenzene system measured by DSC

Figure 5.2 illustrates how the exothermic heat release changed with styrene mass fraction using different normalization methodology. Both curves showed a roughly linear relationship regarding the mass fraction of styrene, and when the heat was calculated based on the weight of reactive monomer, the sloped of the fitting line decreased. As explained above, the addition of diluent lowered over the reaction extent by relieving the gel-effect. The reaction heat of the mixture system under other styrene mass concentrations could be obtained from Figure 5.2 by interpolating.

5.2. Thermal Hazard Analysis of the Styrene-Ethylbenzene System in APTAC

The runaway behavior of the above styrene-ethylbenzene mixture samples was also characterized under adiabatic conditions employing one of the best instruments serving such studies. The larger sample size was used in which case the heat and mass transfer effects became more significant, which adequately mimics the real reaction vessels. The results of the respective measurements are summarized in Table 5.2. The corresponding temperature and pressure trajectories are shown in Figure 5.3 and Figure 5.4, respectively. The first column of Table 5.2 represents the onset temperature (T_0) of the adiabatic reaction, which is taken as the temperature when the self-heating rate of the reaction exceeds 0.1 °C/min, and the APTAC enters adiabatic mode from heat-wait-search mode. The apparent adiabatic temperature rise was calculated as the difference between the maximum temperature at the end of the exothermic process and the onset temperature. This number was multiplied by the φ factor to obtain the true adiabatic temperature rise (ΔT_{ad}) as shown in the second column. The time-to-maximum rate (*TMR*) is the time needed for the runaway reaction to reach its maximum self-heating rate. The maximum

pressure increase (ΔP) was calculated by subtracting the initial value of the adiabatic pressure from the peak pressure. The last two columns of Table 5.2 display the maximum pressure-rise rate (dP/dt_{max}) and maximum self-heating rate (dT/dt_{max}) during the adiabatic reaction.

Table 5.2 Thermokinetic data of the styrene-ethylbenzene system from APTAC

Styrene fraction (%)	T_0 **(°C)**	ΔT_{ad} **(°C)**	***TMR*** **(min)**	ΔP **(kPa)**	$(dP/dt)_{max}$ **(kPa/min)**	$(dT/dt)_{max}$ **(°C/min)**
100	106 (±2)	290 (±8)	121 (±6)	1299 (±16)	241 (±25)	58 (±6)
85	109 (±0.5)	238 (±3)	134 (±7)	1403 (±24)	78 (±2)	10 (±0.1)
70	117 (±0.1)	177 (±5)	145 (±1)	1254 (±56)	21 (±2)	2 (±0.1)
55	126 (±4)	104 (±4)	181 (±10)	822 (±33)	3 (±0.3)	0.6 (±0.02)

The data during the heat-wait-search period was omitted in Figure 5.3 and Figure 5.4, and the time in these two figures was normalized by setting the onset time at 0 min. For a pure styrene system, the detected adiabatic onset temperature was 106 °C, denoting the polymerization reaction started to have a self-heating rate higher than 0.1 °C/min at this temperature. Soon after the onset, a steep increase in temperature was observed starting at 100 min of the reaction, resulting in a temperature increment of 200 °C within 15 min. Such rapid, explosive-like reaction behavior indicates the severity of uncontrolled thermal polymerization of pure styrene. Correspondingly, the pressure inside the test cell increased by 1300 kPa (189 psi), indicating how severe threat to process vessels and relief

valves a runaway can pose. These data also explain why it is a common practice in the industry to avoid using 100% pure styrene for polymer production. The maximum temperature obtained was about 20 °C below the decomposition onset temperature of polystyrene in nitrogen, as obtained by Peterson,[114] indicating that no decomposition was initiated by the runaway reaction.

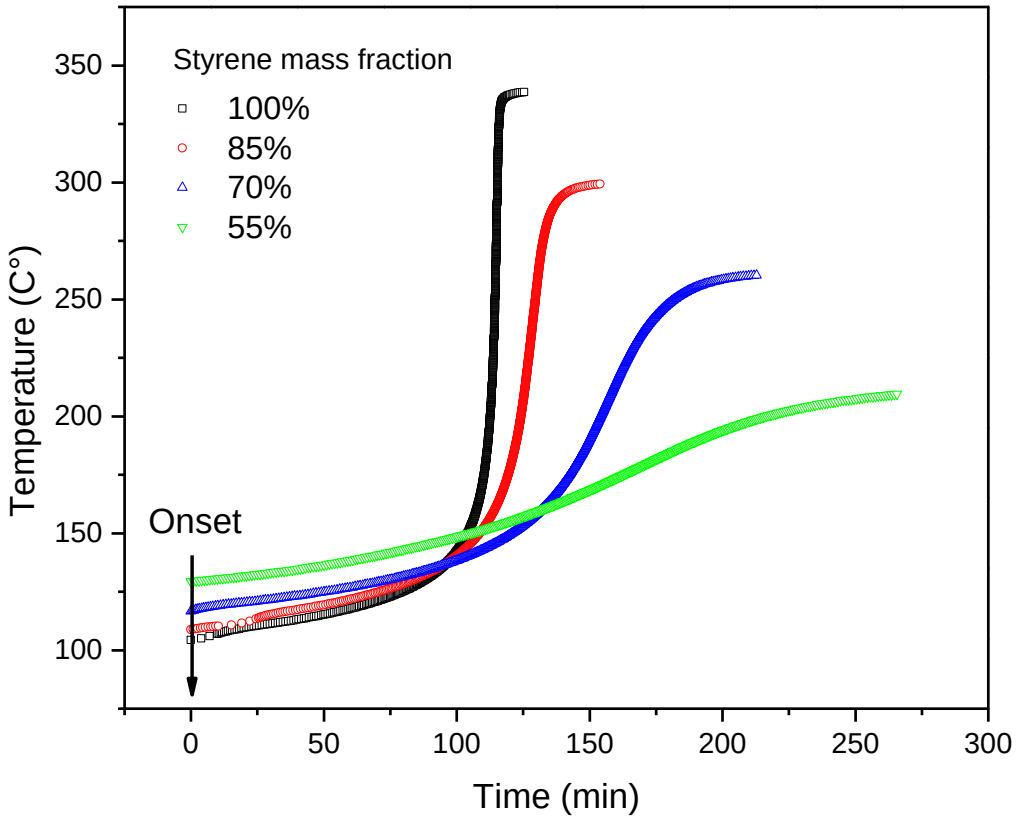

Figure 5.3 The adiabatic temperature rises during the adiabatic runaway reaction of styrene-ethylbenzene systems at various styrene mass fractions

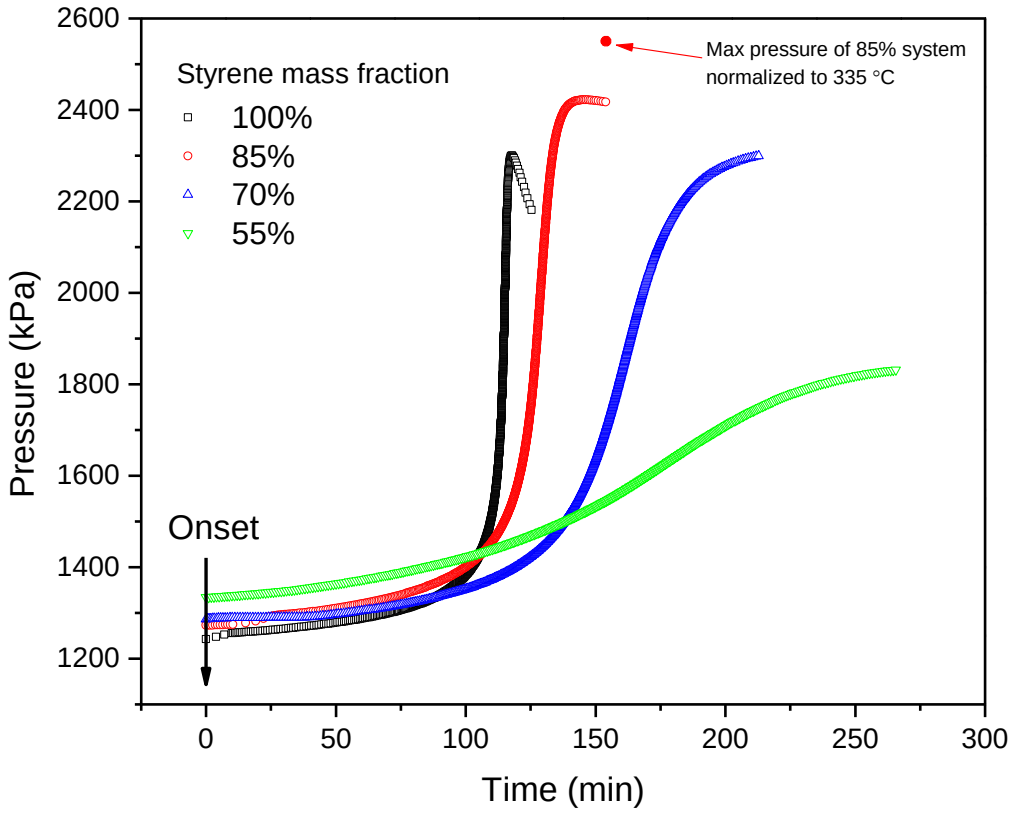

Figure 5.4 The adiabatic pressure rises during the adiabatic runaway reaction of styrene-ethylbenzene systems at various styrene mass fractions

From the temperature data, it is clear that as monomer mass fraction decreased, heat generated by the reaction dissipated to the solvent, and a significant delay and mitigation of thermal polymerization was observed. The adiabatic onset temperature increased to 126 °C for 55% styrene. It is a clear indication that the solvent will delay a potential runaway such that the same self-heating rate was achieved at a much higher temperature for diluted samples. Additionally, the adiabatic temperature rise dropped from 290 °C to 104 °C, which was almost 1/3 of the value for pure styrene when the mass

fraction was reduced to 55%. Unsurprisingly, the time for the reaction to reach its summit increased as styrene mass fraction dropped. For all samples, the main exothermic activity was observed after 100 min. For pure styrene, it took only 121 min for the adiabatic reaction to reach its maximum speed. As the mass content dropped, a longer time was required for the polymerization to develop fully, and the TMR prolonged. The 55% styrene-ethylbenzene system took almost 3 hours to reach its maximum heat release rate. It is clear that the pure styrene system brings difficulties to hazard mitigation or emergency responding, and adding solvents is a practical solution to mitigate sudden temperature increase. In the case of a loss-of-cooling scenario, systems with longer TMR have a lower risk of catastrophic consequences as more time is available to respond and implement mitigation measures.

However, the effect of styrene concentration on pressure change was not as straightforward as the temperature. All experiments had approximately the same initial pad pressure of 1000 kPa (147 psi), but their onset temperatures were different, leading to a slight variation on the initial pressure at the onset point. The peak pressure and pressure difference did not change monotonically with mass content. When styrene was diluted from 100% to 85%, a higher pressure building-up was observed. The pressure changes then declined upon further ethylbenzene addition. As there was no non-condensable gas production during this reaction, the pressure increases primarily consisted of two parts: 1) The vapor pressure of volatile components, which is also a function of temperature; 2) The expansion of pad gas at higher temperature practically obeying the gas law. For the polymer mixture system, the former one was also affected by the polymers produced.

According to Flory's free volume theory[115], the vapor pressure of polymer itself is usually omitted, but the polymer chains had significant effects on the activity of solvent and monomer, leading to a change of vapor pressure of these volatile species. In this study, the pure styrene system had the highest temperature increase, leading to a higher expansion of the nitrogen pad. At the same time, as no solvent was present, monomers reacted to form a non-volatile polymer, which contributed very little to the total pressure. The pressure trajectory denoted that the system pressure reached its maximum before the end of the adiabatic reaction, and gradually decreased afterward. Similar pressure behavior was also observed by Gibson[53] in the Dewar bottle and Tou[52] in Accelerating Rate Calorimeter (ARC), where the maximum pressure during the runaway reaction of styrene was significantly higher than the final pressure. The experimental data reinforced the speculation that monomer vapor pressure contribution first increases and then decreases during the reaction.

For the 85% styrene-ethylbenzene system, the lower temperature increment resulted in a less-expanded nitrogen pad. However, the ethylbenzene was not consumed during the reaction and then contributed to building up vapor pressure. The summation of these two factors led to an overall higher pressure (2400 kPa) than the pure system (2200 kPa). It is worth mentioning that this higher pressure was observed at a lower temperature (298 °C) compared to that of the pure styrene (335 °C). If this maximum pressure was normalized to 335 °C, then the potential pressure rise could increase further to around 2562 kPa, which was also denoted in the figure. As more solvent was added, reaction extent and temperature increase were lowered, even though more solvent vaporized at a

lower temperature, and the expansion of pad gas was not significant, resulting in a lowered total pressure increase. From a safety perspective, the real hazard of a runaway reaction is the uncontrolled pressure, as the direct cause of the loss of containment is the overpressure. Toxic or flammable reactants may be released when the pressure buildup exceeds the ultimate strength of the process vessel, followed by fire or explosion. Although diluting the monomer by 15% helps lower heat release, the elevated pressure change may pose another concern of possible loss of containment. The key hazard indicators obtained from adiabatic tests were plotted in Figure 5.5.

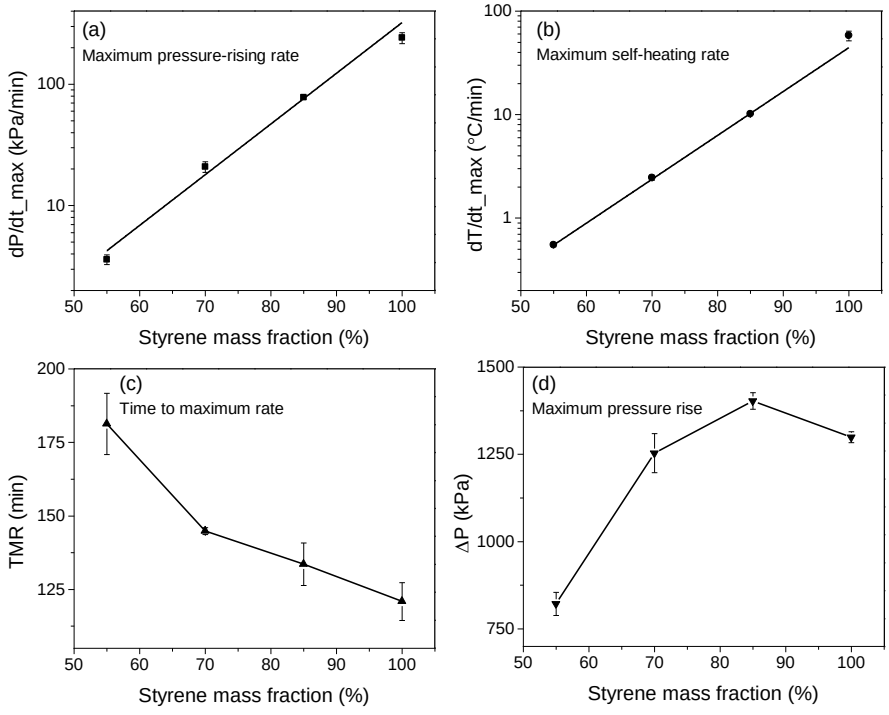

Figure 5.5 The summary of styrene mass fraction effects on the adiabatic runaway behavior of the ethylbenzene-styrene system: (a) the maximum pressure rising rate, (b) the maximum self-heating rate, (c) the time to the maximum rate, (d) the maximum pressure increase

5.3. Pseudo-First-Order Kinetic Fitting

In order to predict the thermal runaway behavior of the styrene-ethylbenzene system, the adiabatic experimental data were used to fit the Townsend nth-order kinetic model, as previously reviewed in the experimental section. The model is a simplified one but serves as a powerful tool to help safety engineers obtain the overall reaction kinetic parameters in a less-complicated way compared to other detailed, multi-step models.

The pseudo-first-order model has been pervasively used in dealing with adiabatic runaway reaction data. Generally, it is assumed that the early stage of the reaction is pseudo-first-order, then the log self-heating rate can be linearly correlated to the reciprocal of absolute temperature and maximum temperature. In such a way, the pseudo-first-order rate constant k, the pre-exponential factor A, and the overall activation energy E_a can be derived according to Equation (20).

$$\ln\left(\frac{dT}{dt}\right)_0 = \ln(A \cdot \Delta T_{\mathrm{ad}}) - \frac{E_a}{R}\left(\frac{1}{T}\right) \tag{20}$$

The average heat of reaction for styrene polymerization can be calculated by multiplying the adiabatic temperature rise by the mixture specific heat capacity. The fitted curves of pseudo-first-order reaction are plotted in dash lines in Figure 5.6. It is obvious that the polymerization was not a first-order reaction in any solution composition at higher conversion. The initial reaction rate can only be fitted by the first-order model up to 40% of total conversion. The linear regression on the logarithm of initial self-heating rate regarding the reciprocal of the absolute temperature resulted in a rate constant was expressed as follows in Equation (21):

$$\ln k = 9467 - \frac{13.54}{T(K)} \tag{21}$$

The apparent activation energy E_a obtained for pure styrene system from the simple pseudo-first-order model was 79 (±0.7) kJ/mol, which was in good agreement with the value of 84.0 kJ/mol obtained by Chen,[55] and 80.6 kJ/mol by Leung.[56] The specific heat of reaction was determined to be around 708 J/g. A significant deviation from the simple pseudo-first-order kinetic was observed for adiabatic tests at higher conversions.

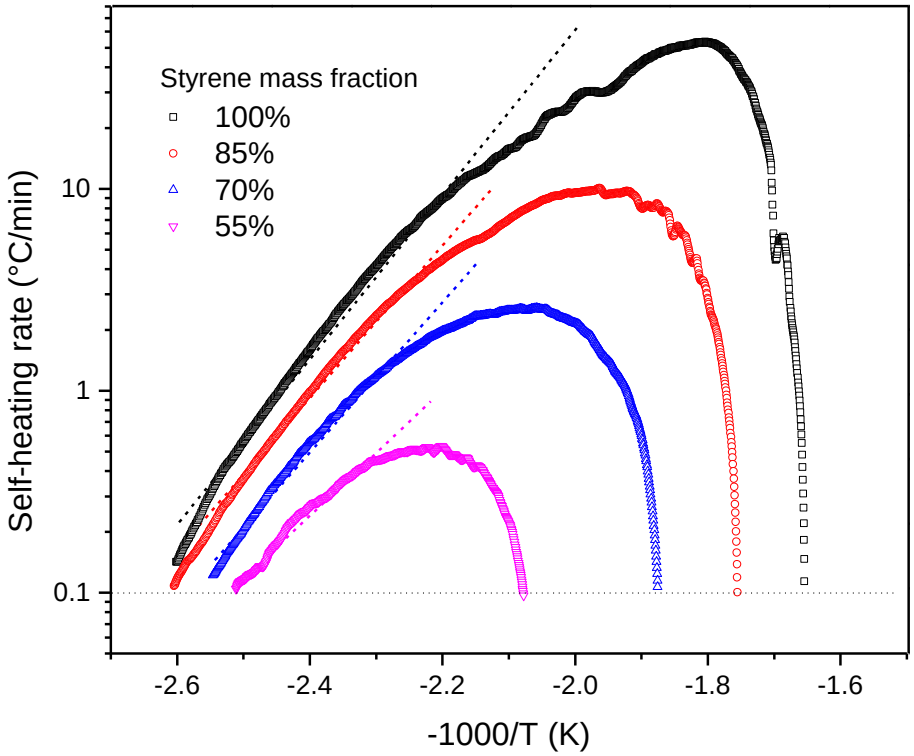

Figure 5.6 Self-heating rate during adiabatic runaway reaction for different styrene mass fractions and the pseudo-first-order kinetic fitting

5.4. Lumped Kinetic Modeling

5.4.1. Temperature Correlation Adopting H-H model

In order to predict the thermal runaway behavior of the styrene-ethylbenzene system and also obtain the optimum solvent dosage ratio to minimize both thermal and pressure hazard, a more detailed kinetic simulation needs to be carried out. The Design Institute for Emergency Relief Systems (DIERS)[116] has recommended the use of Hui and Hamielec[50] model to predict the thermal runaway temperature profile of the thermally initiated styrene polymerization in ethylbenzene in a bulk quantity (32 L). This model was developed in the 1970s for the thermally initiated polymerization of styrene, taking into consideration of gel effect and viscosity change at higher conversions. The initiation was assumed to be a third-order reaction with respect to the monomer concentration. Other reaction rate constants were empirically correlated with the polymer mass fraction and temperature. The overall polymerization rate of Hui & Hamielec kinetic model can be cast as follows:

$$\frac{dx}{dt} = A[M]^{\frac{3}{2}}x \tag{22}$$

$$A = A_0 \exp\left(A_1 x_p + A_2 x_p^2 + A_3 x_p^3\right) \tag{23}$$

$$A_0 = 1.964 \times 10^5 \exp\left(\frac{-10040}{T}\right) \tag{24}$$

$$A_1 = 2.57 - 5.05 \times 10^{-3}\, T \tag{25}$$

$$A_2 = 9.56 - 1.76 \times 10^{-2}\, T \tag{26}$$

$$A_3 = -3.03 + 7.85 \times 10^{-3}\, T \tag{27}$$

Where x is the mass fraction of styrene in the system; x_p is the mass fraction of polymer; $[M]$ is the monomer molar concentration in mol/L; temperature-related parameters A_0,A_1, A_2, A_3 are independent of conversion.

For the styrene/ethylbenzene/polystyrene system in this study, thermodynamic properties such as density, heat capacity, pure component vapor pressure were calculated with empirical correlations as listed in Table 5.3.[56]

Table 5.3 The thermodynamic properties of the chemical system used for simulation

Component	Correlation for properties
Styrene	$C_{p\_styrene} = 2.954 - \frac{13.26}{10^3}T + \frac{39.75}{10^6}T^2 - \frac{29.76}{10^9}T^3$ (kJ/kg·K) $\rho_{styrene} = 1209.8 - 1.3435T + \frac{1.557}{10^3}T^2 - \frac{1.726}{10^6}T^3$(kg/m^3) $P^0_{styrene} = \exp\left(144.02929 - \frac{9630.666}{T} - 19.36771\mathrm{Ln}(T) + 0.001775372T\right)$(N/m^2)
Ethylbenzene (EB)	$C_{p\_EB} = 1.595 - \frac{2.899}{10^3}T + \frac{13.98}{10^6}T^2 - \frac{8.36}{10^9}T^3$ (kJ/kg·K) $\rho_{EB} = 1210.9 - 1.7219T + \frac{2.78}{10^3}T^2 - \frac{3.094}{10^6}T^3$(kg/m^3) $P^0_{styrene} = \exp\left(88.88045 - \frac{7716.472}{T} - 9.8965206\mathrm{Ln}(T) + 6.0871529 \times 10^{-6}\,T^2\right)$(N/m^2)
Polystyrene (PS)	$C_{p\_PS} = 0.945 + \frac{2.400}{10^3}T$ (kJ/kg·K) $\rho_{PS} = 1250.1 - 0.6050T$(kg/m^3)

5.4.2. Pressure Correlation Using Free-Volume Theory

The total pressure of the system was also simulated by considering both pad gas pressure and vapor pressure. The vapor pressure of volatile components (monomer and ethylbenzene) was calculated based on the partial vapor pressure of each component over a monomer/polymer/solvent system via the following Flory-Huggins equation[42] to correct the respective activities. P_i^0 is the pure compound vapor pressure; ϕ_i is the volume fraction of the compound; ϕ_p is the volume fraction of polymer chains; χ is the polymer-solvent interaction parameter, which was measured by Flory to be around 0.45 for polystyrene in ethylbenzene.[117]

$$\frac{P_i}{P_i^0} = \phi_i \exp(\phi_p + \chi \phi_p^2) \tag{28}$$

5.4.3. Modeling Results

The thermodynamic equations, together with the temperature and pressure correlations were coded in Matlab to model the temperature and pressure change of the components and the overall system during the adiabatic thermal runaway reaction of styrene. An ODE45 solver was utilized to generate the temperature and pressure file with respect to time starting from the onset of the thermal polymerization reaction. The simulation was carried out for different runs employing 55−100% monomer mass fraction in the solution for which adiabatic measurements were performed. The heat loss correction was performed using the thermal inertia factor obtained in the experimental section.

The comparison of the self-heating rate between experimental results and the simulated ones are shown in Figure 5.7. As can be seen from the figure, the empirical rate

equations provided by Hui & Hamielec were in good agreement with the adiabatic experimental data in terms of self-heating rate change regarding the reciprocal of temperature.

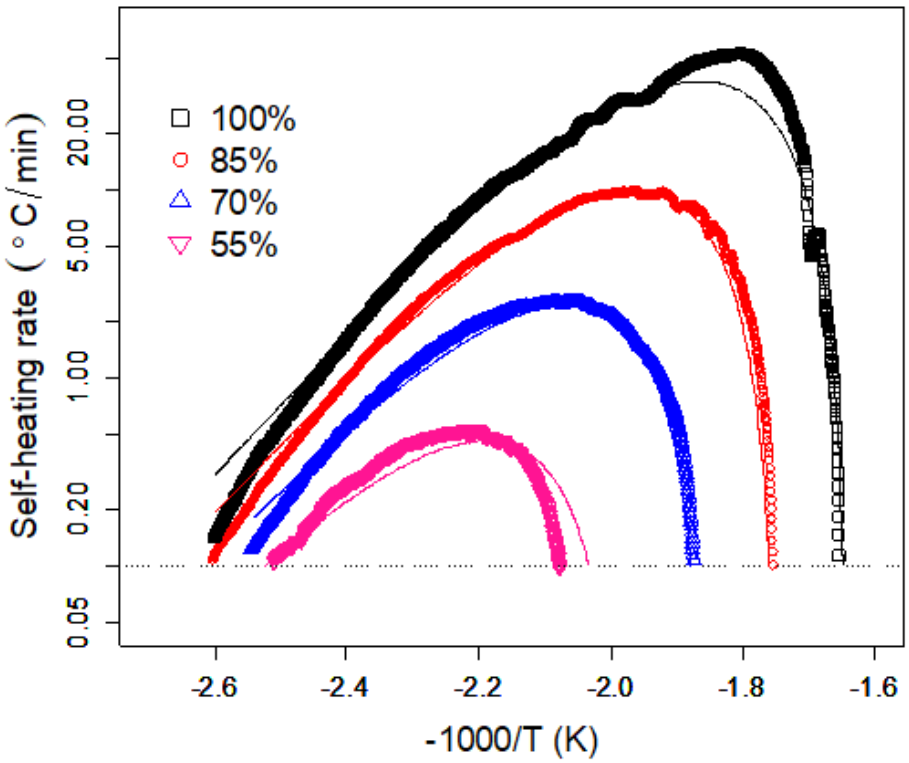

Figure 5.7 The self-heating rate during adiabatic runaway reaction for different styrene-ethylbenzene mass fractions and Hui & Hamielec kinetic prediction (solid lines)

Figure 5.8 shows a comparison of a series of simulation results with experimentally detected maximum temperature and maximum self-heating rates. The model showed a linear trend of maximum adiabatic temperature increase and an exponentially increasing peak self-heating rate with monomer mass fraction. The model

predicted a slightly lowered maximum self-heating rate for all cases. Adjustment of the value of parameters A_0 - A_3 using experimental data may result in more accurate predictions of the self-heating rates and pressures.

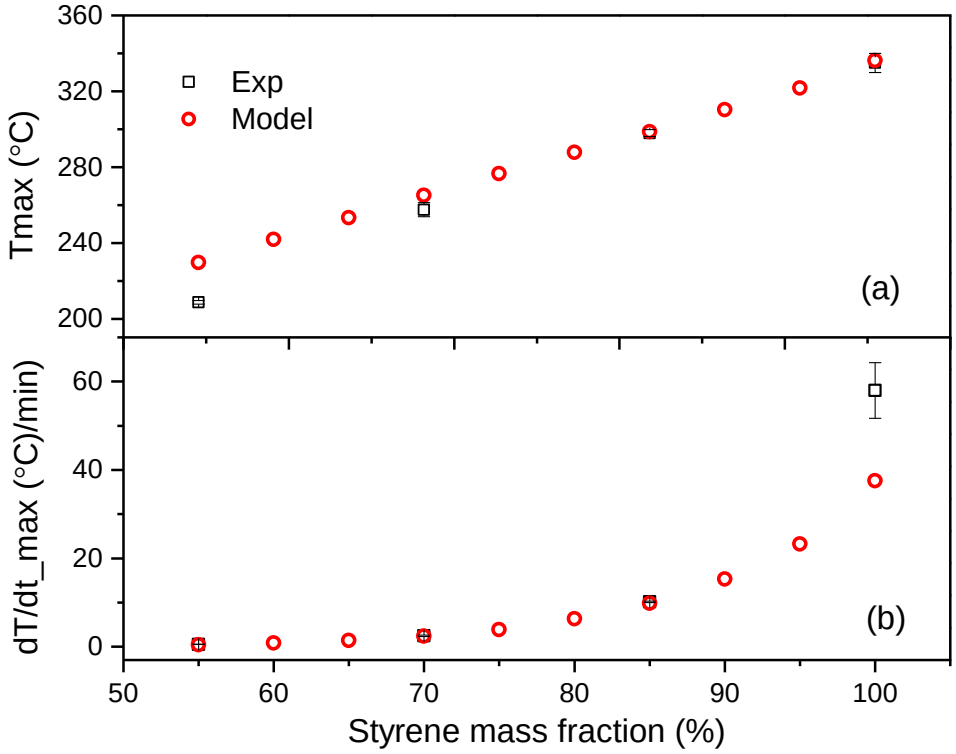

Figure 5.8 Hui & Hamielec model results and APTAC experiment results: (a) maximum adiabatic temperature, (b) maximum temperature rising rate

The pad-pressure change of nitrogen was assumed to follow the ideal gas law, while the gas-phase temperature increased during exotherm, and the headspace volume expanded due to the contraction of the liquid phase caused by polymerization. In such a way, each pressure contributor was simulated separately, as shown in Figure 5.9.

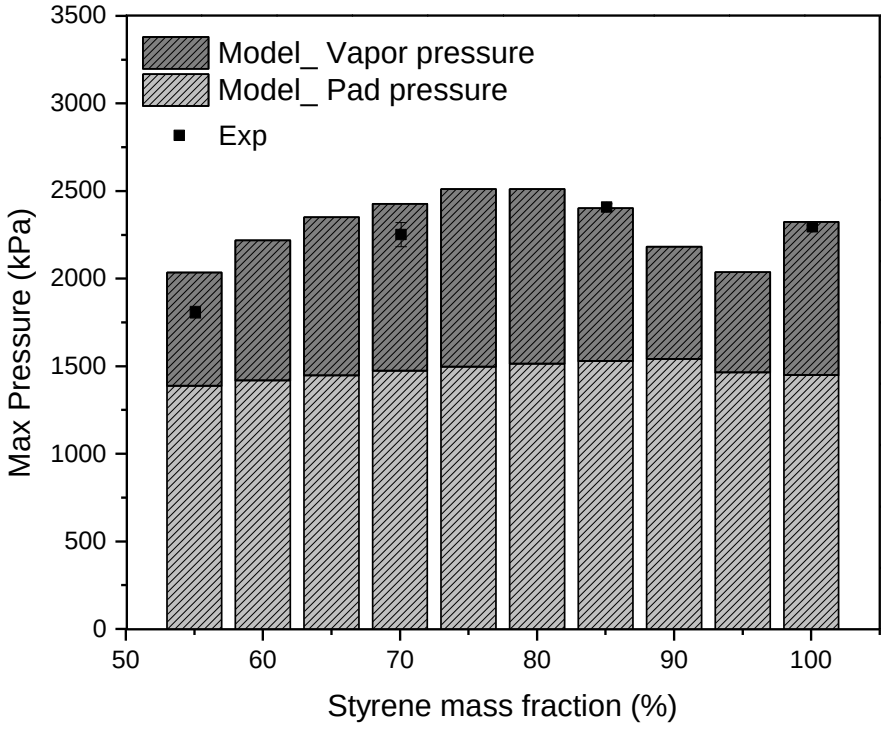

Figure 5.9 Hui & Hamielec kinetic modeling and experiment results of the maximum pressure change for ethylbenzene-styrene systems

The simulation results showed that the maximum pressure during the adiabatic thermal runaway was not a monotonic function of the monomer mass fraction, which was confirmed by the experiments. It was expected that as the reaction temperature increased during the adiabatic runaway polymerization, the pad gas expansion would result in a respective rise of pressure. However, as the monomer with lower density gradually reacted to build up polymer chains with higher density, a contraction of the liquid phase and an expansion of the gas phase was introduced. This volume change counterbalanced the temperature change effect and moderated the pad-pressure increase. The vapor pressure of monomer and ethylbenzene increased with temperature, while at the same time, the

monomer was consumed, and thus its contribution to the total vapor pressure during the reaction decreased.

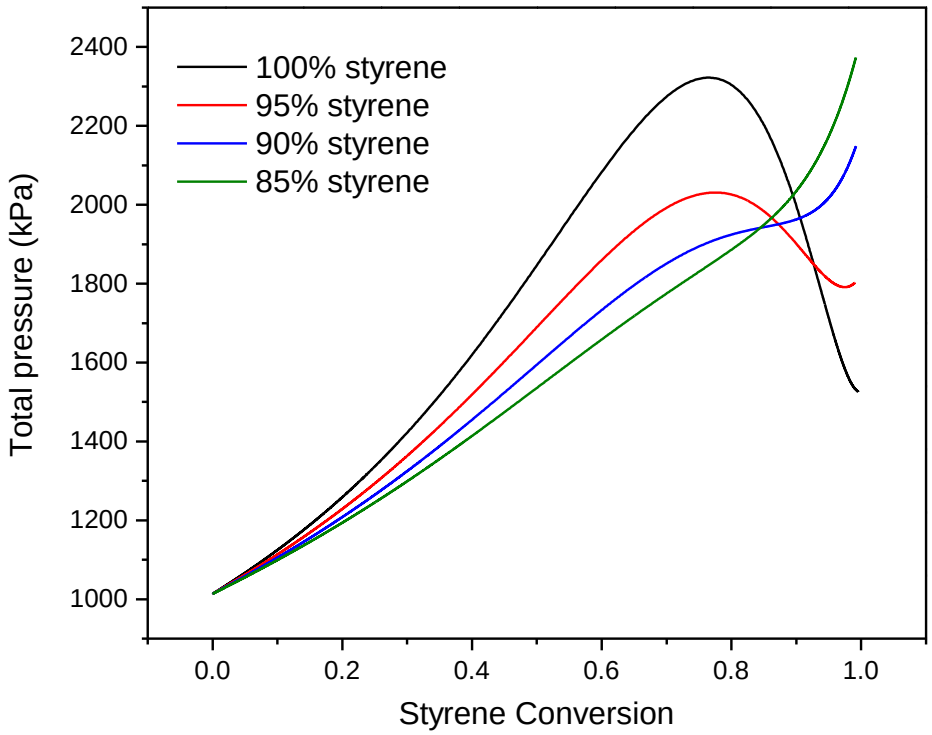

Figure 5.10 Hui & Hamielec kinetic modeling of pressure change as a function of styrene conversion for selected ethylbenzene-styrene systems

When the mass fraction of monomer increased from 55% to 100%, the non-reactive volatile components fractions dropped, and the total pressure increase with conversion showed a significant change. Two different pressure change patterns were observed as shown in Figure 5.10.

For samples with monomer mass fraction below 95%, the calculated maximum pressure was observed at the end of the reaction ($P_{max} = P_{final}$). In these cases, although the monomer was completely consumed at the final stage, the solvent vapor pressure reached its maximum and had a significant contribution to the total pressure. The simulations for a styrene mass fraction of 95% and 100% showed that the total pressure first increased with conversion and then dropped at the end of the reaction ($P_{max} > P_{final}$). In other words, the peak thermal hazard and peak pressure hazard appeared at different stages of the adiabatic runaway reaction. For the pure styrene sample, simulation denoted peak pressure value was at around 77% monomer conversion, at which point 23% of the monomer still had a significant contribution to the total pressure. After more monomers were consumed, the simulated vapor pressure of monomer dropped to 0 psi at the endpoint (100% conversion). The total pressure was then equal to the pad gas pressure. The experimental results were in good agreement with the prediction within the mutual error. The results showed that the addition of the solvent or the lowering of the mass fraction was an effective measure to prolong TMR and moderate the rate of heat release. However, volatile solvents lead to a higher pressure rise even at lower temperatures, which introduces a different kind of hazard, which must be taken into consideration when designing the vapor relief systems.

The experimental and lumped kinetic modeling results reported herein should be considered in the light of some limitations. First of all, other species that are present in the polymer production such as initiators, chain-transfer agents, or possible contaminants, may also have an impact on the thermal runaway behavior. Other scenarios and further

studies are necessary to be conducted to evaluate the synergistic effects which arise from their presence. At the same time, the lumped kinetic simulation with Hui & Hamielec model matched well with the adiabatic self-heating rate for the concentrated samples at a higher temperature range while overestimated the rate of polymerization at the initial stage. This deviation may be caused by the simplified empirical correlation, which was insufficient to provide detailed expressions of rate constants for individual steps in the free-radical polymerization reaction. A series of more detailed kinetic studies have been carried out by a working party of the International Union of Pure and Applied Chemistry (IUPAC) since 1988[118, 119] to obtain the accurate values of the critical rate constants for a variety of free-radical polymerization systems. More specifically, for the styrene system, the pulsed laser polymerization-size exclusion chromatography method (PLP-SEC) method was first used to obtain the benchmark value of the propagation rate coefficient of styrene.[120] The change of initiator efficiency of azobisisobutyronitrile (AIBN) in styrene was evaluated under different temperature and pressure conditions.[121] Most importantly, the experimental method to accurately assess the termination rate coefficient has been carefully reviewed for various free-radical polymerization systems,[122, 123] followed by a recent experimental evaluation of the styrene termination rate coefficient that covers the entire conversion range.[124] These benchmark values and IUPAC recommended PLP-SEC experimental method have facilitated the development of numerous new kinetic models as summarized by Achilias.[57] The future utilization of these detailed non-empirical kinetic modeling would enable a deeper understanding of styrene polymerization thermal runaway behavior at bulk quantities.

5.5. Conclusions

The effect of styrene mass fractions on the thermally initiated polymerization runaway hazards of the styrene-ethylbenzene system was studied using screening and adiabatic calorimeters. DSC results confirmed a multi-peak reaction exotherm between 100 °C and 300 °C. The addition of diluent effectively reduced overall heat release by affecting the late stage of the reaction at higher temperatures (> 150 °C). Adiabatic tests identified a delayed and milder self-polymerization upon dilution, with higher detected "onset" temperature and linearly decreased adiabatic temperature rise. Both screening and adiabatic test results confirmed that the overall heat release and reaction severity was reduced by the addition of solvent. At the same time, pressure build-up rate and temperature rate exponentially decreased with lower monomer mass fraction, proving that dilution with solvent is an effective measure to moderate reaction thermal hazards and as such it may form a sound inherently safer design option, especially when the monomer mass fraction drops below 0.8. However, when the monomer was diluted in ethylbenzene to 85% w/w, the presence of volatile species resulted in a higher pressure-rise during reaction runaway compared to the pure styrene system even at lower temperatures. The lumped kinetic model, developed by Hui & Hamielec, presented an excellent agreement with the experimental data for both thermal and pressure hazards during the adiabatic thermal runaway. The study revealed the complex role of solvent (ethylbenzene) regarding the polymerization runaway hazards. The addition of solvents into the polymerization system to mitigate the thermal risk may introduce pressure risks because of the volatile

nature of the solvent. Optimum process design should be based on a thorough assessment of all types of hazards present in the system.

6. EFFECT OF INITIATORS ON THE THERMAL HAZARD OF STYRENE [3]

In the previous chapter, the thermal runaway hazard of the styrene-ethylbenzene system was investigated using a combination of calorimetric study and kinetic modeling. The results revealed that the thermal and pressure hazards of the polymerization were strongly altered by the addition of solvent at around 15% (wt.), which was a common recipe for the industrial-scale polystyrene production. Based on the results of the binary system, initiators were added into the styrene-ethylbenzene system to further investigate the effect of radical generators on the thermal hazards of the polymerization system.

Based on a fault-tree-analysis, the deviation from a normal recipe or designed operation condition may lead to auto-accelerated temperature and pressure rise, followed by rupture of reaction vessels, fire, and explosion. Mischarging of initiators (radical generators) is one of the most common credible mal-operation cases, which has only been studied to a limited extend. In this section, benzoyl peroxide (BPO) and azobisisobutyronitrile (AIBN) were used as initiators for styrene-ethylbenzene solution polymerization at a series of high concentrations to mimic the mischarging scenarios. Both screening and adiabatic tests were performed to obtain the most critical safety parameters such as onset temperature, adiabatic temperature rise, and the time to maximum rate.

[3] Part of this section is reprinted with permission from "Study of the Initiator Mischarging Effect on Runaway Reaction of Styrene Polymerization" by Lin Zhao, Maria I. Papadaki, M. Sam Mannan, and Mustafa Akbulut. *2019 Spring Meeting and 15th Global Congress on Process Safety*. Copyright 2019 by American Institute of Chemical Engineers.

6.1. Initiator Triggered Free-Radical Polymerization

The reaction scheme of the initiator-triggered free-radical polymerization of styrene was reviewed in chapter one, and the reaction steps were illustrated in Equation (1)−(10). The two most commonly used initiators, BPO, and AIBN both thermally decompose to generate free radicals and further react with monomers to initiate the free-radical polymerization process.

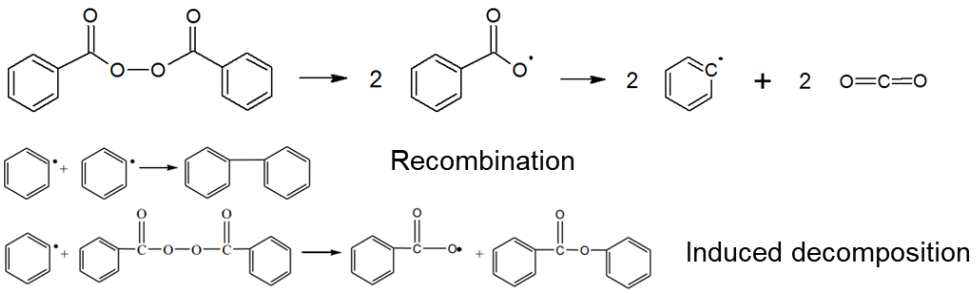

Figure 6.1 Thermal decomposition routine of benzol peroxide

BPO is a kind of diacyl peroxides and has a 10-hour half-life at 73 °C in benzene.[45] Figure 6.1 illustrated the major reaction steps that related to free-radical generation and recombination when BPO is heated.[125-127] The primary thermal decomposition of BPO involves the generation of two benzoyloxy radicals, a very reactive intermediate. Further decomposition of the benzoyloxy radical results in the generation of carbon dioxide gas and phenyl radicals. The recombination between benzoyloxy radicals and phenyl radicals leads to a non-reactive by-product and a “waste” of the initiator. At the same time, the

decomposition of BPO can be induced by the phenyl radicals, giving it an auto-catalytic nature.

AIBN is another kind of free-radical generators that find prevalent usage in the manufacturing of all types of engineering plastics. It belongs to the azo family where the N=N double bond decomposes under heat or light. The 10-hour half-life temperature for AIBN in toluene is experimental measured to be around 63 °C.[128] The thermal decomposition routine of AIBN is shown in Figure 6.2.[129] Upon heating, the nitrogen double bond breaks, leading to the non-condensable nitrogen gas generation and the production of carbon radical (2-cyano-2-propyl radical).

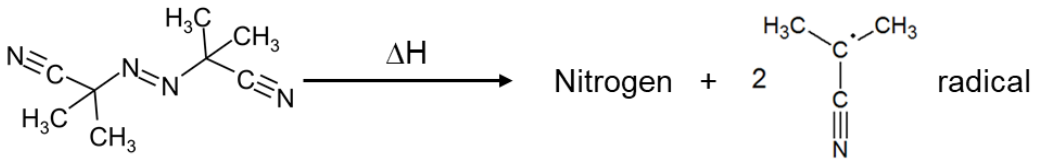

Figure 6.2 Thermal decomposition routine of azobisisobutyronitrile

Comparing these two initiators, they both thermally decompose under heat to generate free-radicals and non-condensable gas. BPO has a more complex decomposition scheme that the reaction can be induced by the product, while the thermal decomposition of AIBN follows a simpler scheme and usually well described with a first-order kinetic model. At the same time, the reaction decomposition rate for AIBN is approximately independent of the solvent type. BPO, on the other side, has a more substantial solvent effect that the decomposition rate can be significantly altered by the polarity and kind of

the solvent been used. In addition to that, the 10-hour half-life temperature reported in the literature denoted that AIBN has a faster decomposition rate than BPO.

6.2. Thermal Decomposition Analysis of Initiators

To understand how the mischarging of both initiators affect the thermal runaway behavior of the styrene-ethylbenzene-initiator system, the very first step would be an accurate assessment of the thermal decomposition of the pure initiator itself. Evaluating the standalone thermal decomposition thermal hazards of the initiators served as the cornerstone in terms of understanding the thermal behavior of the complex polymerization system initiated by the decomposition of the initiators. Next, the thermal decomposition of the initiator was investigated in the diluent (ethylbenzene) to identify the effect of the solvent.

6.2.1. Thermal Decomposition Hazard Analysis of Solid Initiators in MDSC

In this section, the thermal decomposition behavior of the pure initiators was discussed. There were several technical difficulties associated with the accurate evaluation of the thermal decomposition hazards of the initiators. First of all, the initiators decompose to generate a tremendous amount of heat, usually over 1000 J/g, as summarized by Prana.[130] Such acute, almost explosive thermal decomposition also brought a significant amount of non-condensable gas, as shown in Figure 6.1 and Figure 6.2. The temperature-increase and pressure building-up during the test would possibly exceed the mechanical strength of the test cell if the sample size were too large. In addition to that, both BPO and AIBN are solids under ambient temperature and have a melting temperature very close to

the decomposition onset temperature, leading to an overlapping of the heat signal in a DSC test.

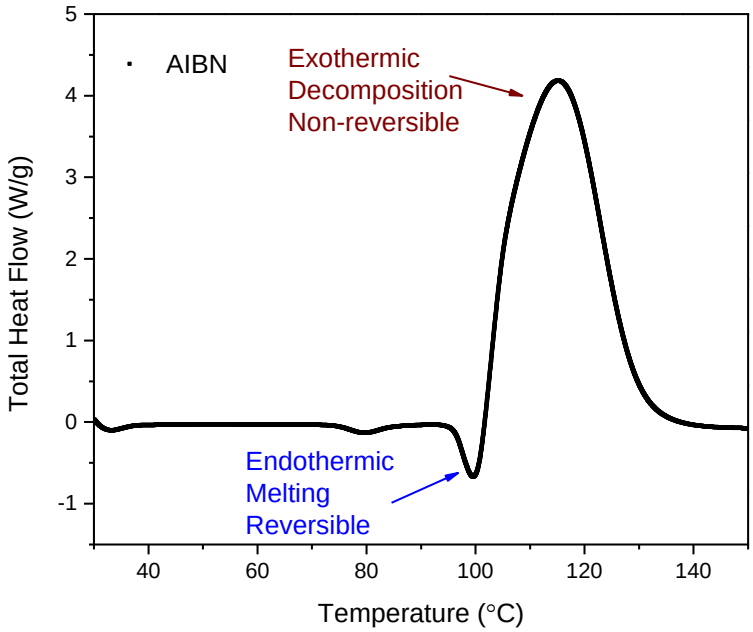

Figure 6.3 The overall heat flow curve of AIBN tested in DSC

Figure 6.3 shows the heat flow curve of the solid AIBN heated in DSC from room temperature to 150 °C at a constant heating rate of 4 °C/min using 2 mg of sample in the high-pressure sample pan. It was noticed that at around 95 °C, a small endothermic peak emerged, which was related to the melting of the solid AIBN particles to its liquid phase. The tail of this endothermic peak overlapped with the thermal decomposition exothermic peak, which had a peak temperature of around 115 °C. The overall heat flow curved denoted a mixed signal consisting of both phase change and reaction; thus, it was

impossible to tell exactly at which temperature the thermal decomposition of AIBN actually onsets. If the endothermic peak was not properly separated from the total signal, the accurate measurement of the initiator decomposition heat was not possible.

Two different approaches have been reported to solve the puzzle. Zhang[69] compared two different decoupling methods to rule out the effect of phase change on the thermal hazard evaluation of AIBN. The first methods utilized inert solvent aniline to dissolve the solid AIBN and thus eliminate the phase change. Mathematical extrapolation of the peaks was also adopted to split the overall heat signal peak into the endothermic part and the exothermic part. The two methods yielded similar results regarding the "true" onset temperature and exothermic decomposition heat. Under a heating rate of 4 °C/min, AIBN started to decompose at around 94 °C thermally, and the exothermic heat release was around 1300 J/g.

In this work, a novel Modulated DSC (MDSC®) test method, developed by TA instruments, was adopted to decouple the combined heat effect of initiators during the parallel melting-decomposition process. The working mechanism of the MDSC method was reviewed in a series of technique documents published by TA Instruments.[131-134] The key difference between the conventional DSC and MDSC is that the latter applies a sinusoidal oscillating or modulated heating rate to the test sample, as shown in Figure 6.4(a). The green curve shows the actual temperature change applied to the test sample in the MDSC test. The signal oscillates around the average temperature change (shown in blue line) of 4 °C/min, and the derivative of the modulated temperature regarding temperature follows a sinusoidal pattern.

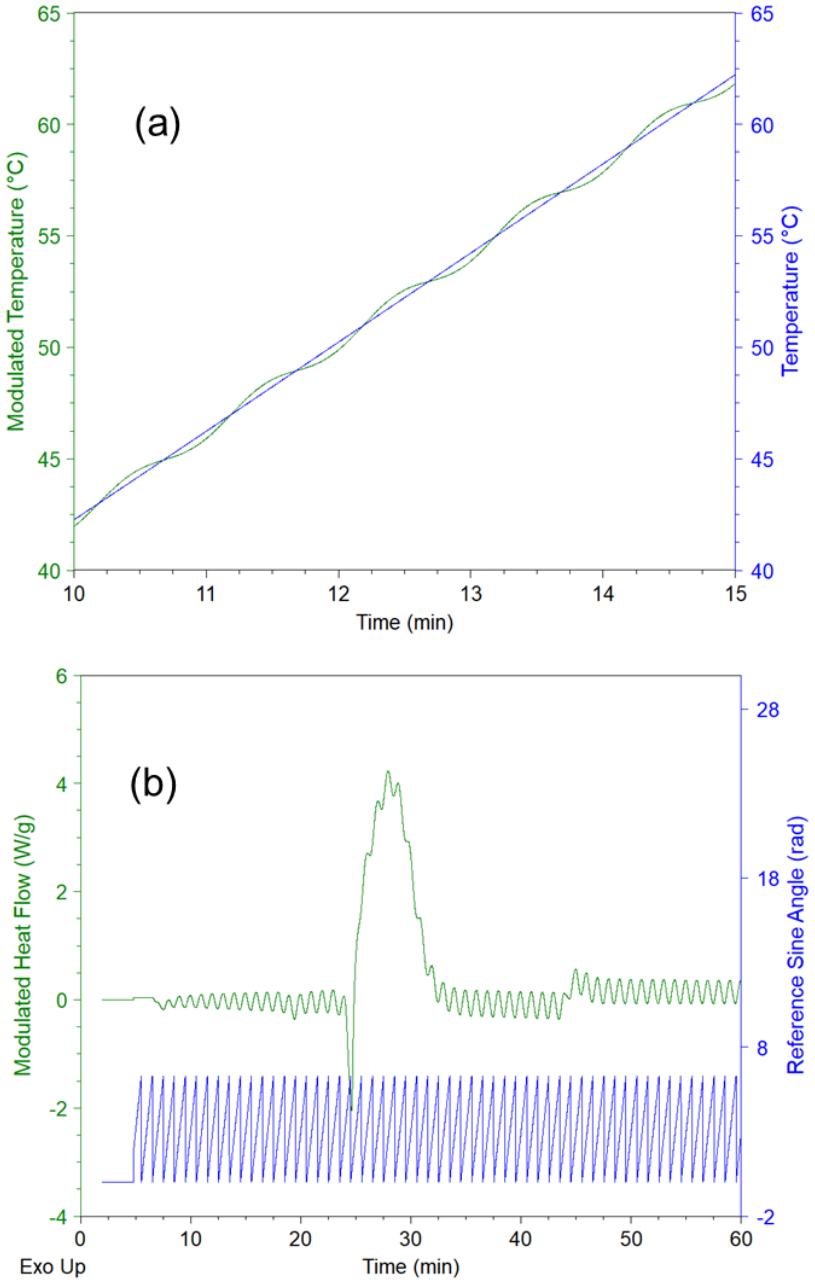

Figure 6.4 MDSC test of the thermal decomposition of solid AIBN: (a) modulated and average temperature, (b) modulated heat flow

The heat flow signal generated by applying the MDSC heating rate is calculated with Equation (29).

$$\frac{dH}{dt} = C_p \frac{dT}{dt} + f(T, t) \tag{29}$$

In the above equation, dH/dt was the overall heat flow signal in watt (W), which consisted of two different terms, the reversing term $C_p \frac{dT}{dt}$ and the kinetic term $f(T, t)$. The first term on the right side of the equation represented those thermal activities that linearly related to the heat capacity of the sample. A typical example of these thermal activities was the melting of solids, and this type of thermal signal was identified to be the "reversing signal" that responds to heating rate change. The other term in the equation denoted "non-reversing signal" that related to the kinetic processes, including decomposition, chemical reaction, and relaxation. This part of the signal, on the contrary, only responded to the absolute temperature/time. In this research, all samples were heated up at a fixed average heating rate of 4 °C/min oscillating at 0.6 °C per 60 s. The total heat flow signal was processed with the TA Universal Analysis software to split the reversing signal (melting) and the non-reversing signal (thermal decomposition). The modulated heat flow signal is shown in Figure 6.4(b).

The decoupled thermal decomposition signal of the two solid initiators using MDSC are summarized in Figure 6.5. The non-reversing heat flow curve denoted one single exothermic peak, which was the thermal decomposition process. The reversing heat flow curve showed a single endothermic peak, overlapped with the non-reversing heat

flow, which was identified as the melting process of the initiator from the solid state to the liquid state.

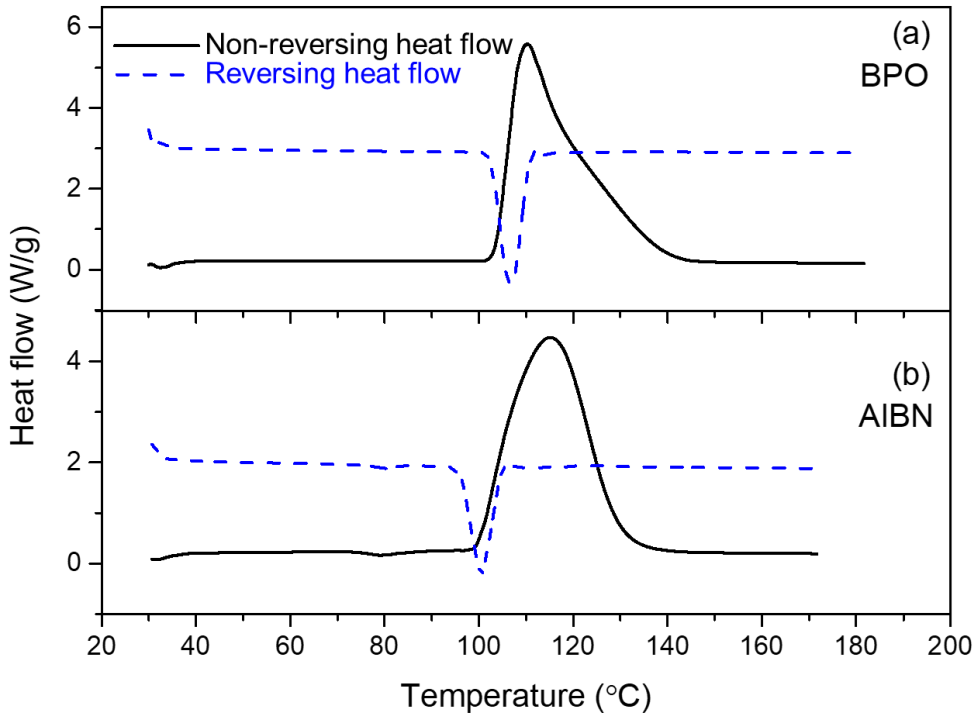

Figure 6.5 Split heat flow of the two solid initiators during thermal decomposition from the MDSC experiments: (a) BPO, (b) AIBN

As it is clearly shown in Figure 6.5 when compared to Figure 6.3, MDSC provided a convenient way to separate overlapping thermal activities and rule out the phase transition from the hazardous exothermic behavior. As a result, the determination of the onset temperature of the thermal decomposition became straightforward. The non-reversing heat flow denoted the onset temperature of solid BPO and AIBN was 103 °C

and 100 °C, respectively. The heat of decomposition integrated from the non-reversible heat flow was 1352 J/g for BPO, and 1140 J/g for AIBN, which were slightly higher than the heat of decomposition obtained from the traditional method,[66, 70] implying the MDSC decoupling method provided a more conservative estimate of the reaction heat and thermal hazard.

6.2.2. Thermal Decomposition Hazard Analysis of 5% Initiator in DSC

Next, the solid initiators were dissolved in ethylbenzene at a weight percentage of 5% in the total sample. The initiator-solvent system was heated up in DSC to investigate the solvent effect on the thermal decomposition hazard of the initiators. In general, industrial practices utilize initiators that dissolved in the solvent to trigger the polymerization reaction, and the thermal decomposition of the two initiators was examined in ethylbenzene following the kinetic method documented in ASTM E698 standard (Ozawa method)[94]. Four different scanning rates (β) were applied to the 5% initiator-ethylbenzene mixture varying from 2 °C/min to 10 °C/min. The peak temperature of the major exothermic peak and the overall reaction heat summarized in Table 6.1.

In Table 6.1, the peak temperature (T_p) corresponding to the maximum heat generation was recorded for each heating ramp. The activation energy (E_a) of thermal decomposition in the solvent was obtained by using Equation (30), where E_a is the activation energy of thermal decomposition, R is the gas constant, β is the heating rate in °C /min, and T_p is the peak temperature in Kelvin.

$$E_a \cong -2.19R[\mathrm{d}\,\mathrm{Log}_{10}\beta/\mathrm{d}(1/T_p)] \tag{30}$$

Table 6.1 The thermal decomposition of 5% initiator in ethylbenzene in DSC

β	BPO		AIBN	
(°C/min)	T_p (°C)	ΔH (J/g)	T_p (°C)	ΔH (J/g)
2	115(±0.5)	1341(±46)	112(±1)	1394(±8)
4	126(±3)	1320(±12)	119(±1)	1478(±43)
8	138(±1)	1319(±7)	127(±4)	1477(±11)
10	141(±2)	1257(±27)	129.5(±1)	1304(±14)

When initiators were dissolved in ethylbenzene, the phase transition was eliminated, and the reversing heat flow became a trivial part. The overall heat flow obtained was identical to the non-reversible heat flow through the process of thermal decomposition, as shown in Figure 6.6.

When initiators were dissolved in ethylbenzene, the thermal decomposition became detectable at a significantly lower temperature when compared to the concentrated solid form. For the heating rate of 4 °C /min, 5% BPO in ethylbenzene onset at around 84.8 °C, and the 5% AIBN in ethylbenzene onset at around 70.7 °C. The maximum temperature of the exothermic peak increased with a higher heating rate. The activation energy E_a obtained of 5% initiators in ethylbenzene was 79.7 kJ/mol for BPO and 108.1 kJ/mol for AIBN.

The experimental results in the solvent denoted that the solvent had significantly altered the thermal behavior of the onset of the thermal decomposition of the two initiators. Both AIBN and BPO showed an early decompose when dissolved in solvent compared to the onset temperature of around 100 °C in the solid state. The overall heat of reaction,

normalized based on only the mass of the initiators, had no substantial change. Thus, the results implied that the thermal decomposition reaction extent was not affected by the presence of the solvent, while the reaction scheme shifted to a lower temperature range.

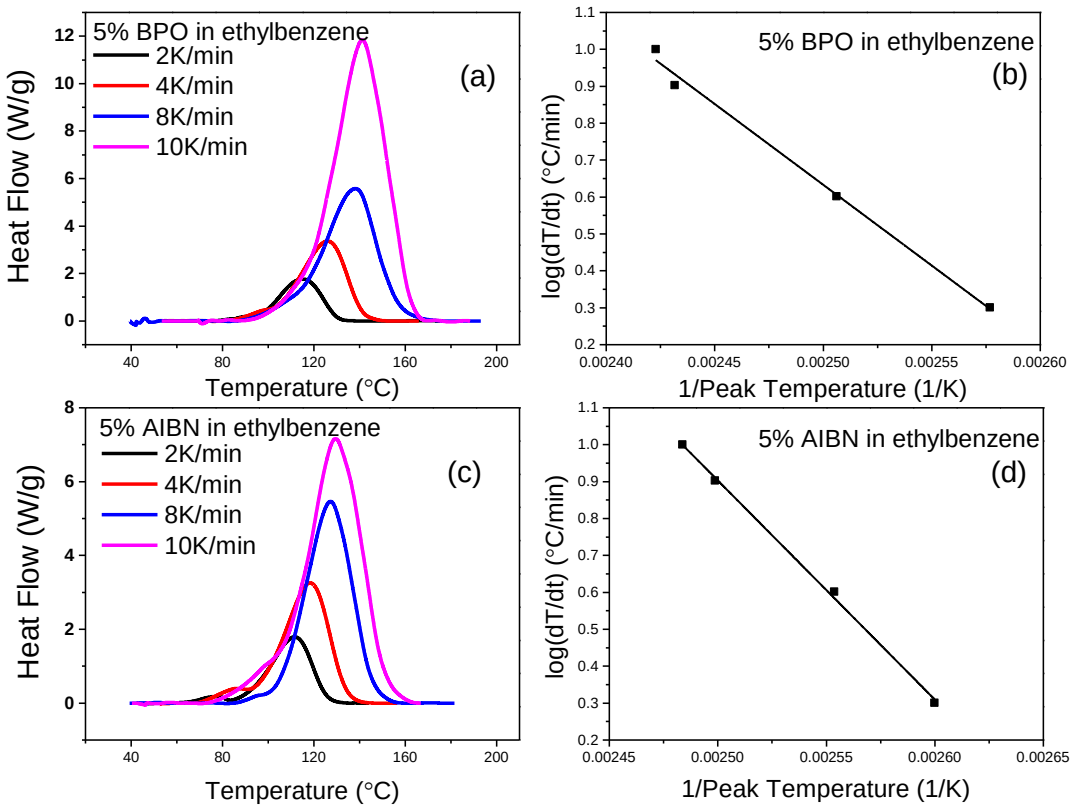

Figure 6.6 Heat flow of the 5% initiator-ethylbenzene solution at different heating rates in the DSC and the kinetic fitting: (a), (b) BPO, (c), (d) AIBN

We speculate the presence of solvent changed the phase of the test sample from solid to liquid, in which case the thermal conductivity of the sample elevated and resulted in a better heat transfer from the bottom heating plate to the sample. When the solid sample was added in the test cell, the BPO and AIBN particles were loosely packed and had poor

contact with the sample holder, raising difficulties in the heat transfer from the heater to the bulk of the sample. At the same time, the addition of the solvent eliminated the endothermic melting peak of both initiators, which might be another reason that a lowered onset temperature was observed.

6.3. Thermal Hazard Analysis of Initiator-Styrene-Solvent System in DSC

After the thermal decomposition hazard of the initiators was assessed in both the solid form and in the solvent, the initiators were then mixed with 85% styrene-15% ethylbenzene at a series of initiator concentrations in DSC. The heat flow results are depicted in Figure 6.7 and Figure 6.8 for the ternary systems initiated by BPO and AIBN, respectively. For free-radical polymerization triggered by both initiators, the total heat flow was equal to the non-reversing heat flow, and the kinetic related thermal activity dominated the whole reaction.

The thermal hazard of runaway polymerization triggered by both initiators expressed some common trends when the dosage of the initiator was altered. First, more than one exothermic peak emerged upon heating, denoting a complex reaction pathway, including initiation, chain propagation, chain-transfer, and termination. Compared to the thermal polymerization of styrene without an initiator, Liao[36] identified two major peaks to represent two different types of reaction patterns. However, when the initiators were present, peak numbers increased, and no clear conclusion can be drawn whether the peaks were associated with a specific reaction step as they highly overlapped with each other.

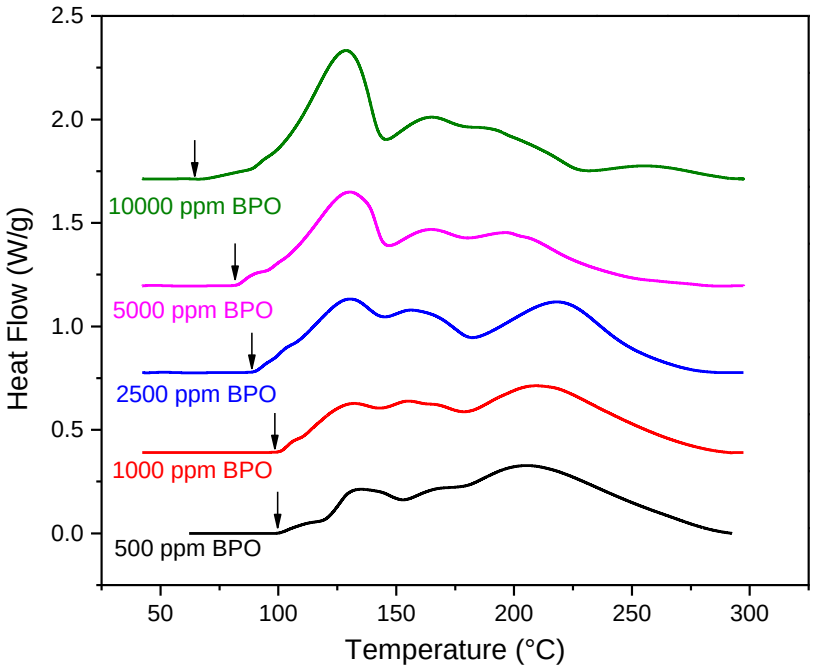

Figure 6.7 Heat flow of the polymerization of styrene-ethylbenzene with different BPO concentrations in DSC at 4 °C/min

A significant difference regarding the onset temperature and the relative peak area was noticed under different initiator dosages. For both BPO and AIBN, the free-radical polymerization reaction started to onset at a lower temperature when the initiator concentration was increased. The lowest onset temperature for AIBN initiated polymerization was 71.3 °C, which was identical to the starting temperature of the thermal decomposition of AIBN in ethylbenzene at 5%. For BPO initiated system, the lowest onset temperature obtained at 10000 ppm BPO in styrene-ethylbenzene was 70.1 °C, which was even lower than the thermal decomposition of BPO in ethylbenzene (84.8 °C). This finding implied that the presence of the monomer further promoted the decomposition of BPO.

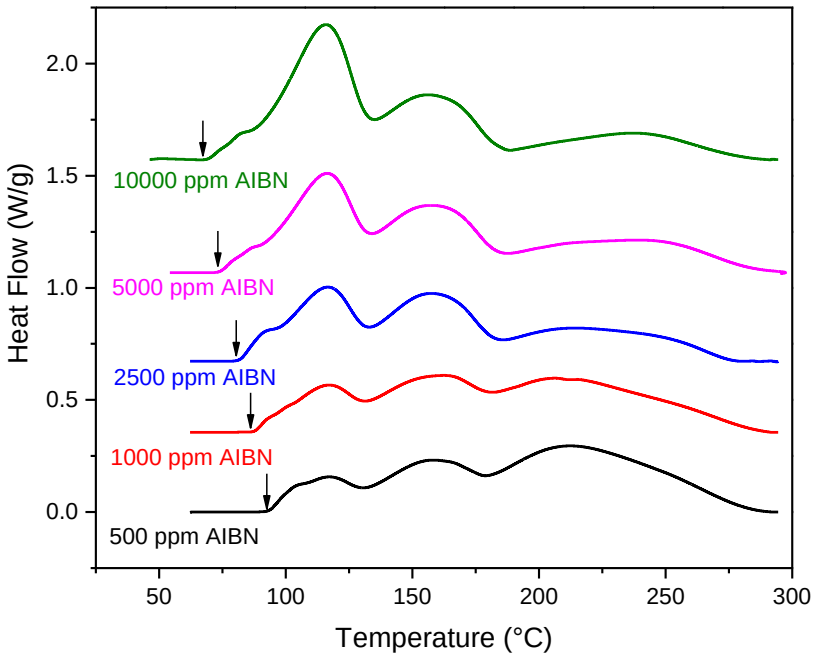

Figure 6.8 Heat flow of the polymerization of styrene-ethylbenzene with different AIBN concentrations in DSC at 4 °C/min

Another difference noticed from the DSC results was that the main exothermic peak shifted to a lower temperature upon the addition of both initiators. The area under the heat flow curve represents the heat generated during the reaction, and thus the relative size and position of the peak can be used to estimate the heat release and at different temperatures, in other words, to assess the severity of the thermal hazards. When BPO and AIBN dosage was low (500 ppm), the major exothermic reaction took place at the late stage of the reaction at around 210 °C. With the addition of the initiators, the main heat release was observed at a much-lowered temperature. For systems with 10000 ppm of BPO or AIBN, the maximum heat generation was observed at around 120 °C; and the sharper, narrower peak denoted a sudden heat released during a short period. The overall

heat of reaction for the ternary system was calculated for all test samples and summarized in Table 6.2, together with the onset temperatures.

Table 6.2 Thermal kinetic data for the polymerization of 85% styrene-ethylbenzene with different initiator concentrations in DSC

Initiator concentration (ppm)	**BPO**		**AIBN**	
	T_0 **(°C)**	ΔH **(J/g)**	T_0 **(°C)**	ΔH **(J/g)**
500	102(±1)	478(±28)	94(±1)	503(±7)
1000	100(±2)	531(±2)	87(±1)	499(±18)
2500	91(±1)	558(±13)	81(±1)	500(±18)
5000	83(±1)	585(±21)	75(±1)	565(±7)
10000	70(±3)	596(±8)	71(±0.2)	637(±25)

The change of these important thermal hazard indicators obtained from the DSC study with respect to the initiator dosage was depicted in Figure 6.9. As shown in Figure 6.9(a), when BPO was used to trigger the polymerization of styrene in ethylbenzene, the reaction heat increased monotonically upon BPO addition, and this increase was most significant when the BPO concentration was below 5000 ppm. At the same time, adding BPO to the monomer-solvent system also lowered the onset temperature, and the lowest onset temperature obtained was around 15 °C lower than the initial thermal decomposition temperature of BPO itself when dissolved in ethylbenzene at 5%. When compared to the case of AIBN in figure 6.9(c) and Figure 6.9(d), it was noticed that the reaction heat roughly remained constant when AIBN concentration was below 2500 ppm, and the

further charging of AIBN resulted in a sharp increase of reaction heat. The onset temperature of the polymerization system with different AIBN dosage showed a similar declining trend as what was observed for the case of BPO. However, the lowest onset temperature was not affected by the presence of the monomer.

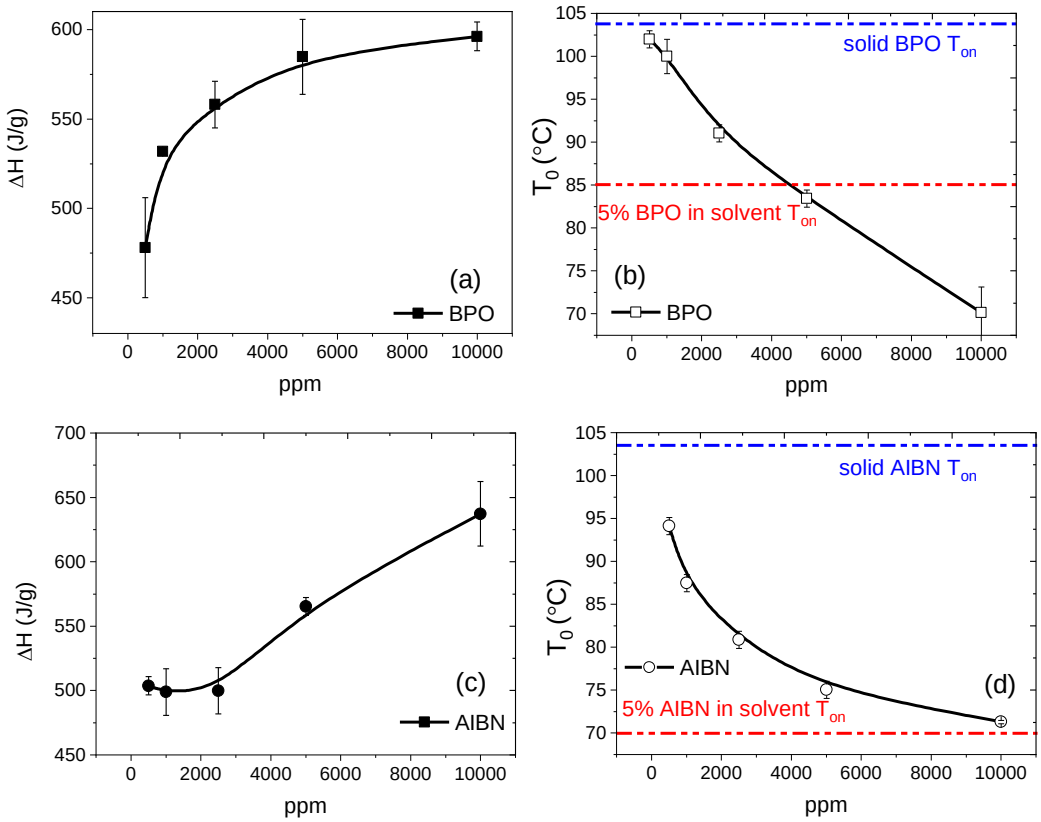

Figure 6.9 The onset temperature and heat of reaction for the polymerization of 85% styrene-ethylbenzene with different initiator concentrations in DSC at 4 °C/min: (a), (b) BPO in styrene-ethylbenzene, (c), (d) AIBN in styrene-ethylbenzene

The change in the detected onset temperature can be explained by the change in overall heat release when the initiators were added into the styrene polymerization system.

The relationship between the reaction rate and the onset temperature was illustrated by Hofelic,[135] also shown in Figure 6.10 in the solid green line.

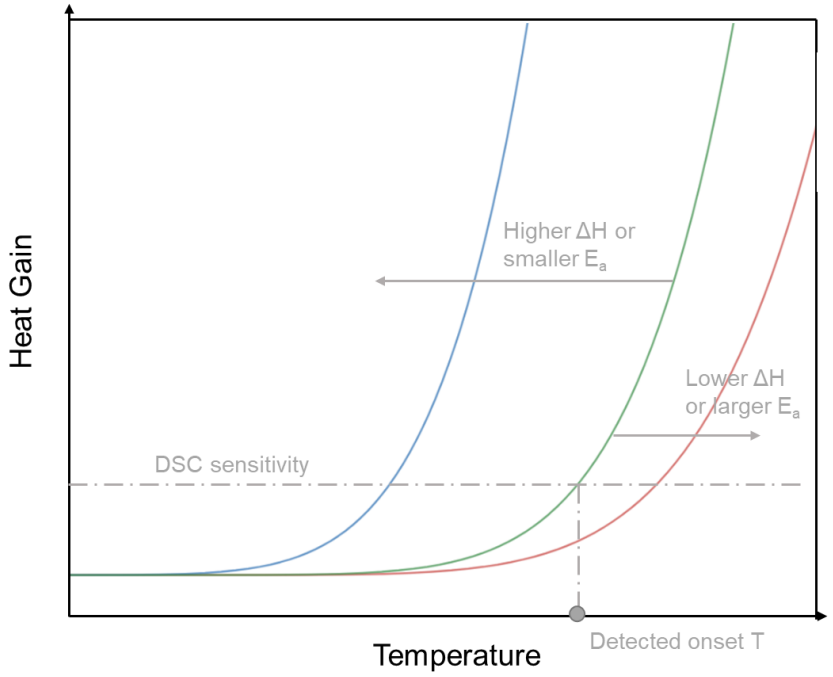

Figure 6.10 The Arrhenius plot of heat gain vs. temperature in a DSC test

For a chemical reaction, whose reaction rate follows the Arrhenius law, the reaction rate shows an exponential relationship regarding temperature. When the heat release of the reaction exceeds the detection threshold of the calorimeter (45mW/g for DSC), the reaction can be noticed or "seen" on the heat flow curve. For the exothermic reactions studied in this research, the overall heat gain was expressed as the product of both reaction specific heat release and the reaction rate. In other words, reaction with

higher specific heat release or higher reaction rate led to a lower onset temperature in a DSC test and vice versa.

Form the DSC test of 5% initiator decomposition insolvent, the activation energy of BPO was determined to be around 80 kJ/mol with a specific heat release of 1319 J/g. The activation energy value for 5% AIBN decomposition was 108 kJ/mol, and a slightly higher heat release of 1477 J/g was observed. For thermally initiated 86% styrene in the solvent, the overall activation energy measured in the previous sections was 79 kJ/mol. The activation energy for the initiation stage of the reaction was estimated by Equation (31) and (32), as shown below.

$$E_a = E_p + \frac{1}{2}(E_d - E_t) \tag{31}$$

$$E_d = 2(E_a - E_p + \frac{1}{2}E_t) \tag{32}$$

The value of $E_p + \frac{1}{2}E_t$ was obtained from the experimental study of Barr[136] to be 26 kJ/mol, then the activation energy for the initiation steps of thermal polymerization of styrene was calculated to be 108 kJ/mol. By comparing the activation energy and heat release in all three types of polymerization (BPO initiated, AIBN initiated, thermally initiated), it was noticed that BPO significantly reduced the activation energy of initiation and increase heat release, leading to the lowest onset temperature. For the AIBN initiated system, the activation energy slightly decreased with the presence of the azo initiator, and the heat release was elevated. Thus, the onset temperature was still lowered. The thermally initiated polymerization, on the other hand, had the highest activation energy and moderate

heat release, and the reaction was not detected by the DSC until a higher temperature was achieved.

6.4. Thermal Hazard Analysis of Initiator-Styrene-Solvent System in APTAC

The DSC provided a preliminary heat generation information of the samples at a small scale, where the heat and mass transfer did not play an essential role in the overall reaction. The thermal runaway behavior of the polymerization process with various initiators dosages was further investigated in APTAC. BPO and AIBN were added into the 85% styrene-15% ethylbenzene system at 500 ppm, 2500 ppm, and 10000 ppm. The adiabatic temperature rise with respect to time and the self-heating rate with temperature is shown in Figure 6.11.

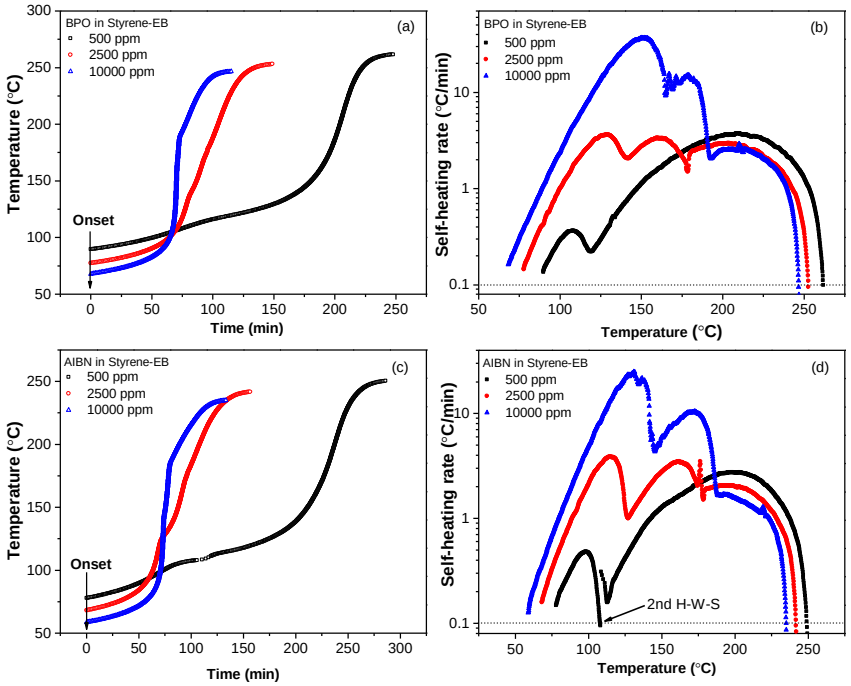

Figure 6.11 The adiabatic runaway behavior of styrene-ethylbenzene system with various initiator charges: (a), (b) BPO, (c), (d) AIBN

The detected onset temperature of the adiabatic thermal runaway reaction, time to maximum rate under adiabatic conditions (TMR), the maximum self-heating rate (dT/dt_{max}), and the maximum pressure-rising rate (dP/dt_{max}) were calculated and summarized in Table 6.3 and Table 6.4.

Table 6.3 Thermal kinetic data for the polymerization of 85% styrene-ethylbenzene with different BPO concentrations in APTAC

Initiator (ppm)	**BPO**			
	T_0 **(°C)**	***TMR* (min)**	dT/dt_{max} **(°C/min)**	dP/dt_{max} **(kPa/min)**
500	84(±6)	207(±3)	4(±1)	23(±2)
2500	73(±2)	78(±9)	4(±0.3)	18(±0.5)
10000	63(±6)	70(±3)	37(±4)	106(±7)

Table 6.4 Thermal kinetic data for the polymerization of 85% styrene-ethylbenzene with different AIBN concentrations in APTAC

Initiator (ppm)	**AIBN**			
	T_0 **(°C)**	***TMR* (min)**	dT/dt_{max} **(°C/min)**	dP/dt_{max} **(kPa/min)**
500	71(±2)	236(±11)	3(±0.3)	18(±2)
2500	63(±3)	69(±6)	4(±0.1)	18(±2)
10000	55(±1)	74(±1)	25(±2)	93(±12)

The adiabatic onset temperature monotonically decreased with initiator dosage for both BPO and AIBN, which was consistent with the observations in MDSC tests. At the

same time, the results emphasized the necessity of employing an adiabatic calorimeter in thermal hazard assessment, as a more conservative and realistic value can be obtained. The lowest onset temperature obtained in this study was 55.1 °C when 10000 ppm of AIBN was charged into the 85% styrene-ethylbenzene system. This value was around 50 °C below the normal recognized thermal decomposition temperature of pure AIBN in its pure state, and also much lower than the onset of thermal polymerization temperature of styrene of around 100 °C. Mischarging of a small quantity of AIBN into the system may result in an unexpected thermal activity at a very low temperature.

At the same time, a significant decrease in TMR was noticed when the initiator concentration was higher than 2500 ppm for both BPO and AIBN. This can be observed in Figure 6.11(a) and Figure 6.11(c) that as BPO and AIBN was 500 ppm in 85% styrene-ethylbenzene, the polymerization reaction activity became notable between 70−80 °C, and the temperature building-up was relatively slow as only around 20 °C increase in temperature was observed in the first two hours. The main temperature increase was noticed after 200 min of the onset, where a temperature increment of over 100 °C was achieved within less than an hour. The time used for the system to reach its maximum self-heating rate (TMR) was 206.7 min for BPO and 236.8 min for AIBN, respectively. When initiators were mischarged into the polymerization system at 2500 ppm, the TMR was shortened to around 80 min for both initiators; a steep temperature increment was observed, denoting that the runaway behavior changed to almost explosive type upon initiator mischarging. The corresponding massive heat release in such a short time may

result in a massive increase in cooling demand, which might not be able to meet by the equipment design.

The energy release, or the heat generation that needs to be taken care of by proper cooling, is expressed as the self-heating rate versus temperature in Figure 6.11(b) and Figure 6.11(d). The polymerization of 85% styrene in ethylbenzene initiated by BPO and AIBN went through multiple exothermic steps, which resulted in several peaks on the curve. When BPO dosage was 500 ppm, the self-heating rate exceeded 0.1 °C/min at 83.8 °C and resulted in a mild exothermic peak with a maximum self-heating rate of 0.2 °C/min before 125 °C. This peak was followed by a major exotherm with a peak temperature of over 200 °C. The latter reaction step also possessed a characteristic of auto-acceleration as the self-heating rate was first linearly related to the reciprocal of temperature (pseudo-first-order) and then had a negative deviation after around 145 °C. This unique heat generation pattern represented a typical free-radical polymerization process with a gel-effect. The gel-effect poses a significant threat to the polymer production as the polymerization rate, and the heat production rate suddenly increases due to the reduced mobility of the long polymer chains after the conversion achieved a certain critical point. For the case of 500 ppm in AIBN, a similar temperature pattern was observed only that the initial exothermic step was not able to generate enough heat to sustain the following reaction at around 110 °C. The APTAC entered heat-wait-search (H-W-S) mode and then heated the system up again to 120 °C; the following reaction developed to complete after that. The temperature rate curve confirmed that when BPO and AIBN dosage was at 500 ppm, the thermal risk associated with the polymerization reaction was due to the sudden

heat release affected by the gel-effect at high temperature, and the maximum self-heating rate was below 4 °C/min. When the initiator dosage was increased to 2500 ppm, three exothermic peaks were observed for both BPO and AIBN. The maximum self-heating rate of the reaction was achieved in the first reaction step at a lowered temperature of around 125 °C for BPO and 114 °C for AIBN, and the value of this peak self-heating rate had no visible change when compared to the case of 500 ppm initiator. Further increasing of initiator concentration to 10000 ppm resulted in a remarkable change of maximum self-heating rate, which was almost ten times higher than that of the 500-ppm case. The heat release rate of the first reaction step overwhelmed the following reactions.

The change of the maximum pressure-rising rate with respect to initiator concentration also followed the same trend. As summarized in Table 6.3, there is no significant change in the peak pressure-building up rate until the initiator concentration increased from 2500 ppm to 10000 ppm. The polymerization of the styrene-ethylbenzene system was a *vapor system* according to the Design Institute for Emergency Relief Systems (DIERS) classification; as such, the pressure increase was solely related to the vaporization of the volatile species. When initiators were present, the decomposition of the BPO resulted in the release of oxygen, while the AIBN generated nitrogen upon heating, which also contributed to the total pressure of non-condensable gases. However, in this study, the initiator dosage remained at a very low concentration (less than 1%), and the contribution of oxygen/nitrogen generation was trivial. The pressure building-up was related to the vapor pressure change caused by the temperature rise.

6.5. Conclusions

In this section, the runaway behavior and thermal hazard of the mischarging of two initiators (BPO and AIBN) into the styrene-ethylbenzene polymerization system were investigated using screening and adiabatic calorimeters. The thermal decomposition of the solid initiators was first characterized by a novel MDSC method to decouple the endothermic phase change and the exothermic decomposition reaction. The onset temperature and the activation energy of the thermal decomposition of initiators in ethylbenzene were investigated by DSC, revealing that when dissolved in ethylbenzene, the thermal decomposition of initiators became notable at a much-lowered temperature when compared to their solid state.

DSC studies on the runaway behavior of styrene-ethylbenzene with different initiator charges discovered that the thermal hazard of free-radical polymerization was strongly related to the initiator dosage regardless of the initiator type. When the BPO and AIBN were mischarged into the system at an elevated concentration, the exothermic onset temperature dropped 30 °C when compared to the thermal polymerization temperature of styrene and also the thermal decomposition temperature of the initiators themselves. Furthermore, the total heat generated by the system with over-dosed initiators increased monotonically with the increase of BPO concentration and had an approximate linear increment after AIBN concentration was over 2500 ppm. The overcharging of both initiators also resulted in a shift of main exothermic activity temperature from around 200 °C to around 120 °C.

The adiabatic runaway test of bulk samples also demonstrated a similar trend that the free-radical polymerization started onset at lower temperature upon initiator dosage, and the time required for the reaction to develop to its maximum self-heating was significantly reduced. With an elevated initiator dosage of 10000 ppm, increased peak heat-release was observed at a lowered temperature associated with higher pressure building-up. The adiabatic data provided extremely useful information regarding thermal behavior and pressure profile for large-scale samples regarding scenarios of mischarging initiators into the polymerization system.

7. INCOMPATIBILITY STUDY OF THE THERMAL HAZARD OF STYRENE

In the previous sections, the thermal hazard of the pure styrene, the binary system of styrene and solvent, and the ternary system containing styrene, solvent, and initiators were evaluated using calorimeters and kinetic modeling. The data obtained suggested that the thermal hazards of the styrene polymerization were significantly impacted by the other species interacting with styrene. The previous experiment successfully covered those chemical pairs that are commonly seen in a commercial styrene processing process.

Another credible scenario that would lead to the catastrophic thermal runaway reaction of styrene is the contamination of the reactive monomer. In this section, the hazard evaluation was carried out to understand how other unwanted species would possibly affect the thermal runaway polymerization of styrene. Both screening and pseudo-adiabatic calorimeters were adopted to obtain the critical safety indicators experimentally, and the data were fitted into lumped kinetic models.

7.1. Incompatibility Screening of Styrene and Other Chemicals

The literature review in the first section identified the inadequacy regarding the incompatibility study between styrene and other chemicals. Quantitative calorimetric evaluation of thermal hazards upon contamination of styrene was only available for the styrene-absorbent system.

Following the hazard evaluation strategy summarized previously, when no detailed incompatibility information is available, desktop screening methods were adopted

to search for clues regarding possible contamination hazards. Typical incompatible species recorded by hazard handbooks are summarized in Table 7.1.[16, 18, 19]

Table 7.1 List of possible incompatible chemical species with styrene

Reference	Chemical species incompatible with styrene
Bretherick	oxygen, butyllithium, alkali-metal-graphite compound, trichlorosilane, initiators
Sax	chlorosulfonic acid, oleum, sulfuric acid, chlorine, iron(iii) chloride (above 50°c). oxidizing materials
Wiley	acids, rust, catalysts for vinyl polymerization, peroxides, hydroperoxides, metal salt

From the table, it was noticed that the most frequently mentioned incompatible species with styrene were the free-radical generators (initiators) and strong acids. Free-radical generators like peroxides and azo compounds thermally decompose to produce highly-active free radicals and trigger the polymerization of styrene, as we investigated before. The presence of initiators significantly lowered polymerization onset temperature, and during which process, the major exothermic peak appeared much earlier, leaving less response time for emergencies.

Health	Flammability	Instability	Styrene incompatibility chart	Sodium Hydroxide solution	Sulfuric acid	Water	Styrene, stabilized
3	0	1	Sodium Hydroxide solution				
3	0	2	Sulfuric acid	N			
0	0	0	Water	C	C		
2	3	2	Styrene, stabilized	N	N	C	SR

Figure 7.1 Styrene incompatibility chart obtained from CRW software

Next, the Chemical Reactivity Worksheet (CRW) was used to further analyze the incompatible pairs and provide screening guidance on possible mixing hazards of styrene and other chemical species. Figure 7.1 shows the incompatibility chart of stabilized styrene and possible contaminants predicted by CRW, where N stands for incompatible, C stands for a caution under certain conditions, and SR denotes the self-reaction of the chemical. The National Fire Protection Association (NFPA) ratings for the corresponding chemicals were also listed. As denoted in the chart, stabilized styrene is not compatible with the sodium hydroxide solution and sulfuric acid.

Furthermore, CRW suggests that caution needs to be taken when stabilized styrene is mixed with water. The CRW also identifies the self-polymerization nature of stabilized

styrene. However, CRW only provides a qualitative hazardous rating of stabilized styrene in contact with other chemicals, which can only be used as an estimate regarding thermal hazards identification and mitigation. More detailed and critical thermal safety indicators, including the onset temperature of unwanted exothermic activity, the overall heat generation, and the rate of temperature increment, still need to be experimentally evaluated. This information is essential in terms of designing the protection layers and developing mitigation measures for runaway reactions.

This study aims to carry out a quantitative assessment of the thermal runaway hazards of styrene in contact with water, alkaline, and acid in calorimeters. DSC and ARSST were employed to provide a comprehensive understanding of the thermal characteristic at both microgram and bulk scale.

7.2. Thermal Hazard Analysis of Styrene and Contaminants in DSC

The thermal behavior of styrene in contact with various contaminants was first investigated in DSC to obtain the preliminary results of heat generation information. The reaction mixture contained 5 mg of purified styrene and 1 mg of aqueous contaminant, including the deionized water (DI), 5N sulfuric acid (H_2SO_4), and 5N sodium hydroxide (NaOH). Due to the immiscible nature between styrene and the aqueous contaminants, a phase-separation of the reaction mixture was immediately noticed before the test, as shown in Figure 7.2. When the water phase was dispersed in the oil phase, it tended to form a spherical shape to reduce the surface area and minimize the system surface energy.[137] As a result, the effective contact between the water phase contaminants and

styrene was highly limited in the DSC cell, leading to poor mass transfer between the styrene and the contaminants.

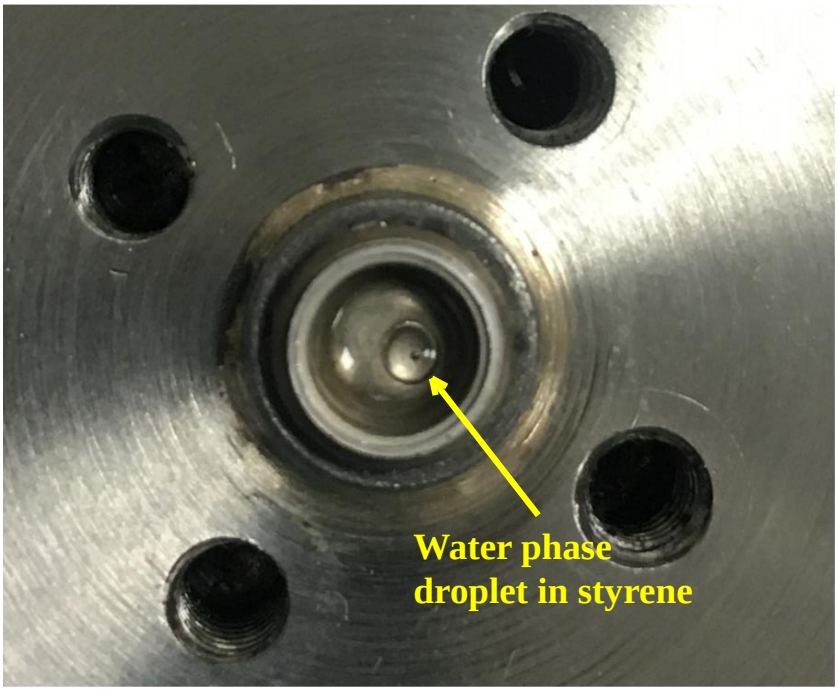

Figure 7.2 Phase separation of water phase contaminant in styrene

Figure 7.3 summarizes the typical thermal curves from DSC tests, describing the heat flow during the thermal runaway reaction of styrene in contact with various aqueous contaminants. For purified styrene without any contaminants, the exothermic thermal polymerization was first detected at around 101 °C, then the heat flow kept increasing, exhibiting multiple exothermic peaks before the end of the reaction. The maximum heat release was observed at a peak temperature of around 205 °C.

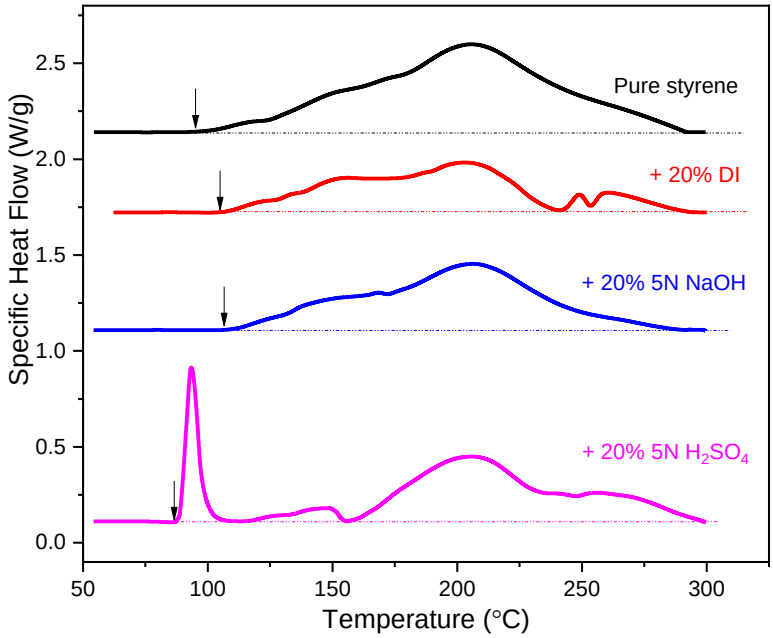

Figure 7.3 DSC results of polymerization heat release profile of styrene in contact with various contaminants

This multi-peak heat release behavior has also been observed by many other researchers,[77, 138] and was related to the complex thermal-initiated polymerization process of styrene. This thermal initiation process had a high initiation rate, and the most well-accepted mechanism was proposed by Mayo[48] and further developed by Hui and Hamielec[50] where the two styrene molecules dimerize to form a Diels-Alder adduct and initiate the polymerization. The heat of styrene polymerization obtained was 629.3 J/g, which was in good agreement with the literature value.[138] In the following cooling and re-heating process, no other exothermic peak was observed, denoting the polymerization was complete at the end of the heating process, and the 100% conversion of styrene monomer was achieved. The safety characteristic parameters including the initial exothermic onset temperature (T_0) and the heat of reaction (ΔH) were listed in Table 7.2.

Table 7.2 DSC results of polymerization of styrene in contact with contaminants

Contaminant	T_0 (°C)	ΔH (J/g)
None	101 (±1)	629 (±21)
Water	105 (±5)	313 (±11)
5N NaOH	116 (±7)	493 (±26)
5N H_2SO_4	84 (±7)	384 (±36)

With 20% of DI water (wt. to styrene) in the system, the thermal polymerization behavior of styrene significantly changed. First, the initiation of the exothermic reaction was slightly delayed as the onset temperature was 5 °C higher than the pure styrene. At the same time, the overall heat release significantly reduced to 313.4 J/g. This value denoted that only 50% of the styrene monomers polymerized. This DSC results revealed that by adding 20% of water into the system, the severity of the runaway reaction was strongly suppressed. It was reported by other researchers that water is an effective quenching agent to mitigate the polymerization thermal runaway.[139, 140] These results may be explained by the speculation that polymerization was "tempered" by the endothermic evaporization of water, which has a latent heat of as high as 2257 J/g.[141] At the same time, this two-phase mixture may possess different mass and heat transfer characteristics when compared to the pure styrene system, and thus affect the mobility and interaction of polymer chains.

While this experiment proved that adding water to the polymerization system is a valid practice to intervene the runaway reaction of styrene, it is not a universal practice

for all types of polymerization processes. For monomers that may react with water (e.g., ethylene oxide), adding water into the system may result in unexpected exothermic reactions,[81] and in which case, non-aqueous quenching materials need to be used.

The soluble species type also strongly affected the thermal behavior of styrene polymerization. With the presence of NaOH in water, the onset of exothermic was further delayed to around 116 °C. The heat of reaction was measured to be 492.8 J/g of styrene, which was only around 78% of the value of pure styrene. When the contaminant water contained 5 N of H_2SO_4, a sharp exothermic peak emerged at as early as 84 °C, lowering the onset temperature of the exothermic reaction by 20 °C. A series of other exothermic peaks following this early peak was also observed. The total heat of reaction for styrene in contact with the H_2SO_4 solution was higher than the case in contact with pure DI.

These experiments illustrated that the overall heat release of thermal polymerization was reduced when styrene was in contact with 20% water-based impurities under static mixing conditions regardless of the impurity type. A series of complex peaks were observed during the course of the polymerization, among which the 5N of sulfuric acid caused an early and sharp exothermic peak.

7.3. Thermal Hazard Analysis of Styrene and Contaminants in ARSST

7.3.1. Thermal Hazard Analysis of Styrene with Various Water Contents

The DSC tests only provide preliminary heat release information during the runaway polymerization when styrene and contaminants have minimal contact due to the phase separation. At the same time, the styrene/contaminant systems in DSC tests consisted of 20% (wt) of water, which may strongly affect the overall heat capacity and

other physical properties of the mixture. Therefore, it is crucial to conduct a thermal hazard assessment of the styrene/water system in other calorimeters to understand how water affects the thermal behavior of the runaway process. The ARSST tests enabled the pseudo-adiabatic evaluation of styrene/water mixtures in bulk quantity with magnetic stirring to enhance the inter-phase contact, in which case, mimics the real process vessel.

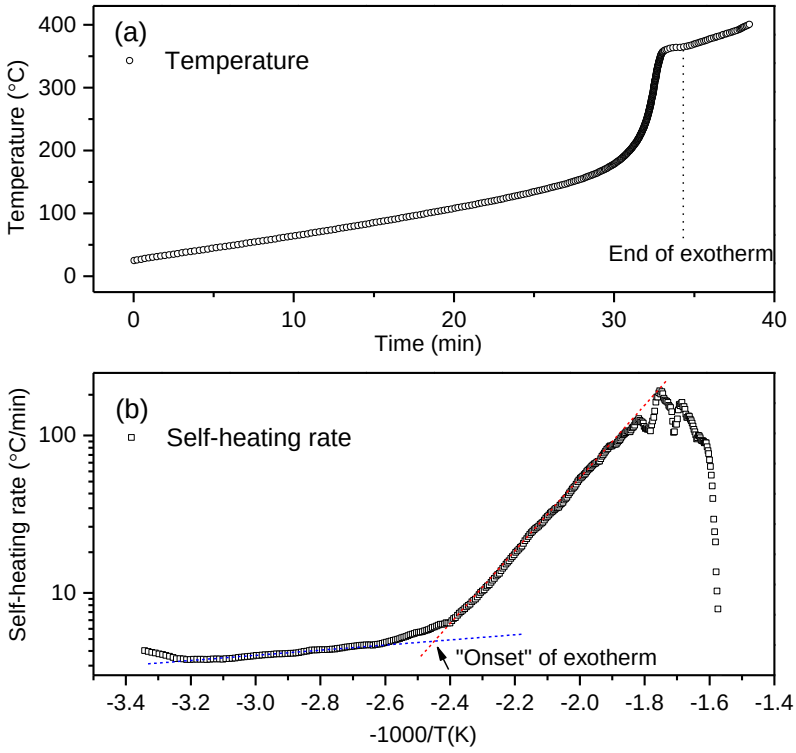

Figure 7.4 The thermal runaway polymerization of purified styrene in ARSST: (a) temperature profile as a function of time, (b) temperature rising rate

Figure 7.4 illustrated typical ARSST measurements of the pure styrene thermal polymerization process in ARSST. The pseudo-adiabatic temperature rise as a function of

time was recorded in Figure 7.4(a). The temperature-rising rate shown in Figure 7.4(b) was used to calculate the onset temperature (T_0) of the exothermic reaction as described by Wen [103] and discussed in section three.

The heat of polymerization (ΔH) was also obtained from the figure by multiplying the average reactant heat capacity with temperature rise and the thermal inertia factor (ϕ), as defined in Equation (33).

$$\Delta H = C_p \cdot \varphi \cdot (T_{max} - T_0) \tag{33}$$

For purified styrene without any contaminants, the exothermic polymerization onset temperature was observed at around 136 °C from three identical repetition tests. The difference between the onset temperature obtained from DSC and ARSST denoted that the onset threshold value strongly depends on the instrument sensitivity, the experiment procedure by which the test is performed, and the calculation process adopted.[142] The heat of styrene polymerization obtained from ARSST was 674 J/g, which was in agreement with the value in the DSC tests (629 J/g) and APTAC tests (708 J/g). It was denoted that the pseudo-adiabatic calorimeter provided a more conservative estimate on the heat release when compared to the data from DSC tests, as the heat loss to the environment is compensated by larger sample size used and corrected by the thermal inertia factor. However, although the cell and containment vessel was pressurized before heating, the evaporization of the reactant still tempered the reaction and resulted in a lowered overall heat of reaction when compared to APTAC.

The thermal behavior of the styrene/water systems were tested in the ARSST at different water loadings. Around 5 g of purified styrene was mixed with DI with a weight

ratio of the aqueous phase to styrene varied from 0% to 20%. All tests were carried out under the protection of 300 psig nitrogen and continuous stirring, as described in the experimental section. Figure 7.5 summarizes the temperature rate during the thermal polymerization of the styrene/water mixtures utilizing the same heating power.

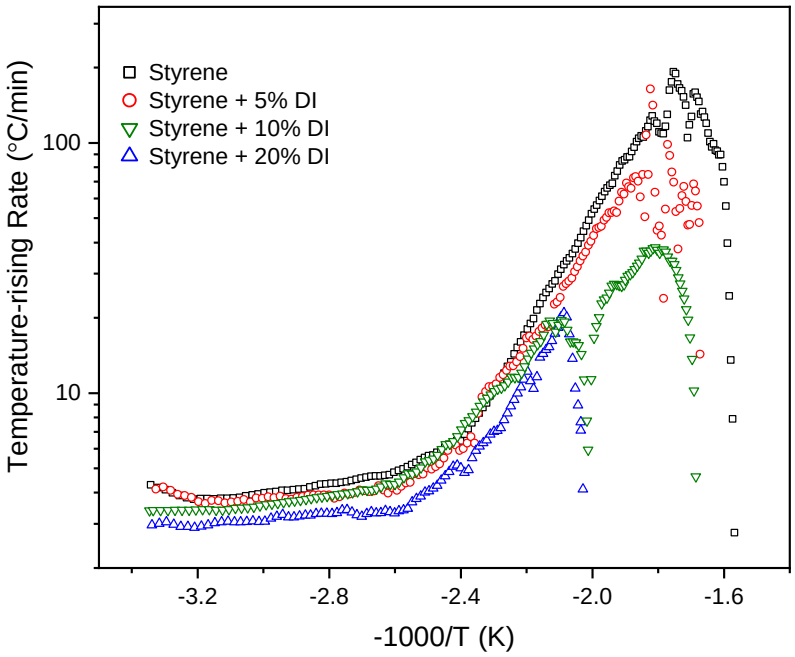

Figure 7.5 The thermal runaway behavior of styrene with various water contents in ARSST

With 5% water in contact with styrene, the maximum temperature was lowered by 25 °C, resulted in a minor drop in the overall heat generation to 640 J/g. At the same time, the temperature rate during almost the entire polymerization process was reduced, denoting 5% of water significantly lowered the overall polymerization reaction rate. When the water addition increased to 10%, the decrease of the temperature rate was most

significant at higher temperatures after 200 °C. Further addition of water to a weight ratio of 20% prohibited the polymerization at the high-temperature range over 220 °C.

As can be noticed from the temperature curve, with 20% of water present, the heat generated from the exothermic polymerization reaction was not sufficient to sustain the polymerization at higher temperatures, and the reaction stopped at around 220 °C before the complete conversion of the polymerization. The overall reaction heat for 20% water in styrene was calculated to be 377 J/g, which resulted in a final conversion of 56%. This value was in good agreement of the conversion obtained from the DSC runs, denoting that approximately the same reaction extent was achieved for the styrene/20% water system regardless of system scale and mixing condition. The ARSST test results further confirmed that adding water into the styrene polymerization system under a near-adiabatic condition mitigated the overall thermal hazard. 20% of water addition was effective in prohibiting the propagation of the polymerization reaction above 220 °C. As discussed in the previous section, the retardation could be explained by the tempering effect of water due to its high latent heat and heat capacity. In addition to that, when mixing was available, and water was dispersed in the styrene as a discontinuous phase, system viscosity, mass transfer, and heat transfer behavior might have significantly changed when compared to the pure styrene system. It is well accepted that the gel-effect played a critical role in the auto-accelerated polymerization and thermal runaway of styrene due to the viscosity change and heat transfer difficulties.[79, 143] The retarded polymerization with the presence of water might be the consequence of reduced system viscosity and enhanced heat/mass transfer.

7.3.2. Thermal Hazard Analysis of Styrene with Acid and Alkaline Solution

The thermal runaway behavior of styrene in contact with water discussed in the previous section provides a baseline to understand the contamination effect of aqueous impurities on the polymerization of styrene. Following that, ARSST tests were carried out for styrene in contact with water containing 5 N H_2SO_4 or 5 N NaOH. The weight ratio of water with respect to styrene was fixed at 5% to minimize the quenching effect of water.

The temperature rate during the thermal polymerization of the mixtures was displayed in Figure 7.6. Corresponding runaway characteristics including the onset temperature (T_0), the overall heat of the reaction (ΔH), the maximum temperature rate $(dT/dt)_{max}$, the peak pressure-rising rate $(dP/dt)_{max}$, and the maximum reaction pressure (P_{max}) are summarized in Table 7.3. Kinetic fitting was also carried out on the temperature rate to obtain the kinetic parameters by adopting the pseudo-first-order model developed by Townsend and Tou.[99] The maximum temperature (T_f), the temperature rate (dT/dt) and the system temperature (T) were used to calculate the apparent reaction rate coefficient (k) as expressed in Equation (19). Thus, the activation energy (E_a), the pre-exponential factor (A) for runaway reactions was derived from the Arrehuis equation, as also shown in Equation (19) and Equation (20), where R is the gas constant.

$$k = \frac{dT}{dt} \cdot \left(\frac{1}{T_f - T} \right) \tag{19}$$

$$\ln \left(\frac{dT}{dt} \right)_0 = \ln(A \cdot \Delta T_{\mathrm{ad}}) - \frac{E_a}{R} \left(\frac{1}{T} \right) \tag{20}$$

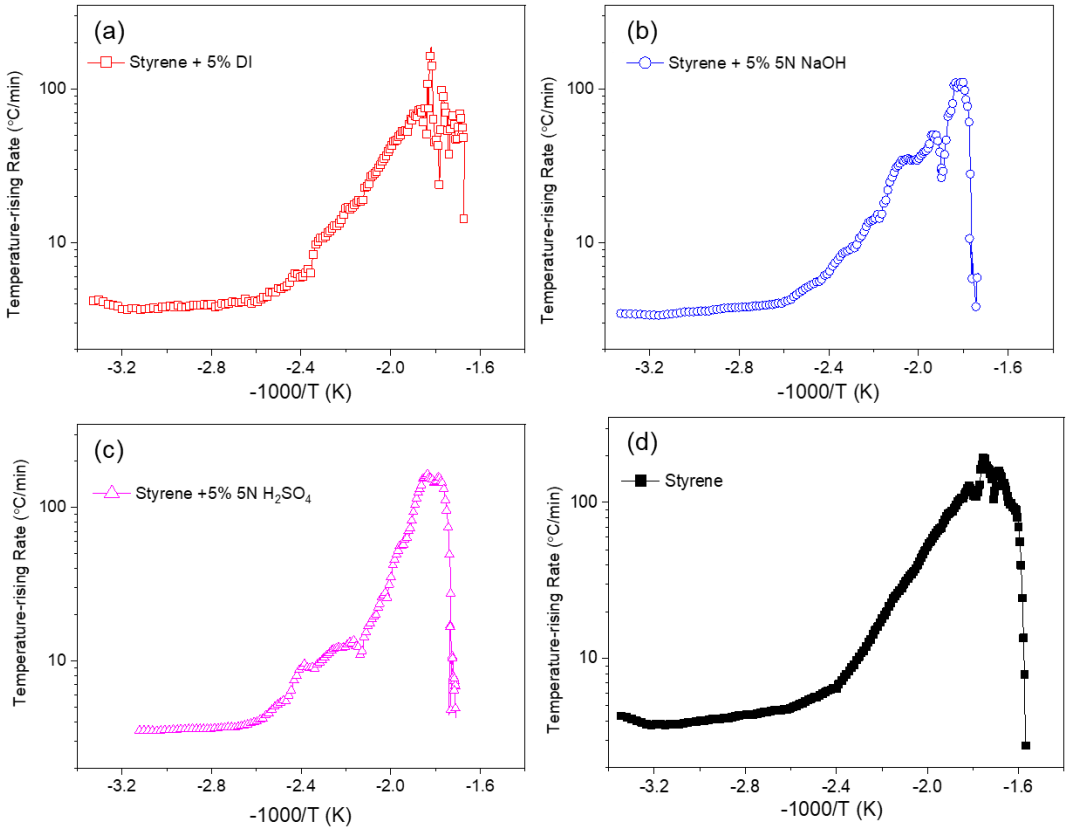

Figure 7.6 The temperature-rising rate of styrene in contact with 5% aqueous contaminants in ARSST

The mixture system with styrene and 5% water was used as the baseline to understand how solute type affected the thermal behavior during the polymerization. With only 5% of the water in the system, the quenching effect was minimized. When NaOH was dissolved in the water phase, the temperature rate, shown in Figure 7.6(b), had a similar trend with the sample contains 5% pure water. The onset temperature, overall heat of reaction, and the activation energy also remained roughly the same.

When the active component in 5% water was H_2SO_4, in contrast, the temperature rate during the polymerization showed a substantial change. Two distinct exothermic peaks emerged with a slightly lowered onset temperature for the first peak at around 123 °C, as shown in Figure 7.6(c).

Table 7.3 Thermal runaway results of styrene in contact with different contaminants in ARSST

Contaminant	T_0 **(°C)**	**ΔH (J/g)**	E_a **(kJ/mol)**	dT/dt_{max} **(°C/min)**
None	136 (±1)	674 (±31)	62 (±4)	203(±24)
5% Water	125(±3)	640 (±11)	56 (±1)	186 (±6)
5% 5N NaOH	127(±4)	617 (±84)	59 (±7)	115 (±23)
5% 5N H_2SO_4	123(±3)	609 (±50)	1st peak 38(±3) 2nd peak 98 (±7)	223 (±23)

Meanwhile, the temperature rate for the first peak between onset and 180 °C was significantly higher than the styrene/5% water system. This observation was consistent with the results obtained in the DSC tests that H_2SO_4 solution promoted early stage of thermal polymerization. ARSST results further confirmed that this promoting effect could be observed even when the mass ratio of the acid was low. By fitting the temperature rate data to the initial and late peak, the corresponding kinetic parameters were obtained for both peaks and listed in Table 7.3. The activation energy of the first stage was calculated to be 37.8 kJ/mol. This significantly dropped activation energy denoted a lowered energy

barrier and a more sensitive response of reaction rate to temperature change. In this case, the H_2SO_4 acted like a catalyst that effectively lowered the energy required to initiate the thermal polymerization. This styrene/5% 5N H_2SO_4 system also showed the highest maximum temperature rising rate compared to styrene and other mixtures tested in ARSST, as summarized in the Table. The peak pressure for all samples remained roughly constant at around 345 psi, and the maximum pressure-rising rate showed no substantial change with contaminant type. The highest pressure rate obtained was around 38 psi/min.

The activation energy from the test was used to estimate the time to the maximum rate (TMR) using Equation (34) for any given storage temperatures.[144-146] The data obtained, assuming the styrene-contaminant system was stored at 323 K (50 °C) are summarized in Figure 7.7. This value is a critical indicator representing how much time was required for the system to develop to its maximum reaction rate under specific storage conditions. For a given temperature of 50 °C, when 5% of 5 N sulfuric acid get in contact with the styrene, the time to maximum rate reduced by around 50%, denoting the thermal stability of the monomer was strongly impacted, and the acid solution promoted the unintended thermal runaway reaction. DI showed no substantial effect on the storage safety of styrene, while the presence of caustic solution slightly retarded the polymerization.

$$\ln \mathrm{TMR}_{ad} \cong \frac{E_a}{RT} - \ln A \tag{34}$$

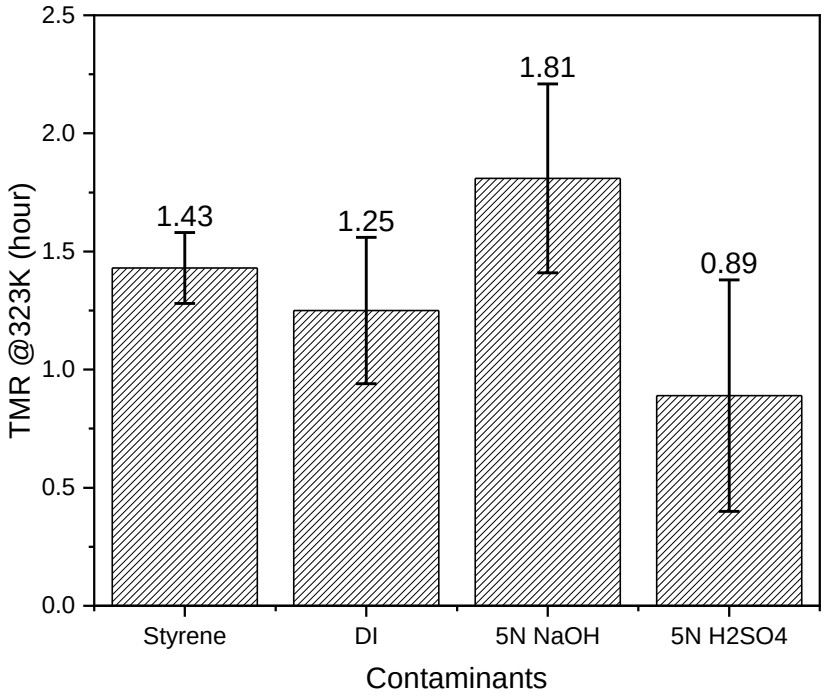

Figure 7.7 The calculated TMR for the styrene-contaminant system under 323 K

7.3.3. The Instantaneous Mixing Hazards of Styrene and Concentrated Acid

Both DSC and ARSST experiments had confirmed that 5N H_2SO_4 promoted the thermal polymerization of styrene at the early stage. The onset temperature was lowered by 20 °C when the acid solution and styrene were in static contact in DSC. The exothermic temperature rate was significantly elevated when the acid solution and styrene were under continuous stirring in ARSST. It is critical to conduct further experiments to understand how concentrated H_2SO_4 would affect the thermal polymerization of styrene to represent the worst-case contamination scenario.

DSC tests were first attempted to screen the contamination effect between styrene and concentrated (98%) H_2SO_4. It was noticed that when the 98% H_2SO_4 was dropped

into the DSC cell that containing purified styrene, the mixture instantaneously reacted upon contact, releasing a large amount of heat and the styrene gelled up in the DSC cell within a short period of time. Thus, the DSC test could not be performed for this system.

An open-cup mixing (injection) experiment was conducted in ARSST according to the procedure stated in the experimental section to further analyze the thermal hazard of styrene in contact with 98% H_2SO_4. The temperature trajectory is shown in Figure 7.8.

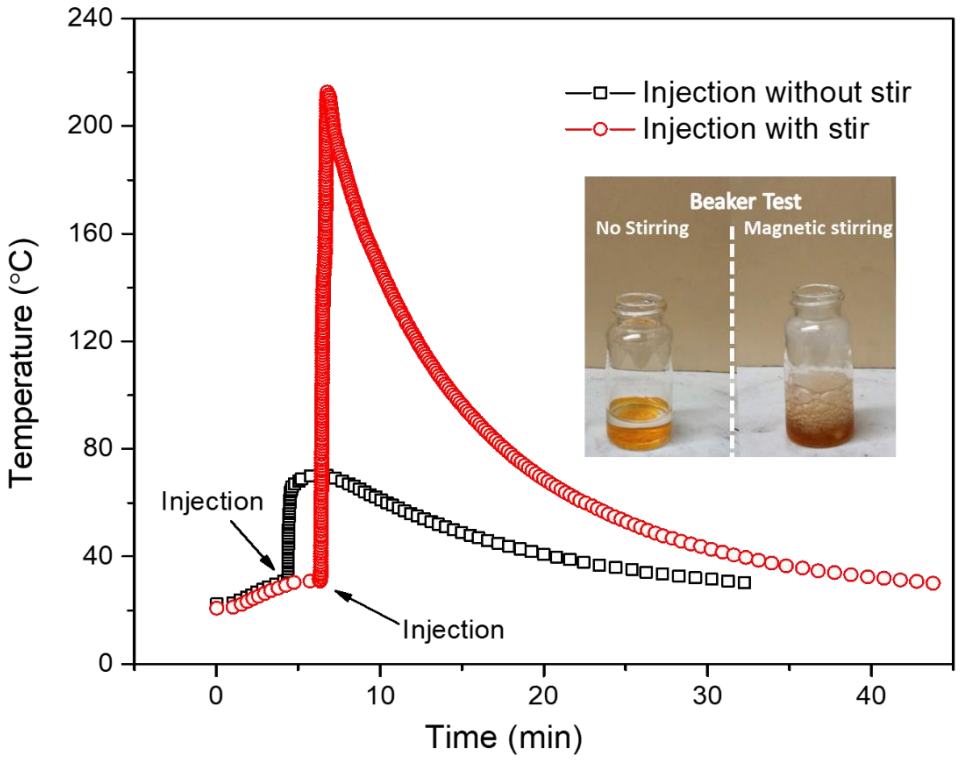

Figure 7.8 The thermal hazards of styrene in contact with 98% sulfuric acid upon mixing

It was noticed that the thermal hazard of the system upon contact was strongly affected by the mixing condition. When 0.2 g of 98% H_2SO_4 was dropped into 4 g of styrene under a static condition, the temperature instantaneously rose, and the maximum temperature during the mixing was measured to be 60.8 ± 8.5 °C. The inserted digital photography depicted how the reactant changed by conducting the identical mixing experiment in an open vail (beaker test).

When the concentrated sulfuric acid was added into purified styrene without stirring, no boiling was observed as the peak temperature was well below the boiling point of styrene, which is 146 °C.[147] A clear phase-separation was also observed in the vail that brownish product precipitated at the bottom. On the contrary, when concentrated sulfuric acid was dropped into styrene under vigorous magnetic stirring (300 RPM), the reaction was violent and explosive. The system temperature spontaneously increased above the boiling point of styrene to a maximum of around 183.9 ± 26.2 °C, leading to the boiling of the reactant mixture.

The violent reaction between styrene and concentrated sulfuric acid has also been observed by Tsuda[148] at temperatures as low as −78 °C when methylene chloride was used as the solvent. Asami and Tokura further confirmed the "flash polymerization" of styrene in the presence of 98% sulfuric acid in liquid sulfur dioxide at 0 °C.[149] This rapid, non-stationary polymerization catalyzed by sulfuric acid has been identified to follow the cationic polymerization pathway with an extremely fast initiation process.[150, 151] The sudden, explosive temperature rise observed during the mixing test in ARSST was in consistent with the cited literature. Furthermore, the experiment revealed that the thermal

severity of the polymerization (maximum temperature, gas generation) was strongly enhanced by the stirring.

A possible explanation for the lowered thermal hazard under static conditions may be the coating of the active catalyst by product oligomers. It was supposed that when the concentrated sulfuric acid droplets got in contact with styrene, the oligomer was produced instantaneously at the surface of the droplet, and then acted as an insulation layer to separate the active sulfuric acid from unreacted styrene. Due to the high chain-transfer and termination rate, the chain growth quickly stopped. At the same time, as the maximum temperature under no-stirring condition was significantly lower than the normal initiation temperature of the thermal polymerization of styrene, no further polymerization was observed. While under vigorous stirring, the sulfuric acid droplet was well dispersed into smaller droplets, and thus resulted in more reaction sites. With continuous stirring, the fast polymerization reaction was not hindered by the mass transfer, and tri-folded temperature rise was observed, which would adequately represent the worst-case scenario of styrene in contact with concentrated sulfuric acid.

7.4. Conclusions

In this section, both differential scanning calorimeter (DSC) and advanced reactive system screening tool (ARSST) were used to investigate the thermal incompatibility between styrene and various contaminants under different mixing conditions. The static contact between styrene and 20% aqueous contaminants in DSC showed a significantly lowered heat release during the polymerization, which might be caused by the tempering effect caused by water evaporation. When 5 N sulfuric acid was dissolved in water, the

polymerization reaction initiated at a reduced temperature with rapid heat release, denoting the promotion effect of sulfuric acid on styrene polymerization. The ARSST test of styrene in contact with various amounts of water further confirmed the quenching effect of water on the runaway polymerization when the weight ratio of water was higher than 5%. The incompatibility study in ARSST with 5% aqueous contaminants under constant stirring denoted that 5 N sodium hydroxide had a trivial effect on the thermal polymerization of styrene. At the same time, 5 N sulfuric acid lowered the energy barrier of the polymerization and elevated the maximum temperature rising rate, which significantly increased the thermal hazard of the system.

The open-cup mixing test between concentrated sulfuric acid and styrene showed an explosive runaway reaction with a rapid temperature increase. Under the worst-case-scenario, the instantaneous boiling of the reactant and a temperature-rise over 150 °C was observed when continuous stirring was present. It is concluded that the sulfuric acid promoted the thermal runaway polymerization of styrene, and the severity of the reaction depended on the mixing condition and the concentration of the acid. In order to prevent the unintended thermal runaway of styrene, the monomer should be kept away from sulfuric acid.

8. CONCLUSIONS AND FUTURE WORK

8.1. Conclusions

In this work, a comprehensive thermal hazard analysis was conducted to investigate the unintended thermal runaway polymerization of the styrene. Styrene is one of the most critical reactive monomers to produce polystyrene and other copolymers and has caused a significant number of major incidents that lead to injuries and fatalities. The processing of styrene monomer and the production of polystyrene are naturally hazardous, and the thermal and pressure hazards associated with these processes need to be carefully evaluated to provide guidance to enhance the safety management of these processes.

This research advanced the understanding of the thermal runaway polymerization hazards of styrene under various scenarios. A systematic fault-tree-analysis was first conducted based on the kinetics to identify the root causes of runaway incidents. Following that, calorimetric evaluation and kinetic modeling were performed to obtain quantitative assessment regarding different hazardous scenarios. Screening calorimeter (DSC), pseudo-adiabatic calorimeter (ARSST), and adiabatic calorimeter (APTAC) were adopted to assess the safety indicators during the runaway polymerization of the styrene system.

Major findings regarding the thermal hazard analysis of the styrene system are listed as follows:

1) By adopting the fault-tree-analysis of the styrene polymerization system, three direct causes that lead to unintended runaway polymerization were identified,

including fast initiation, fast propagation, and slow termination. The root causes associated with these direct causes were identified to be the deviations from a normal recipe. For the complex styrene polymerization system, deviation in inhibitor concentration, solvent concentration, initiator type, initiator concentration, and contaminant species was concluded to be the most credible scenarios triggering a hazardous thermal runaway event.

2) Two inhibitor removal methods were experimentally investigated regarding the inhibitor removal efficiency and their corresponding impact on the thermal runaway hazards of thermally initiated polymerization of styrene. The presence of 4-tert-butylcatechol (TBC) effectively retarded the thermal polymerization of styrene by delaying the onset of an exothermic reaction. Washing styrene with caustic solution promoted the reversible hydrolysis of TBC and thus reduced the TBC concentration in the monomer. Passing the styrene through an aluminum oxide-packed column, on the contrary, effectively removed all the inhibitor from the monomer. DSC results revealed that the onset of thermal polymerization of styrene was delayed by over 50 °C when TBC was present. The adiabatic temperature rise obtained from the APTAC test showed that the overall heat release was reduced by 55% when TBC was not properly removed. The experiment suggested that the elimination of inhibitor was a prerequisite regarding the accurate assessment of the thermal runaway hazards of the styrene system.

3) The effect of thermal inertia factor on the adiabatic thermal runaway test was investigated to locate the optimum sample size in an APTAC test. When 9 g of purified styrene was loaded in a 25 mL glass test cell, the thermal inertia factor of 1.26 was achieved.
4) Both screening and adiabatic calorimeters were adopted to study the effect of styrene mass fractions on the thermally initiated polymerization runaway hazards of the styrene-ethylbenzene system. The addition of diluent effectively reduced overall heat release by affecting the late stage of the reaction at higher temperatures (> 150 °C) in the DSC test. Under the adiabatic condition, the styrene had an explosive thermal runaway reaction after around 150 °C, and the addition of diluent significantly reduced the overall heat release and prolonged the time to the maximum rate (TMR). Both the self-heating rate and the pressure-rising rate exponentially reduced with the addition of diluent. However, when the monomer was diluted in ethylbenzene to 85%, the presence of volatile species resulted in a higher pressure-rise during reaction runaway compared to the pure styrene system even at lower temperatures.
5) Kinetic modeling was conducted to simulate the temperature and pressure profile of the thermally initiated polymerization of styrene in the presence of a diluent. Hui & Hamielec model was adopted for the temperature correlation, while the Flory free-volume theory was utilized to generate the pressure profile. The lumped model showed a good agreement with the adiabatic data

and suggested the vapor pressure of the volatile diluent was the culprit of total pressure building up.

6) A novel modulated differential screening calorimetry (MDSC) method was used to investigate the thermal decomposition hazards of two initiators (BPO and AIBN) used in the initiator-styrene-ethylbenzene system. MDSC method enabled an accurate assessment of the onset temperature of initiator decomposition by decoupling the overlapping heat effect of endothermic phase change and exothermic decomposition reaction. The non-reversing heat flow from the MDSC denoted the onset temperature of solid BPO and AIBN was 103 °C and 100 °C. When dissolved in ethylbenzene at 5% (wt.), the exothermic thermal decomposition of both initiators was noticed at a much lower temperature between 71 °C and 85 °C. The ASTM E698 Ozawa method was utilized to fit the kinetic experiment data, and the activation energy of the initiator decomposition reaction was 79.7 kJ/mol for BPO and 108.1 kJ/mol for AIBN.

7) The thermal behavior of the initiator-styrene-ethylbenzene system was calorimetric analyzed under a series of initiator mischarging scenarios. The thermal profile during the runaway reaction was strongly altered by the addition of the initiator exceeding the normal recipe. The major exothermic peak shifted to a lower temperature upon the addition of both initiators, as well as the onset of the exothermic reaction. A synergetic effect was observed in

the BPO-styrene-ethylbenzene system that the ternary system had the lowest onset temperature of around 70 °C.

8) The adiabatic runaway test on the initiator-styrene-ethylbenzene ternary system demonstrated that the addition of initiators lowered the onset temperature of the polymerization reaction to around 70 °C. The shifting of major exothermic peak reduced the time to maximum rate by over 100 min, and the maximum pressure and temperature rising rate were mitigated by the presence of 500 ppm of initiators. Mischarging of both initiators to over 10000 ppm resulted in a sudden and acute increase of initial reaction rate and temperature/pressure rising rate.
9) The incompatibility between purified styrene and contaminants was first screened using the Chemical Reactivity Worksheet (CRW) and the calorimetrically evaluated in both DSC and ARSST. The screening calorimeter assessed the runaway behavior of styrene mixed with contaminants under static conditions. When the aqueous contaminant solution contained 5 N of sulfuric acid, an early and sharp exothermic peak was noticed at 84 °C. The presence of water or the caustic solution containing 5N sodium hydroxide exhibited a tempered runaway reaction with less heat release in the DSC test.
10) ARSST tests were carried out to assess the incompatibility hazards between styrene and contaminants under vigorous mixing to enhance heat/mass transfer. The ramped heating test confirmed that 5 N sulfuric acid promoted the onset of the styrene thermal polymerization. The onset temperature was

lowered by 13 °C with the presence of the sulfuric acid solution. The pseudo-first-order reaction model revealed that the activation energy of the reaction was lowered by over 30 kJ/mol.

11) An instantaneous, explosive polymerization reaction was identified upon the mixing of styrene and concentrated sulfuric acid. The severe incompatibility thermal hazard was quantified with an injection experiment in ARSST under different mixing conditions. During the worst-case-scenario that the concentrated sulfuric acid contacted with styrene under vigorous mixing, the instantaneous boiling of the reactant and a temperature-rise over 150 °C was observed.

In summary, this work first adopted the fault-tree-analysis to identify the root causes for a runaway polymerization incident for a complex reaction system involving reactive monomer, inhibitor, initiator (s), and solvent. This top-down method enabled the discovery of underlying causes regarding a runway event. Four hazardous scenarios were investigated in various calorimeters to obtain quantitative hazard information, including the onset temperature of the runaway reaction, the temperature rise, the pressure rise, the time to the maximum rate, and the rate of temperature/pressure building up. These safety indicators were further used to fit into kinetic models to generate important reaction kinetic parameters. The calorimetric data and kinetic model obtained in this research would serve as guidance regarding the design of a safer process and installation of protection layers.

8.2. Recommendations for Future Work

This section summarizes the recommendations for future work to solve the challenges facing by current research. Research opportunities to enhance data quality and fulfill the gaps between calorimeters and industrial vessels are presented below.

8.2.1. Calorimetric Analysis

One primary concern regarding the calorimetric analysis of the polymerization reaction system is the control of the atmosphere. In this research, the stainless-steel DSC capsule was sealed in the open air, and the headspace containing oxygen might dissolve into the purified and purged styrene along with the test. Frurip[152] and other researchers[153] developed a capillary glass tube with exceptionally high mechanical strength (up to 21 MPa) and the capability to precisely control the headspace gas composition. Further modification on the glass sample capsule and the detailed 3-D design was documented by Min[154]. Adopting this glass-capillary sample cell and sealing the cell under nitrogen would rule out the oxygen from the system and enhance the data quality of the DSC test.

Moreover, the experimental results regarding the incompatibility study between styrene and contaminants revealed that the thermal behavior was strongly impacted by the mass transfer between different species. The auto-acceleration of the polymerization reaction was also the result of enhanced viscosity and reduced mass transfer at higher conversion. This research adopted magnetic stirring in adiabatic and pseudo-adiabatic calorimetric tests, which might not be powerful enough to stimulate the system after the polymer solution gelled up. The calorimeters used in this research were not capable of conducting mechanical stirring. In order to study the mixing effects on the thermal hazards

of styrene runaway polymerization, reaction calorimeters (RC1e) with mechanical stirring and in-line product analysis probe shall be used.

8.2.2. Kinetic Modeling and Process Simulation

In this research, a simplified pseudo-first-order model was used to process the adiabatic data and obtain the overall activation energy of the polymerization process. For the purified styrene or styrene-ethylbenzene system that the self-heating plot showed only one exothermic peak, this method was able to capture the kinetic information by relating the initial temperate-rising rate to the reciprocal of temperature. However, for the ternary system consisted of initiator-styrene-ethylbenzene, multiple exothermic peaks emerged on the self-heating plot, suggesting a complex reaction scheme. A more detailed kinetic model needs to be developed to fit the adiabatic thermal runaway data.

The multi-peak behavior was also observed for all the monomer-containing reaction systems tested in DSC under 4 °C/min. The Kissinger kinetic modeling of the DSC data was only performed on the thermal decomposition of the initiators, where only one exothermic peak was observed on the heat flow diagram. For this complex reaction system with overlapping reaction steps, the International Confederation for Thermal Analysis and Calorimetry (ICTAC)[155]has suggested applying a model-free (iso-conversional) method to obtain the relationship between the activation energy and the reaction extent. A more recent study by Muravyev[156] compared different kinetic models that utilizing deconvolution or model-free kinetic methods to deal with the overlapping heat effect. These kinetic modeling methods can be applied to the styrene-containing reaction system after the heat flow data is obtained under other heating rates.

8.2.3. Risk Matrix

In this work, different hazardous scenarios regarding the runaway polymerization of the styrene system were analyzed using calorimetry and kinetic modeling. The results enhanced the understanding of the inherent hazard associated with the system and can be further adapted to assess the "thermal risk" of a polymerization process. The risk of a process, defined as the product of the severity of an incident by the frequency of incident occurrence, is used to describe the chance that a catastrophic runaway incident will happen. Stoessel[157] has proposed a method to relate the incident consequence to the overall adiabatic heat release, while the probability (frequency) is represented by the time to the maximum rate.

A case study can be carried out on an industrial scale process vessel by combining our data with the thermal risk methodology. With a given process with size, operation, and safety protection layer (relief valve) specifications, the kinetic obtained in this study can be adopted to predict the thermal and pressure behavior of runaway events. Following that, these data can be further used to obtain the severity and probability information of the system and eventually generate a risk matrix.

REFERENCES

1. Johnson, R. W.; Rudy, S. W.; Unwin, S. D. *Essential practices for managing chemical reactivity hazards*. John Wiley & Sons: 2010; Vol. 17.

2. Center for Chemical Process Safety. *Guidelines for safe storage and handling of reactive materials*. John Wiley & Sons: 2010.

3. Lees, F. *Lees' Loss prevention in the process industries: Hazard identification, assessment and control*. Butterworth-Heinemann: 2012.

4. Liu, Y.-S.; Rogers, W. J.; Mannan, M. S. Screening reactive chemical hazards. *Chemical Engineering Progress* **2006,** *102* (5), 41-47.

5. Barton, J.; Nolan, P. Incidents in the chemical industry due to thermal runaway chemical reactions. *Hazards X: Process Safety in Fine and Speciality Chemical Plants* **1989,** *115*, 3-18.

6. Chemical Safety Board. *Improving reactive hazard management*. US Chemical Safety and Hazard Investigation Board: 2002.

7. Sales, J.; Mushtaq, F.; Christou, M.; Nomen, R., Study of major accidents involving chemical reactive substances: analysis and lessons learned. *Process Safety and Environmental Protection* **2007,** *85* (2), 117-124.

8. Mihailidou, E. K.; Antoniadis, K. D.; Assael, M. J. The 319 major industrial accidents since 1917. *International Review of Chemical Engineering* **2012,** *4* (6), 529-540.

9. Saada, R.; Patel, D.; Saha, B. Causes and consequences of thermal runaway incidents—will they ever be avoided? *Process Safety and Environmental Protection* **2015,** *97*, 109-115.

10. Ibeh, C. C., *Thermoplastic materials: properties, manufacturing methods, and applications*. CRC Press: 2011.

11. Besserman, J.; Mentzer, R. A. Review of global process safety regulations: United States, European Union, United Kingdom, China, India. *Journal of Loss Prevention in the Process Industries* **2017,** *50*, 165-183.

12. Leggett, D. J. Safe process development from reaction hazards testing. *Thermochimica Acta* **2001,** *367*, 351-365.

13. Center for Chemical Process Safety. *Guidelines for engineering design for process safety*. John Wiley & Sons: 2012.

14. Center for Chemical Process Safety. *Guidelines for chemical reactivity evaluation and application to process design*. John Wiley & Sons: 1995.

15. National Fire Protection Association. *Standard system for the identification of the hazards of materials for emergency response*. National Fire Protection Association: 2017.

16. Lewis, R. J.; Sax, N. *Sax's dangerous properties of industrial materials*. New York: 1996; Vol. 8.

17. Carson, P. A. *Hazardous chemicals handbook*. Elsevier: 2002.

18. Bretherick, L. *Bretherick's handbook of reactive chemical hazards*. Elsevier: 2016.

19. Pohanish, R. P.; Greene, S. A. *Wiley guide to chemical incompatibilities*. John Wiley & Sons: 2009.

20. Melhem, G.; Shanley, E. On the estimation of hazard potential for chemical substances. *Process Safety Progress* **1996,** *15* (3), 168-172.

21. Lothrop, W. C.; Handrick, G. R. The relationship between performance and constitution of pure organic explosive compounds. *Chemical Reviews* **1949,** *44* (3), 419-445.

22. Shanley, E.; Melhem, G. The oxygen balance criterion for thermal hazards assessment. *Process Safety Progress* **1995,** *14* (1), 29-31.

23. Murphy, M. R.; Singh, S. K.; Shanley, E. S. Computationally evaluate self-reactivity hazards. *Chemical Engineering Progress* **2003,** *99* (2), 54-61.

24. Shanley, E. S.; Melhem, G. A. A review of ASTM CHETAH 7.0 hazard evaluation criteria. *Journal of Loss Prevention in the Process Industries* **1995,** *8* (5), 261-264.

25. Grewer, T.; Frurip, D. J.; Harrison, B. K. Prediction of thermal hazards of chemical reactions. *Journal of Loss Prevention in the Process Industries* **1999,** *12* (5), 391-398.

26. Pasturenzi, C.; Dellavedova, M.; Gigante, L.; Lunghi, A.; Canavese, M.; Cattaneo, C. S.; Copelli, S. Thermochemical stability: a comparison between experimental and predicted data. *Journal of Loss Prevention in the Process Industries* **2014,** *28*, 79-91.

27. Center for Chemical Process Safety. *Guidelines for chemical reactivity evaluation and application to process design*. American Institute of Chemical Engineers: 1995.

28. Rowe, S. M. Thermal stability: a review of methods and interpretation of data. *Organic Process Research & Development* **2002,** *6* (6), 877-883.

29. Donoghue, E. Identifying hazardous chemical reactivity. *Journal of Thermal Analysis* **1997,** *49* (3), 1609-1616.

30. Gustin, J. Thermal stability screening and reaction calorimetry. Application to runaway reaction hazard assessment and process safety management. *Journal of Loss Prevention in the Process Industries* **1993,** *6* (5), 275-291.

31. Frurip, D.; Chakrabarti, A.; Hofelich, T.; Martinez, S.; Whiting, L. Hazard evaluation of polymerizable compounds. *Process Safety Progress* **1995,** *14* (2), 79-86.

32. Melville, H.; Watson, W. Inhibition and retardation in polymerisation reactions. *Transactions of the Faraday Society* **1948,** *44*, 886-905.

33. Riga, A. T. Inhibitor selection for vinyl monomers by differential scanning calorimetry. *Polymer Engineering & Science* **1976,** *16* (12), 836-840.

34. Cohen, S. G. Inhibition and retardation of the peroxide initiated polymerization of styrene. *Journal of the American Chemical Society* **1947,** *69* (5), 1057-1064.

35. Darvishi, A.; Rahimpour, M. R.; Raeissi, S. A theoretical and experimental study for screening inhibitors for styrene polymerization. *Processes* **2019,** *7* (10), 677.

36. Liao, C.; Wu, S.; Su, T.; Shyu, M.; Shu, C. Thermokinetics evaluation and simulations for the polymerization of styrene in the presence of various inhibitor concentrations. *Journal of Thermal Analysis and Calorimetry* **2006,** *85* (1), 65-71.

37. Kirchner, K.; Rintelen, T. Continuous free-radical polymerization of styrene in the stirred tank reactor: Effect of retarders. *Applied Macromolecular Chemistry and Physics* **1986,** *141* (1), 85-93.

38. Chen, S. A.; Tsai, L. C. Kinetics and mechanism of inhibition of an antioxidant type inhibitor in free radical vinyl copolymerizations. *Macromolecular Chemistry and Physics* **1986,** *187* (3), 653-666.

39. Allen, T. L. Oxygen inhibition of the polymerization of styrene. *Journal of Chemical Technology and Biotechnology* **1954,** *4* (6), 289-290.

40. Batch, G. L.; Macosko, C. W. Oxygen inhibition in differential scanning calorimetry of free radical polymerization. *Thermochimica Acta* **1990,** *166* (Supplement C), 185-198.

41. Walling, C.; Briggs, E. R. The thermal polymerization of methyl methacrylate. *Journal of the American Chemical Society* **1946,** *68* (7), 1141-1145.

42. Flory, P. J. *Principles of polymer chemistry*. Cornell University Press: 1953.

43. Wünsch, J. R. *Polystyrene: Synthesis, production and applications*. Smithers Rapra Publishing: 2000; Vol. 112.

44. Chen, C. C. Continuous production of solid polystyrene in back-mixed and linear-flow reactors. *Polymer Engineering & Science* **2000,** *40* (2), 441-464.

45. Mark, H. *Encyclopedia of polymer science and technology, 15 volume set*. Wiley New York: 2014; Vol. 14.

46. Scheirs, J.; Priddy, D. *Modern styrenic polymers: polystyrenes and styrenic copolymers*. John Wiley & Sons: 2003; Vol. 6.

47. Mishra, M.; Yagci, Y. *Handbook of vinyl polymers: radical polymerization, process, and technology*. CRC press: 2016.

48. Mayo, F. R. The dimerization of styrene. *Journal of the American Chemical Society* **1968,** *90* (5), 1289-1295.

49. Flory, P. J. The mechanism of vinyl polymerizations. *Journal of the American Chemical Society* **1937,** *59* (2), 241-253.

50. Hui, A. W.; Hamielec, A. E. Thermal polymerization of styrene at high conversions and temperatures. An experimental study. *Journal of Applied Polymer Science* **1972,** *16* (3), 749-769.

51. Husain, A.; Hamielec, A. Thermal polymerization of styrene. *Journal of Applied Polymer Science* **1978,** *22* (5), 1207-1223.

52. Whiting, L.; Tou, J. Thermal hazard evaluation of styrene polymerization by accelerating rate calorimetry. *Journal of Thermal Analysis and Calorimetry* **1982,** *24* (1), 111-132.

53. Gibson, N.; Maddison, N.; Rogers, R. In *Case studies in the application of diers venting methods to fine chemical batch and semi-batch reactors*, Hazards from pressure: exothermic reactions, unstable substances, pressure relief and accidental discharge: a three-day symposium, Pergamon Pr: 1987; p 157.

54. Chen, C.-C.; Shu, C.-M.; Chang, R.-S.; Shyu, M.-L.; Chen, S.-C. In *Thermal hazard analysis of styrene monomer at low temperature conditions during storage and transportation*, Conference of NATAS, 2002.

55. Chen, C.-C.; Duh, Y.-S.; Shu, C.-M. Thermal polymerization of uninhibited styrene investigated by using microcalorimetry. *Journal of Hazardous Materials* **2009,** *163* (2), 1385-1390.

56. Leung, J. C.; Fauske, H.; Fisher, H. Thermal runaway reactions in a low thermal inertia apparatus. *Thermochimica Acta* **1986,** *104*, 13-29.

57. Achilias, D. S. A review of modeling of diffusion controlled polymerization reactions. *Macromolecular Theory and Simulations* **2007,** *16* (4), 319-347.

58. Noronha, J.; Juba, M.; Low, H.; Pascoe, W.; Schiffhauer, E.; Simpson, B. Kinetic model and tests for runaway thermally initiated styrene polymerization. *Journal of Hazardous Materials* **1979,** *3* (1), 91-106.

59. Hungenberg, K.-D.; Nieken, U.; Zöllner, K.; Gao, J.; Szekely, A., Modeling safety aspects of styrene polymerization processes. *Industrial & Engineering Chemistry Research* **2005,** *44* (8), 2518-2524.

60. Su, W.-F. *Principles of polymer design and synthesis*. Springer Berlin Heidelberg: 2013.

61. Denisov, E. T. *Liquid-phase reaction rate constants*. Springer Science & Business Media: 2012.

62. Graham, S. R.; Hodgson, R.; Vechot, L.; Essa, M. I. Calorimetric studies on the thermal stability of methyl ethyl ketone peroxide (MEKP) formulations. *Process Safety and Environmental Protection* **2011,** *89* (6), 424-433.

63. Ho, T. C.; Duh, Y. S.; Chen, J. Case studies of incidents in runaway reactions and emergency relief. *Process Safety Progress* **1998,** *17* (4), 259-262.

64. Duh, Y. S.; Hui wu, X.; Kao, C. S., Hazard ratings for organic peroxides. *Process Safety Progress* **2008,** *27* (2), 89-99.

65. Liu, S.-H.; Shu, C.-M.; Hou, H.-Y. Applications of thermal hazard analyses on process safety assessments. *Journal of Loss Prevention in the Process Industries* **2015,** *33*, 59-69.

66. Liu, S.-H.; Lin, W.-C.; Hou, H.-Y.; Shu, C.-M. Comprehensive runaway kinetic analysis and validation of three azo compounds using calorimetric approach and simulation. *Journal of Loss Prevention in the Process Industries* **2017**, *49*, 970-982.

67. Guo, S.; Wan, W.; Chen, C.; Chen, W. Thermal decomposition kinetic evaluation and its thermal hazards prediction of AIBN. *Journal of Thermal Analysis and Calorimetry* **2013,** *113* (3), 1169-1176.

68. Bessiere, J.-M.; Boutevin, B.; Loubet, O. Determination of kinetic parameters for isothermal decomposition of azo initiators of polymerization by differential scanning calorimetry. *Polymer Bulletin* **1993,** *30* (5), 545-549.

69. Zhang, C.-X.; Lu, G.-B.; Chen, L.-P.; Chen, W.-H.; Peng, M.-J.; Lv, J.-Y. Two decoupling methods for non-isothermal DSC results of AIBN decomposition. *Journal of Hazardous Materials* **2015,** *285*, 61-68.

70. Tsai, L.-C.; Chen, J.-W.; Hou, H.-Y.; Liu, S.-H.; Shu, C.-M. Exothermic behaviors in decomposition of three solid organic peroxides by DSC and VSP2. *Journal of Thermal Analysis and Calorimetry* **2012,** *109* (3), 1303-1309.

71. Huang, Y.-H.; Yet-Pole, I.; Chen, N.-C.; Wu, S.-H.; Horng, J.-J.; Wu, Y.-T.; Wen, I.-J. Thermal runaway reaction evaluation of benzoyl peroxide using calorimetric approaches. *Journal of Thermal Analysis and Calorimetry* **2013,** *113* (2), 595-598.

72. Lv, J.; Chen, W.; Chen, L.; Gao, H.; Tian, Y.; Sun, X. In *Experimental study and theoretical analysis on decomposition mechanism of benzoyl peroxide*. 2013 AIChE Annual Meeting, San Francisco, 2013.

73. Maschio, G.; Feliu, J.; Ligthart, J.; Ferrara, I.; Bassani, C. The use of adiabatic calorimetry for the process analysis and safety evaluation in free radical polymerization. *Journal of Thermal Analysis and Calorimetry* **1999,** *58* (1), 201-214.

74. Theis, A. E.; Burelbach, J. P.; Askonas, C. F. Safely scale-up processes and accommodate recipe changes. *Process Safety Progress* **2009,** *28* (2), 135-140.

75. Lee, E. J.; Park, H. J.; Kim, S. M.; Lee, K. Y. Effect of azo and peroxide initiators on a kinetic study of methyl methacrylate free radical polymerization by DSC. *Macromolecular Research* **2018,** *26* (4), 322-331.

76. Rowe, S. In *Polymerisation reaction inhibition: an alternative basis of safety*, Institution of chemical engineers symposium series, hemsphere publishing corporation: 1997; pp 273-284.

77. Uchida, T.; Surianarayanan, M.; Wakakura, M.; Tomioka, H. Hazards of radical polymerizations: Thermokinetic investigation of styrene polymerization methods. *Journal of Chemical Engineering of Japan* **1998,** *31* (6), 960-968.

78. Wang, W.; Fang, J.; Pan, X.; Hua, M.; Jiang, J.; Ni, L.; Jiang, J. Thermal research on the uncontrolled behavior of styrene bulk polymerization. *Journal of Loss Prevention in the Process Industries* **2019,** *57*, 239-244.

79. Liang, X.-M.; Jiang, H.-C.; Fang, J.-L.; Hua, M.-.; Pan, X.-H.; Jiang, J.-C. Thermal analysis of the styrene bulk polymerization and characterization of polystyrene initiated by two methods. *Chemical Engineering Communications* **2019,** *206* (4), 432-443.

80. Gustin, J.-L. Influence of trace impurities on chemical reaction hazards. *Journal of Loss Prevention in the Process Industries* **2002,** *15* (1), 37-48.

81. Liu, J.; Zhang, F.; Xu, W.; Shi, N.; Mu, S. Thermal reactivity of ethylene oxide in contact with contaminants: A review. *Thermochimica Acta* **2017,** *652*, 85-96.

82. Cassona, V.; Sneeb, T.; Maschio, G. Effect of amine compounds on the self-polymerisation of methyl methacrylate. *Chemical Engineering Transactions* **2014,** *36*, 109-114.

83. Moreno, V. C.; Rubinato, A.; Maschio, G. In *A simplified model to describe the effect of alkyl anilines on the polymerization of methyl methacrylate*, Macromolecular Symposia, 2016; pp 26-40.

84. Liu, K.; Wang, C.; Lin, J.; Chang, C.; Li, W.; Tseng, J. Thermal reaction hazard research for isoprene. *Journal of Thermal Analysis and Calorimetry* **2017,** *129* (1), 411-424.

85. Hankin, S. Accelerating rate calorimetry of monomers on absorbents. *Journal of hazardous materials* **1986,** *13* (2), 217-226.

86. Ericson, C. A.; Ll, C. In *Fault tree analysis*, System Safety Conference, Orlando, Florida, 1999; pp 1-9.

87. Lee, W.-S.; Grosh, D. L.; Tillman, F. A.; Lie, C. H. Fault Tree Analysis, methods, and applications: a review. *IEEE Transactions on Reliability* **1985,** *34* (3), 194-203.

88. Charsley, E.; Price, D.; Hunter, N.; Gabbott, P.; Kett, V.; Gaisford, S.; Priestley, I.; Duncan, J.; Royall, P.; Scowen, I. *Principles of thermal analysis and calorimetry*. Royal Society of Chemistry: 2019.

89. Ancsin, J. Melting curves and heat of fusion of indium. *Metrologia* **1985,** *21* (1), 7.

90. TA Instruments. *A review of DSC kinetics methods*. 2010. http://www.tainstruments.com/pdf/literature/TA073.pdf (Accessed April 28, 2020)

91. American Society for Testing and Materials. *Standard test method for kinetic parameters by differential scanning calorimetry using isothermal methods*, West Conshohocken New York (NY): 2013.

92. American Society for Testing and Materials. *Standard test method for estimating kinetic parameters by differential scanning calorimeter using the Borchardt and Daniels method*. West Conshohocken New York (NY): 2013.

93. American Society for Testing and Materials. *Standard test method for kinetic parameters for thermally unstable materials by differential scanning calorimetry using the Kissinger method*. West Conshohocken New York (NY): 2018.

94. American Society for Testing and Materials. S*tandard test method for arrhenius kinetic constants for thermally unstable materials using differential scanning calorimetry and the Flynn/Wall/Ozawa method*. West Conshohocken New York (NY): 2005.

95. Abele, S.; Schwaninger, M.; Fierz, H.; Schmidt, G.; Funel, J.-A.; Stoessel, F. Safety assessment of Diels–Alder reactions with highly reactive acrylic monomers. *Organic Process Research & Development* **2012,** *16* (12), 2015-2020.

96. Schick, H. L. A thermodynamic analysis of the high-temperature vaporization properties of silica. *Chemical Reviews* **1960,** *60* (4), 331-362.

97. Aras, L.; Richardson, M. The glass transition behaviour and thermodynamic properties of amorphous polystyrene. *Polymer* **1989,** *30* (12), 2246-2252.

98. Barton, J.; Rogers, R. *Chemical reaction hazards: a guide to safety*. IChemE: 1997.

99. Townsend, D.; Tou, J. Thermal hazard evaluation by an accelerating rate calorimeter. *Thermochimica Acta* **1980,** *37* (1), 1-30.

100. Noronha, J. A.; Fisher, H. G. DIERS Bench-Scale Apparatus. *Emergency Relief System Design Using DIERS Technology* **1993**, 365-448.

101. Leung, J. C.; Fauske, H. K. Runaway system characterization and vent sizing based on DIERS methodology. *Plant/Operations Progress* **1987,** *6* (2), 77-83.

102. Burelbach, J. P. In *Advanced reactive system screening tool (ARSST)*, North American Thermal Analysis Society, 28th Annual Conference, Orlando, 2000.

103. Zhu, W.; Papadaki, M. I.; Han, Z.; Mashuga, C. V. Effect of temperature and selected additives on the decomposition "onset" of 2-nitrotoluene using Advanced Reactive System Screening Tool. *Journal of Loss Prevention in the Process Industries* **2017,** *49*, 630-635.

104. Center for Chemical Process Safety. *Guidelines for pressure relief and effluent handling systems*. John Wiley & Sons: 2017.

105. Matsas, G.; Faliagas, A.; Simitzis, J. Removal of polymerization inhibitors from styrene based on adsorption. *Applied Macromolecular Chemistry and Physics* **1995,** *227* (1), 35-42.

106. Sebastian, D.; Biesenberger, J. A study of chain addition polymerizations with temperature variations: III. Thermal runaway and instability in styrene polymerization—an experimental study. *Polymer Engineering & Science* **1976,** *16* (2), 117-123.

107. Hu, K.-H.; Kao, C.-S.; Duh, Y.-S. Studies on the runaway reaction of ABS polymerization process. *Journal of Hazardous Materials* **2008,** *159* (1), 25-34.

108. Kehinde, A. J.; Usman, M. A.; Owolabi, R. U. Solvent-initiator compatibility and sensitivity of conversion of styrene homo-polymerization. *Journal of Polymer Engineering* **2013,** *33* (9), 775-783.

109. Loss, C.; Azevedo, E.; Dezotti, M. Treatment of the butadiene washing stream from a synthetic rubber industry and recovery of p-TBC. *Water Science and Technology* **2006,** *54* (10), 17-21.

110. Nédez, C.; Ray, J.-L. Efficient removal of polymerization inhibitors by adsorption on the surface of an optimized alumina. *Langmuir* **1999,** *15* (18), 5932-5936.

111. Díaz, I.; Ovejero, G.; Romero, M. D.; Díez, E. Feasibility analysis of some clays as adsorbents for styrene purification. *Journal of Materials Science and Engineering B* **2015**, 5 (1-2), 96-105.

112. Rivero, M. J.; Ibáñez, R.; Ortiz, M. I. Analysis of the elimination process of polymerisation inhibitors from styrene by means of adsorption. *Journal of Chemical Technology & Biotechnology: International Research in Process, Environmental & Clean Technology* **2003,** *78* (1), 64-72.

113. Casson, V.; Maschio, G. In *Risk analysis in transport and storage of monomers: an accident investigation*, Macromolecular Symposia, 2011; pp 273-279.

114. Peterson, J. D.; Vyazovkin, S.; Wight, C. A. Kinetics of the thermal and thermo-oxidative degradation of polystyrene, polyethylene and poly (propylene). *Macromolecular Chemistry and Physics* **2001,** *202* (6), 775-784.

115. Flory, P. J. Thermodynamics of heterogeneous polymers and their solutions. *The Journal of Chemical Physics* **1944,** *12* (11), 425-438.

116. Fisher, H.; Forrest, H.; Grossel, S. S.; Huff, J.; Muller, A.; Noronha, J.; Shaw, D.; Tilley, B. *Emergency relief system design using DIERS technology: The Design Institute for Emergency Relief Systems (DIERS) project manual*. John Wiley & Sons: 2010.

117. Höcker, H.; Flory, P. Thermodynamics of polystyrene solutions. Part 2. Polystyrene and ethylbenzene. *Transactions of the Faraday Society* **1971,** *67*, 2270-2274.

118. Buback, M.; Garcia-Rubio, L.; Gilbert, R.; Napper, D.; Guillot, J.; Hamielec, A.; Hill, D.; O'Driscoll, K.; Olaj, O.; Shen, J. Consistent values of rate parameters in free radical polymerization systems. *Journal of Polymer Science Part C: Polymer Letters* **1988,** *26* (7), 293-297.

119. Buback, M.; Gilbert, R.; Russell, G.; Hill, D.; Moad, G.; O'Driscoll, K.; Shen, J.; Winnik, M. Consistent values of rate parameters in free radical polymerization systems. II. Outstanding dilemmas and recommendations. *Journal of Polymer Science Part A: Polymer Chemistry* **1992,** *30* (5), 851-863.

120. Buback, M.; Gilbert, R. G.; Hutchinson, R. A.; Klumperman, B.; Kuchta, F. D.; Manders, B. G.; O'Driscoll, K. F.; Russell, G. T.; Schweer, J. Critically evaluated rate coefficients for free-radical polymerization, 1. Propagation rate coefficient for styrene. *Macromolecular Chemistry and Physics* **1995,** *196* (10), 3267-3280.

121. Buback, M.; Huckestein, B.; Kuchta, F. D.; Russell, G. T.; Schmid, E. Initiator efficiencies in 2, 2′-azoisobutyronitrile-initiated free-radical polymerizations of styrene. *Macromolecular Chemistry and Physics* **1994,** *195* (6), 2117-2140.

122. Buback, M.; Egorov, M.; Gilbert, R. G.; Kaminsky, V.; Olaj, O. F.; Russell, G. T.; Vana, P.; Zifferer, G. Critically evaluated termination rate coefficients for free-

radical polymerization, 1. the current situation. *Macromolecular Chemistry and Physics* **2002,** *203* (18), 2570-2582.

123. Barner-Kowollik, C.; Buback, M.; Egorov, M.; Fukuda, T.; Goto, A.; Olaj, O. F.; Russell, G. T.; Vana, P.; Yamada, B.; Zetterlund, P. B. Critically evaluated termination rate coefficients for free-radical polymerization: Experimental methods. *Progress in Polymer Science* **2005,** *30* (6), 605-643.

124. Kattner, H.; Buback, M. Chain-length-dependent termination of styrene bulk polymerization up to high degrees of monomer conversion. *Macromolecules* **2017,** *50* (14), 5308-5314.

125. James, D. H.; Castor, W. *Ullmann's encyclopedia of industrial chemistry*. John Wiley & Sons: 1994.

126. Moad, G.; Solomon, D. H. *The chemistry of radical polymerization*. Elsevier: 2006.

127. Carraher Jr, C. E. *Introduction to polymer chemistry*. CRC Press: 2012.

128. Brandrup, J.; Immergut, E. H.; Grulke, E. A.; Abe, A.; Bloch, D. R. *Polymer handbook*. Wiley New York: 1989; Vol. 7.

129. Tedder, J. M.; Walton, J. C. The importance of polarity and steric effects in determining the rate and orientation of free radical addition to olefins: Rules for determining the rate and preferred orientation. *Tetrahedron* **1980,** *36* (6), 701-707.

130. Prana, V.; Rotureau, P.; Fayet, G.; André, D.; Hub, S.; Vicot, P.; Rao, L.; Adamo, C. Prediction of the thermal decomposition of organic peroxides by validated QSPR models. *Journal of Hazardous Materials* **2014,** *276*, 216-224.

131. Thomas, L. C. *Modulated DSC® paper# 1 Why modulated DSC®?; An overview and summary of advantages and disadvantages relative to traditional DSC*. 2005. http://www.tainstruments.com/pdf/literature/TP006_MDSC_1_MDSCOverview.pdf (Accessed April 28, 2020)

132. Thomas, L. C. *Modulated DSC® paper# 5: Measurement of glass transitions and enthalpic recovery*. 2005. http://www.tainstruments.com/pdf/literature/TP_010_MDSC_num_5_Measurement_of_Glass_Transition_and_Enthalpic_Recovery.pdf (Accessed April 28, 2020)

133. Thomas, L. C. *Modulated DSC® paper# 9: Measurement of accurate heat capacity values*. 2005. http://www.tainstruments.com/pdf/literature/TP 014_MDSC_9_Measurementof-AccurateHeatCapacityValues.pdf (Accessed April 28, 2020)

134. Thomas, L. C., *Modulated DSC® paper# 3 Modulated DSC® basics; Optimization of MDSC® experimental conditions*. 2005. http://www.tainstruments.com/pdf/literature/TP_008_MDSC_num_3_Optimization_of_Experimental_Conditions.pdf (Accessed April 28, 2020)

135. Hofelich, T.; LaBarge. On the use and misuse of detected onset temperature of calorimetric experiments for reactive chemicals. *Journal of Loss Prevention in the Process Industries* **2002,** *15* (3), 163-168.

136. Barr, N.; Bengough, W.; Beveridge, G.; Park, G. The measurement of rates of initiation in the thermal polymerization of styrene. *European Polymer Journal* **1978,** *14* (4), 245-250.

137. De Gennes, P.-G.; Brochard-Wyart, F.; Quéré, D. *Capillarity and wetting phenomena*. Springer: 2004.

138. Lin, S.; Chen, K.; Shu, C. Calorimetric evaluation of polymerization thermokinetics of styrene, α-methylstyrene and trans-β-methylstyrene. *Journal of Hazardous Materials* **2009,** *161* (1), 330-335.

139. Dakshinamoorthy, D.; Khopkar, A.; Louvar, J.; Ranade, V. CFD simulations to study shortstopping runaway reactions in a stirred vessel. *Journal of Loss Prevention in the Process Industries* **2004,** *17* (5), 355-364.

140. Fried, J. R. *Polymer science and technology*. Pearson Education: 2014.

141. Osborne, N. S. Measurements of heat capacity and heat of vaporization of water in the range 0°C to 100°C. *Journal of Research of the National Bureau of Standards* **1939,** *23*, 197-260.

142. Burelbach, J. P. *Quick hazard screening by closed cell ARSST using standard ARC bombs*.1989.https://cdn2.hubspot.net/hubfs/232514/Fauske2017/PDF/QuickHazardScreeningbyClosedCellARSSTUsingStandardARCTMBombs.pdf?t=1494272312789. (Accessed April 28, 2020)

143. Jiang, W.; Pan, X.; Hua, M.; Ni, L.; Jiang, J. Research on thermal runaway process of styrene bulk polymerization. *Process Safety Progress* **2018,** *37* (2), 276-282.

144. Zhang, Y.; Ni, L.; Jiang, J.; Jiang, J.; Zhang, W.; Jiang, J.; Zhang, M. Thermal hazard analyses for the synthesis of benzoyl peroxide. *Journal of Loss Prevention in the Process Industries* **2016,** *43*, 35-41.

145. Chen, L.-P.; Liu, T.-T.; Yang, Q.; Chen, W.-H. Thermal hazard evaluation for iso-octanol nitration with mixed acid. *Journal of Loss Prevention in the Process Industries* **2012,** *25* (3), 631-635.

146. Marco, E.; Cuartielles, S.; Pena, J.; Santamaria. Simulation of the decomposition of di-cumyl peroxide in an ARSST unit. *Thermochimica Acta* **2000,** *362* (1-2), 49-58.

147. Astle, M. J.; Weast, R. C. *CRC handbook of data on organic compounds*. CRC Press: 1986.

148. Tsuda, Y. Hydrogen acid catalyzed polymerization of styrene. *Macromolecular Chemistry and Physics* **1960,** *36* (1), 102-108.

149. Asami, R.; Tokura, N. Cationic polymerization in liquid sulfur dioxide. II. Cationic polymerization of styrene with the friedel-crafts-type and other acid catalysts. *Journal of Polymer Science* **1960,** *42* (140), 553-560.

150. Hayes, M.; Pepper, D. The polymerization of styrene by sulphuric acid-II. The kinetics of polymerization in 1: 2-dichloroethane. *Proceedings of the Royal Society of London. Series A. Mathematical and Physical Sciences* **1961,** *263* (1312), 63-74.

151. Burton, R.; Pepper, D. The polymerization of styrene by sulphuric acid-I. Theory of fast-initiated non-stationary polymerization. *Proceedings of the Royal Society of London. Series A. Mathematical and Physical Sciences* **1961,** *263* (1312), 58-62.

152. Frurip, D. J.; Elwell, T. Effective use of differential scanning calorimetry in reactive chemicals hazard evaluation. *Process Safety Progress* **2007,** *26* (1), 51-58.

153. Whiting, L.; Labean, M.; Eadie. Evaluation of a capillary tube sample container for differential scanning calorimetry. *Thermochimica Acta* **1988,** *136*, 231-245.

154. Sheng, M.; Valco, D.; Tucker, C.; Cayo, E., Lopez, T. Development, practical use of differential scanning calorimetry for thermal stability hazard evaluation. *Organic Process Research & Development* **2019,** *23* (10), 2200-2209.

155. Vyazovkin, S.; Burnham, A. K.; Criado, J. M.; Pérez-Maqueda, L. A.; Popescu, C.; Sbirrazzuoli. ICTAC kinetics committee recommendations for performing kinetic computations on thermal analysis data. *Thermochimica Acta* **2011,** *520* (1-2), 1-19.

156. Muravyev, N. V.; Pivkina, A. N.; Koga, N. J. M. Critical appraisal of kinetic calculation methods applied to overlapping multistep reactions. *Molecules* **2019,** *24* (12), 2298.

157. Stoessel, F. *Thermal safety of chemical processes: risk assessment and process design*. John Wiley & Sons: 2020.